THE SCIENCE CASE FOR MIRANdA

Version of May 1st, 2007

Project Scientist and Editor
S. Johnston[1]

Chapter Authors
R. Ekers[1], I. Feain[1], B. Gaensler[2], G. Hobbs[1], S. Johnston[1],
N. McClure-Griffiths[1], L. Staveley-Smith[3], S. Tingay[4]

Contributing Authors
M. Bailes[4], C. Baugh[5], C. Blake[4], R. Braun[1], S. Chatterjee[2], J. Darling[6],
A. Deller[4], R. Dodson[7], P. Edwards[1], S. Ellingsen[8], M. Haverkorn[9],
A. Hopkins[2], A. Lenc[4], C. Jackson[1], C. James[10], V. Kilborn[4], B. Koribalski[1],
J. Lovell[8], J.-P. Macquart[11], D. Matthews[12], R. Manchester[1], R. Norris[1],
C. Phillips[1], C. Power[4], R. Protheroe[10], B. Schmidt[13], A. Tzioumis[1], M. Walker[14]

Affiliations

1. Australia Telescope National Facility, CSIRO.
2. University of Sydney
3. University of Western Australia
4. Swinburne University of Technology
5. University of Durham, UK
6. University of Colorado, USA
7. Observatorio Astronomico Nacional, Spain
8. University of Tasmania
9. University of California, Berkeley
10. University of Adelaide
11. California Institute of Technology, USA
12. La Trobe University
13. Australian National University
14. MAW Technology Pty. Ltd.

Executive Summary

The future of radio astronomy lies with the Square Kilometre Array (SKA), a telescope currently in the planning stage and expected to be operational in 2020. Much of the Key Science for the SKA calls for a fast survey speed at observing frequencies around 1 GHz.

MIRANdA is an SKA demonstrator which achieves a fast survey speed through a combination of medium sized parabolic dishes equipped with focal plane arrays. The array will be located at Boolardy Station, Western Australia, in one of the most radio quiet regions on Earth and a potential site for hosting the SKA. Although only 1% of the final SKA specifications, MIRANdA is a front-line scientific instrument in its own right which attacks ground-breaking science questions directly relevant to the SKA.

The science goals for MIRANdA include:

- understanding the evolution of the gaseous component of the nearby Universe;
- determining the evolution, formation and population of galaxies throughout cosmic time;
- understanding the interstellar medium of our own Galaxy and the generation and maintenance of its magnetic fields;
- revealing the nature of the transient radio sky;
- discovering and timing up to 1000 radio pulsars;
- providing a vital element of the VLBI network.

The combination of location, technological innovation, scientific program and the outstanding research capability of the Australian astronomical community will ensure that MIRANdA plays a leading role in the years prior to the design and build of the SKA.

Contents

Chapter 1

Introduction

MIRANdA is a next generation radio telescope on the strategic pathway towards the development of the Square Kilometre Array (SKA). MIRANdA has three main goals:

- to carry out world-class, ground breaking observations directly relevant to the SKA Key Science Projects,
- to demonstrate the viability of wide field-of-view technologies with medium sized dishes and focal plane arrays,
- to establish a site in Western Australia where observations can be carried out free from the harmful effects of radio interference.

Significant funding for SKA research in Australia initially came via the Major New Research Facility (MNRF) program initiated by the Federal Government which ran from 2002−2007. The need to achieve a wide field of view at frequencies around 1 GHz led to examinations of initial options for the collector which included Luneberg lenses and cylinders. These ideas were ultimately rejected and subsequent thinking converged on the concept of parabolic dishes equipped with focal plane arrays. Implemented as the New Technology Demonstrator (NTD), and fully funded through MNRF, the key concept behind the NTD is to investigate the viability of wide field-of-view operations on a ∼12 m parabolic dish using a large (∼100 element) focal plane array. This has largely been achieved using two paraboloid dishes equipped with focal plane arrays at the ATNF site in Marsfield, Sydney.

The MIRANdA project grew out of the original NTD concept and is designed to be a front-line scientific instrument in its own right. It builds upon the deliverables from the NTD and other MNRF projects and benefits from

international collaborations with both Canadian and South African partners. MIRANdA will be located near Boolardy Station, Western Australia at the proposed Australian site for the SKA. Initial funding for research and development of MIRANdA came from the CSIRO. Additional funds have since been provided by the Government of Western Australia and from the Federal Government's National Collaborative Research Infrastructure Strategy (NCRIS) which recognised astronomy as a priority area.

MIRANdA is part of the strategic pathway towards the SKA as outlined in the Australian SKA Consortium Committee's "SKA: A Road Map for Australia" document. MIRANdA is seen as '...a significant scientific facility, maintaining Australia's leading role within the SKA partnership and addressing key outstanding computational/calibration risk areas ...'. SKA programs were given the highest priority for Australian radio astronomy in the 2006−2015 Decadal Plan for Astronomy. Although the collecting area of MIRANdA is less than 1% that of the SKA, the technological solutions it proposes are designed to ensure a modular upgrade path towards the 10% SKA Phase I and the full SKA, provided the technical challenges can be met.

1.1 MIRANdA and SKA science

MIRANdA will not only demonstrate 'smart feed' technology for the SKA, it will also demonstrate the feasibility of the science projects envisaged for both SKA Phase I and the full SKA. In particular, five key science projects (KSPs) for the SKA have been adopted by the International SKA Steering Committee. These are

- The cradle of life (Lazio et al. 2004)
- Strong field tests of gravity using pulsars and black holes (Kramer et al. 2004)
- The origin and evolution of cosmic magnetism (Gaensler et al. 2004)
- Galaxy evolution, cosmology and dark energy (Rawlings et al. 2004)
- Probing the dark ages (Carilli et al. 2004)

The MIRANdA system parameters, in particular the frequency range and large field of view capability, are aimed squarely at attacking the middle three of these KSPs. Several other experiments, co-located on the West

Australian site, will target the 'Dark Ages' KSP which requires observing frequencies below about 200 MHz.

The headline science goals for MIRANdA are:

- The detection of 700,000 galaxies in H I emission across the southern sky out to a redshift of 0.2 to understand galaxy formation and gas evolution in the nearby Universe.
- The detection of 6×10^7 continuum sources to determine the evolution, formation and population of galaxies across cosmic time and enabling key cosmological tests.
- The detection of 5×10^5 polarized sources allowing a grid of rotation measures at $10'$ spacing across the sky to understand how the Milky Way generates and maintains coherent magnetic fields on huge scales.
- To understand the evolution of the interstellar medium of our own Galaxy through observations of its atomic, molecular, ionised and magnetic components.
- The characterization of the radio transient sky through detection and monitoring of transient sources such as gamma ray bursts, radio supernovae and intra-day variables.
- The discovery and subsequent timing of up to 1000 radio pulsars.
- To play a key role in the Australian and global VLBI networks.

1.2 System Parameters

The strawman (or base model) parameters for MIRANdA are given in the first column of Table 1.1 and these strawman assumptions have been used throughout this document. However, possibilities exist for an increase in the funding for MIRANdA. Likely upgrade or expansion paths include the addition of further dishes and/or the cooling of the focal plane array elements to provide a lower system temperature. Parameters for this expansion path are listed in the column 2 of Table 1.1.

MIRANdA is designed to be a fast survey telescope. A key metric in this sense is the survey speed expressed in the number of square degrees per hour to a given sensitivity. Survey speeds and sensitivity for an interferometer like MIRANdA have been derived elsewhere (e.g. Johnston & Gray 2006) and the full derivation will not be shown here. To recap, the time, t, required

Table 1.1: System parameters for MIRANdA

Parameter	Strawman	Expansion
Number of Dishes	30	45
Dish Diameter (m)	12	12
Total collecting area (m^2)	3393	5089
Aperture Efficiency	0.8	0.8
System Temperature (K)	50	35
Number of beams	30	30
Field-of-view (deg^2)	30	30
Frequency range (MHz)	$800 - 1700$	$800 - 1700$
Instantaneous Bandwidth (MHz)	300	300
Maximum number of channels	16000	16000

to reach a given sensitivity limit for point sources, σ_s, is

$$t = \left(\frac{2\ k\ T}{A\ N\ \epsilon_a\ \epsilon_c}\right)^2 \frac{1}{\sigma_s^2\ B\ n_p} \tag{1.1}$$

where all parameters have their SI units. B is the bandwidth, n_p the number of polarizations, A is the collecting area of a single element, N is the number of elements and ϵ_a and ϵ_c represent dish and correlator efficiencies. The system temperature is T with k being the Boltzmann constant. The number of square degrees per second that can be surveyed to this sensitivity limit is

$$SS_s = F\ B\ n_p \left(\frac{A\ N\ \epsilon_a\ \epsilon_c\ \sigma_s}{2\ k\ T}\right)^2 \tag{1.2}$$

where F is the field of view in square degrees. The surface brightness temperature survey speed is given by

$$SS_t = F\ B\ n_p \left(\frac{\epsilon_c\ \sigma_t}{T}\right)^2\ f^2\ \epsilon_s^{-2} \tag{1.3}$$

where now σ_t denotes the sensitivity limit in K and f relates to the filling factor of the array via

$$f = \frac{A\ \epsilon_a\ N\ \Omega\ \epsilon_s}{\lambda^2} \tag{1.4}$$

Here, ϵ_s is a 'synthesised aperture efficiency' which is related to the weighting of the visibilities and is always ≤ 1.

There is interplay between these parameters when trying to maximise the survey speed for a given expenditure. For the majority of the science that will be considered here, the value of SS_s and SS_t are critical parameters, although the instantaneous sensitivity is also important. Although these equations are useful, they are not the entire story. For example, the effects of good uv coverage on the image quality do not appear in the equations. Furthermore, one should also not neglect the total bandwidth available for a spectral line survey. If the total bandwidth is insufficient to cover the required bandwidth of a given survey, the survey speed suffers as a result of having to repeat the same sky with a different frequency setting.

In Table 1.2 we list values of the sensitivity and survey speed for different 'typical' surveys for both the strawman and the expansion parameters. The first line gives a continuum survey where the entire 300 MHz of bandwidth is exploited and a desired sensitivity of 100 μJy is required. The second entry gives a spectral line survey, with the third line listing a surface brightness survey needing to reach 1 K rms over 5 kHz channel under the assumption of a $1'$ resolution. The expansion option for MIRANdA offers a factor of almost 5 improvement over the strawman design.

Table 1.2: Sensitivity and survey speeds for MIRANdA

Parameter	Strawman	Expansion
Continuum survey speed (300 MHz, 100 μJy)	250	1150 deg^2/hr
Line survey speed (100 kHz, 5 mJy)	209	960 deg^2/hr
Surface brightness survey speed (5 kHz, 1 K, $1'$)	18	83 deg^2/hr
Point source sensitivity (1 MHz, 1 mJy)	1290	280 sec

1.3 Comparison with other instruments

The large field-of-view (FoV) makes MIRANdA primarily a survey telescope. Although it has a similar collecting area to the Parkes 64-m dish, its uncooled receivers reduces its raw, instantaneous sensitivity. As an interferometer MIRANdA provides low frequency imaging not otherwise available at the Australia Telescope Compact Array (ATCA). Even for single pointings, it also exceeds the ATCA sensitivity at 1400 MHz and may have improved resolution if it also extends beyond 6 km baselines. In terms of survey speed however, it gains by large factors for both line, continuum and surface brightness sensitivity compared to existing facilities and is comparable to

other planned facilities such as the Allen Telescope Array (ATA) in the USA and Apertif in the Netherlands.

As an example comparison, the survey speed for MIRANdA exceeds that of the Parkes 20-cm multibeam receiver by more than an order of magnitude for spectral line surveys. Furthermore, single dish surveys are plagued by problems such as interference, baseline ripple and continuum subtraction, problems which interferometers such as MIRANdA do not have.

The survey speeds of MIRANdA, the ATA and Apertif are almost identical although achieved in different ways. The ATA achieves its survey speed through a large number of small dishes each with a single pixel feed. Apertif has a focal plane array system on large dishes; its instantaneous sensitivity is better than that of MIRANdA, but the field of view is significantly smaller. The presence of telescopes with similar survey speed in the northern hemisphere makes for excellent complementarity to MIRANdA and implies that similar surveys can be achieved over the entire sky.

1.4 Configuration of MIRANdA

The configuration of MIRANdA has been the subject of much debate and is still far from determined. As can be seen from the following chapters in this document, there are diverse requirements on the configuration. A number of science projects (pulsar surveys, galactic H I, low surface brightness mapping) require a highly compact array configuration in order to increase the surface brightness survey speed (see equations 1.3 and 1.4). On the other hand science such as continuum and transients require long baselines both to overcome the effects of confusion and to obtain accurate positions for identification at other wavelengths. In the middle is the extragalactic H I survey which needs moderate resolution to avoid over-resolving the sources. With a total of only 30 dishes it is difficult to achieve all these requests simultaneously. However, it may be possibly to change configurations by physically moving the antennas. This would not happen on a regular basis but occasionally as needs arise. As the number of dishes in the array becomes larger, hybrid configurations become more viable and it becomes possible to have both a compact configuration and outlier dishes on long baselines. Such options still need to be explored in more detail.

1.5 Location of MIRANdA

MIRANdA will be located at one of the most radio quiet sites on Earth, at Boolardy Station in Western Australia. This site has been proposed as Australia's candidate SKA site. A radio astronomy observatory is being established on the site and a radio-quiet zone established surrounding the site. The approximate geographical coordinates of the site are longitude 116.5 and latitude -26.7. The choice of site ensures that MIRANdA will be largely free of the harmful effects of radio interference currently plaguing the current generation of telescopes, especially at frequencies around 1 GHz and below. Being able to obtain a high continuous bandwidth at low frequencies is critical to much of the science described in this document. The southern latitude of MIRANdA implies that the Galactic Centre will transit overhead and the Magellanic Clouds will be prominent objects of study.

1.6 Document outline

Seven main science themes have been identified for MIRANdA. These are extragalactic H I science, continuum science, polarization science, Galactic and Magellanic science, VLBI science, pulsar science and the radio transient sky. Each science theme has its own chapter in this document with a final chapter dealing with other science not covered elsewhere. A lead author has been allocated for each chapter; these lead authors have the opportunity to get input from contributing authors on the various subsections of their chapter. All authors are listed on the title page of the document.

1.7 Acknowledgments

The Project Scientist would like to thank all the participants at the 'Science with MIRANdA' international meeting held at the ATNF in March 2007. The Project Scientist is also grateful to the chapter authors of this document for an excellent job in putting together the science case on a very tight timescale.

Chapter 2

Extragalactic H I Science

2.1 Summary

Understanding how galaxies form and evolve is one of the key astrophysical problems for the 21st century. Since neutral hydrogen (H I) is a fundamental component in the formation of galaxies, being able to observe and model this component is important in achieving a deeper understanding of galaxy formation. Widefield H I surveys using the next generation radio telescopes such as MIRANdA and ultimately the SKA will allow unprecedented insights into the evolution of the abundance and distribution of neutral hydrogen with cosmic time, and its consequences for the cosmic star formation and structure of galaxies and the Intergalactic Medium. MIRANdA will provide powerful tests of theoretical galaxy formation models and improve our understanding of the physical processes that shaped the galaxy population over the last ∼7 billion years.

2.2 MIRANdA H I Surveys

MIRANdA excels as a survey telescope as it will be able to spend long periods of time integrating on large areas of sky, resulting in the detection of large numbers of galaxies. Two compelling H I surveys are:

- A shallow hemispheric H I survey lasting a year. This would result in the detection of over 700,000 galaxies, or two orders of magnitude greater than HIPASS. The typical survey depth would be $z \sim 0.05$ with massive galaxies detected out to $z \sim 0.2$ (see Figure 2.1).

- A deep 'pencil-beam' survey covering a single pointing, also lasting a year. Although this would only detect 100,000 galaxies in the example of a non-evolving H I mass function shown in Figure 2.2, the typical depth would be $z \sim 0.05$ with massive galaxies detected out to $z \sim 0.7$.

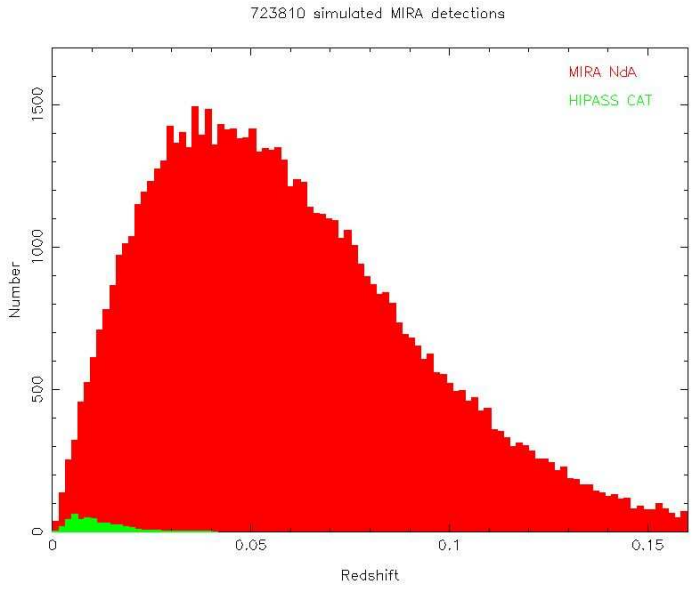

Figure 2.1: Number of galaxies above 5σ as a function of redshift bin for a shallow MIRANdA H I survey lasting a year, covering the southern hemisphere, compared with HIPASS HICAT (Meyer et al. 2004). The simulation assumes the Zwaan et al. (2005) HIPASS mass function, and assumes a bivariate relation between H I mass and velocity width similar to that deduced from HIPASS. The number of predicted detections is over 700,000 although this number quickly reduces for angular resolutions below $1'$.

H I surveys are best carried out with compact configurations. However, the ability to resolve detections greatly increases understanding of the physical properties of galaxies and galaxy populations. A configuration which results in a resolution of around $30''$ at $z = 0$ with a Gaussian natural beam appears a reasonable compromise (Staveley-Smith 2006). However, some science such as imaging the Cosmic Web requires greater column density sensitivity and short baselines, such as might be achieved using a reconfigurable array.

2.3 Cosmic Neutral Gas Density

Neutral atomic hydrogen is the most abundant element in the Universe and it plays a fundamental role in galaxy formation, principally as the raw material from which stars are made. At any given time we expect that the amount of neutral hydrogen in a galaxy will be determined by the competing rates at which H I is depleted (by star formation and various feedback processes) and replenished (by accretion of cold gas from its surroundings and other feedback processes). Understanding how the abundance and distribution of H I in the Universe evolves with redshift therefore provides us with important insights into the physical processes that drive the growth of galaxies and is a powerful test of theoretical galaxy formation models (e.g. Baugh et al. 2004).

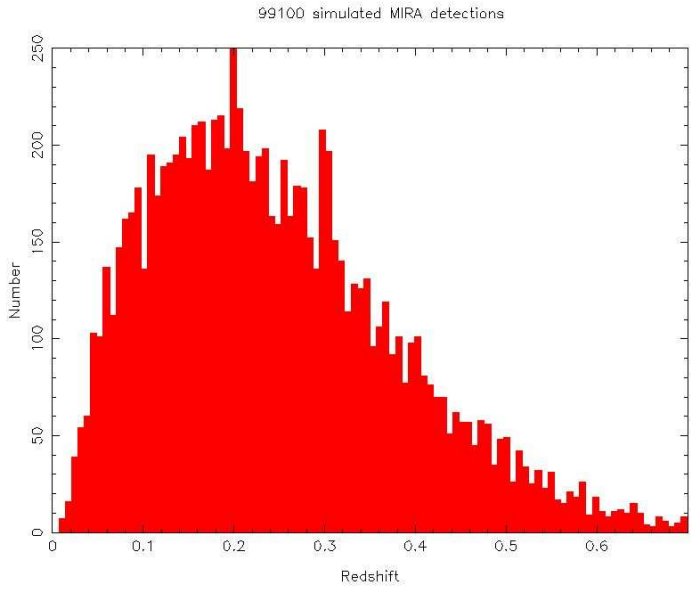

Figure 2.2: Number of galaxies above 5σ as a function of redshift bin for a deep MIRANdA H I survey lasting a year, covering a single pointing of MIRANdA. The simulation is similar to that for the all-sky survey and assumes a non-evolving H I mass function. The number of predicted detections is almost 100,000 and is less sensitive to angular resolution. Standard cosmology is assumed (flat Universe, $H_o = 75$ km s^{-1} Mpc^{-1}, $\Omega_m = 0.3$, $\Omega_\Lambda = 0.7$).

The cosmic H I mass density $\Omega_{\rm HI}$ provides a convenient measure of the abundance of neutral hydrogen at a given epoch. Estimates of $\Omega_{\rm HI}$ at high

redshifts ($z \gtrsim 1.5$) can be deduced from QSO absorption-line systems in general and damped Lyman-α (DLA) systems in particular. DLA systems contain the bulk of H I at high redshifts and imply that $\Omega_{\rm HI} \simeq 10^{-3}$ (e.g. Peroux et al. 2003, Prochaska et al. 2005, Rao et al. 2006). At low-to-intermediate redshifts, however, the only known way to measure accurately $\Omega_{\rm HI}$ is by means of large-scale H I 21-cm surveys.

This has been possible at $z \lesssim 0.04$ using the H I Parkes All-Sky Survey HIPASS (Meyer et al. 2004), which mapped the distribution of H I in the nearby Universe that is observable from Parkes. HIPASS data have allowed accurate measurement of the local H I mass function (HIMF) and HI density, $\Omega_{\rm HI}$ of galaxies (Zwaan et al. 2003, 2005). However, few measurements of the HIMF and $\Omega_{\rm HI}$ using H I 21-cm emission have been possible over the redshift range $0.04 \lesssim z \lesssim 1$ because of insufficient sensitivity of current-generation radio telescopes (though see Lah et al. 2007), and so next generation telescopes such as MIRANdA and ultimately the SKA will be required.

2.3.1 Semi-Analytic Galaxy Formation Models

It is possible to use the semi-analytical galaxy formation code such as GALFORM (Cole et al. 2000) to investigate the predicted evolution with redshift of the HIMF and $\Omega_{\rm HI}$. Semi-analytical models provide a powerful theoretical framework within which we can explore the range of physical processes (e.g. star formation, the release of energy from SNe and AGN, referred to as "feedback") that drive the formation of galaxies and shape their observable properties (see Baugh 2006 for a comprehensive overview of semi-analytical modelling). Numerical simulators call these processes "sub-grid physics". Due the current lack of a detailed understanding of the relevant physics, these phenomena are modelled with recipes or rules which contain parameters whose values can only be set so that appropriate subset of observational data are reproduced in local galaxy populations, e.g. the optical or infrared luminosity functions (see Cole et al. 2000).

For comparison, we consider two of the most successful models implemented in GALFORM: the one proposed by Baugh et al. (2005), which reproduces the abundances of Lyman-break and sub-millimetre galaxies at high redshifts; and the model of Bower et al. (2006), which recovers the observed break in the luminosity function at bright magnitudes particularly well and also matches the evolution of the stellar mass function. Both of these are regarded as viable models. They share many common ingredients

but differ in some important aspects of the sub-grid physics relating to the formation of massive galaxies. In the Bower et al. model, AGN heating suppresses cooling flows in massive haloes. In the Baugh et al. model, the quenching of massive galaxy formation is achieved with a SNe driven wind which ejects cold gas from intermediate mass haloes, thereby removing this material from the low-redshift stages of the hierarchy. A further key difference between the models is that Baugh et al. assume a top-heavy IMF for bursts of star formation triggered by galaxy mergers.

2.3.2 Evolution of $\Omega_{\rm HI}$ with Redshift

In Figure 2.3, we compare the predictions of the Baugh et al. "top-heavy IMF" and the Bower et al. "AGN-heating" models with current observational estimates of the cosmic H I mass density at different redshifts. Here we express $\Omega_{\rm HI}$ as the mean H I mass density $\rho_{\rm HI}$ normalised by the critical density $\rho_{\rm cr}(0)$ at z=0.

At z=0, we find that the Baugh et al. model predicts a cosmic H I mass density which is in good agreement with the HIPASS estimate obtained by Zwaan et al. (2003). In contrast, the Bower et al. model overpredicts the cosmic H I mass density by a factor of $\sim$2. This difference arises because the Baugh et al. model was constrained to match both the z=0 B-band luminosity function and the observed gas fraction versus luminosity relation for late-type galaxies. Bower et al. attached less weight to reproducing the gas content of local spirals when setting the parameters of their model. The gas fraction in this model are somewhat higher than observed and so as a result, the Bower et al. model tends to overpredict local global density of cold gas.

At $z > 0$, we find that the Baugh et al. model predicts a cosmic H I mass density that increases by a factor of ~ 3 between $0 \lesssim z \lesssim 2$ before rolling over and assuming a roughly constant value of $\sim 10^{-3}$ at $z \gtrsim 2$. The bump at $z \simeq 6$ reflects the treatment of the effect of photoionisation – $z < 6$, cooling is suppressed in haloes with virial circular velocities $V_c < 60$ kms^{-1}. When compared to the observational data of Peroux et al. (2003) (taken from their estimates of $\Omega_{\rm DLA}$ divided by the mean molecular mass μ), we find that the Baugh et al. model predicts a cosmic H I mass density that is systematically higher – by $\sim 60\%$ – than is inferred from observations. In contrast, the Bower et al. model predicts a cosmic H I mass density that is in reasonable agreement with the observational data; it is roughly constant between $0 \lesssim z \lesssim 2$ before declining rapidly[1] at $z \gtrsim 2$.

[1]Note that the Bower et al. (2006) predictions are based on Millennium Simulation

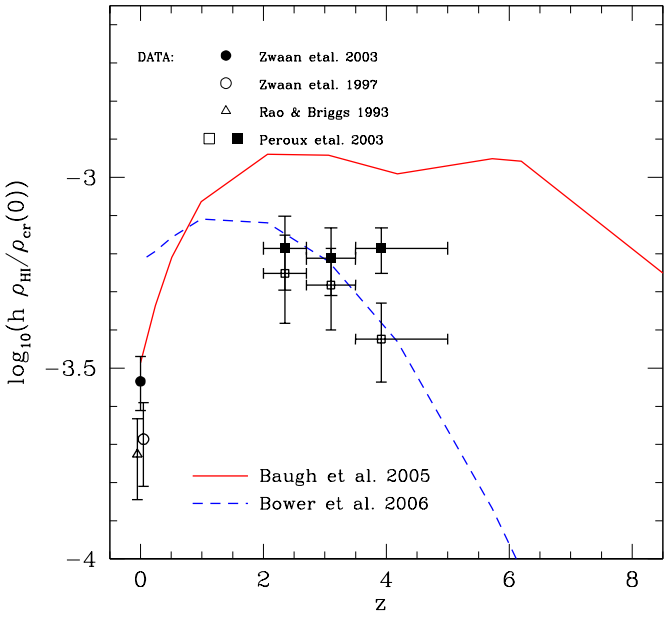

Figure 2.3: Redshift evolution of the mass density of H I (expressed in units of the present day critical density). Predictions based on the Baugh et al. (2005) "top-heavy IMF" and Bower et al. (2006) "AGN-heating" models are shown by solid and dashed lines respectively. We show also recent observational estimates of the H I density at the present day (Rao & Briggs 1993, Zwaan et al. 1997, 2003) and at higher redshifts (Peroux et al. 2003).

The ability of MIRANdA to accurately probe redshifts out to ∼0.8 will fill a significant gap (around 7 Gyr) in our understanding of H I evolution and allow for more refined models to be developed.

merger trees (Springel et al. 2005), and the mass resolution of the simulation is such that the cold gas mass fraction is underestimated at high redshifts.

2.4 Environmental influence on the H I content of Galaxies

Environment plays an important part in the evolution of galaxies. The observation of Butcher & Oemler (1978) that high redshift clusters contain a much higher percentage of spiral galaxies than present day clusters indicates the evolution and transformation of spirals in the highest density regions of the Universe. Further evidence is seen in the star formation rates of galaxies in clusters which are much lower than those galaxies of similar morphology in the field (e.g. Lewis et al. 2002). One outstanding question is whether spiral galaxies are somehow transformed into the present-day lenticular, or S0, galaxies. The mechanism for such a transformation is still not clear: stripping, interactions, and the cessation of star formation leading to the fading of a spiral disk have all been proposed.

H I observations of galaxies in different environments provide an insight into their evolution. One of the main mechanisms of affecting a galaxy's evolution is by stripping the cold H I gas, and thus removing the fuel for future star formation. The effects of gas stripping and tidal interactions are readily observed in the H I content and distribution of galaxies. The H I distribution in late-type galaxies typically extends further than the detectable optical emission, and thus is subject to gravitational forces of any nearby galaxies and group or cluster potentials, before we notice the effects in optical imaging. In addition, stripping processes that are prominent in massive clusters and groups with a hot intra-group medium, affect mainly the gas in galaxies. Detailed observations of interacting galaxies can show large tidal-tails, easily visible in the H I gas, sometimes before the optical observations show any sign of distortion (e.g. Yun et al. 1994). Galaxies in clusters typically contain less H I, or are 'H I deficient' when compared to optically similar galaxies in a low-density environment, suggesting that galaxies are somehow stripped of H I as they enter a dense environment (e.g. Solanes et al. 2001). Because of its wide field of view and ability to simultaneously image huge numbers of objects in a range of physical environments, MIRANdA will be excellent for investigating the effect of environment on the evolution of galaxies.

There are a number of mechanisms that can strip H I gas from galaxies. In dense clusters where there is a hot intra-cluster medium and high velocity dispersions, galaxies can be stripped of their H I via ram pressure stripping (e.g. Gunn & Gott 1972). Observational evidence of ram pressure stripping is seen in H I observations of spiral galaxies in the Virgo cluster (e.g. Kenney

et al. 2004). Harassment and starvation are two other methods for galaxies to lose their gas. Harassment involves a high-speed encounter between two galaxies or a galaxy and the cluster potential, resulting in a loss of gas (Moore et al. 1996). Starvation involves the gas being slowly removed, perhaps due to a hot ICM – the effect is to stop star formation, as the supply of cold gas is thwarted (e.g. Treu et al. 2003). These three mechanisms are most effective in clusters, where there is a massive potential, and extended hot inter-galaxy gas. The other mechanism for galaxy transformation and gas removal is galaxy-galaxy interactions and mergers, a process which is most effective in the group environment.

The group environment is becoming increasingly recognised as one of the most important environments for processing, or changing the evolutionary path, of galaxies. For example, the star formation rate of galaxies begins to drop at the typical group densities (Gomez et al. 2003; Lewis et al. 2002). Over 70% of galaxies live in the group environment (Tully 1987), compared with less than 5% of galaxies that live in clusters (Dressler 1984). Groups have lower velocity dispersions than clusters, providing an ideal environment for interactions and mergers to take place (Mulchaey & Zabludoff 1998). Preliminary results suggest that some galaxies that are members of loose groups may also be H I deficient (e.g. Kilborn et al. 2005; Omar & Dwarakanath 2005; Chamaraux & Masnou 2004), however the group environment is understudied compared to the cluster environment, so the extent of this effect is yet unknown.

As the H I content of galaxies changes with environment, so does the H I mass function.The H I mass function is an essential ingredient in galaxy formation and evolution models, and determinations of the H I mass function provide a test for semi-analytical models. The H I mass function of galaxies at low redshift is known to good precision, thanks to HIPASS (Zwaan et al. 2003). However, how the HI mass function changes with environment is less certain – Springob et al. (2005) found that the low-mass slope became shallower in denser environments, whereas Zwaan et al. (2005) found that it steepens in denser environments.

MIRANdA will allow for the first in-depth and homogeneous investigation of the HI content of galaxies with environment. While the cluster environment has been surveyed extensively in H I, the group environment, where most galaxies reside, remains largely unexplored. The sensitivity of previous H I surveys has been limited an H I mass of about 10^8 – 10^9 $M_\odot$, and for limited numbers of groups, so that effects such as ram pressure stripping in groups, and H I deficiency have not been quantified. The increased sensitivity of MIRANdA over previous studies will allow the determination

of the HI mass function down to much lower masses, and for greater number statistics when investigating the change in the H I mass function with environment. With a spatial resolution of $30''$, MIRANdA will enable the closest galaxies to be automatically mapped – thus we will determine the H I morphology, and thus how the environment is affecting the galaxy, for a large, homogeneous number of nearby galaxies. Combining this data with optical, IR and continuum observations will allow for the first time, a full picture of galaxy evolution in the local Universe.

2.5 Imaging the low redshift Cosmic Web

Extragalactic astronomy has traditionally focused on the regions of extreme cosmic overdensity that we know as galaxies. Only in recent years has the realization emerged that galaxies do not dominate the universal baryon budget but are merely the brightest pearls of an underlying Cosmic Web. Filamentary components extending between the massive galaxies are a conspicuous prediction of high resolution numerical models of structure formation (e.g. Davé et al. 1999, 2001). Such calculations suggest that in the current epoch, cosmic baryons are almost equally distributed by mass amongst three components: (1) galactic concentrations, (2) a warm-hot intergalactic medium (WHIM) and (3) a diffuse intergalactic medium. These three components are each coupled to a decreasing range of baryonic density, namely $\rho_H/\bar{\rho_H} > 10^{3.5}$, 10 – $10^{3.5}$, and < 10, and are correspondingly probed by QSO absorption lines with specific ranges of neutral column density: $N_{HI} > 10^{18}$, 10^{14} – 10^{18}, and $< 10^{14}$ cm^{-2}, as shown in Figure 2.4. The neutral fraction is thought to decrease with decreasing column density from about 1% at $\log(N_{HI}) = 17$, to less than 0.1% at $\log(N_{HI}) = 13$. Although a very wide range of physical conditions can be found within galaxies, the WHIM is thought to be a condensed shock-heated phase of galaxy interaction debris with temperature in the range 10^5 – 10^7 K, while the diffuse IGM is predominantly photo-ionized with temperature near 10^4 K. A complicating factor to this simple picture is the growing suspicion that the gas accretion process, traced by the $\log(N_{HI}) = 14$ – 18 systems, may well occur in two rather different regimes (e.g. Binney 2004, Keres et al. 2005). Low to moderate mass galaxies ($M_{Vir} < 10^{12}$ $M_\odot$) may experience primarily "cold-mode" accretion ($T \sim 10^{4.5}$ K) along filaments, while only more massive systems may be dominated by the more isotropic "hot-mode" accretion ($T \sim 10^{5.5}$ K), which until recently was thought to be universal (e.g. Rees & Ostriker 1977, Davé et al. 2001).

The strongest observational constraints on the Cosmic Web come from the statistics of the QSO absorption lines. Enough of such QSO spectra have been obtained to allow good statistical determinations to be made of the rate of occurrence of intervening absorbers as function of their column density. By binning such data in redshift intervals, it has even been possible to gauge

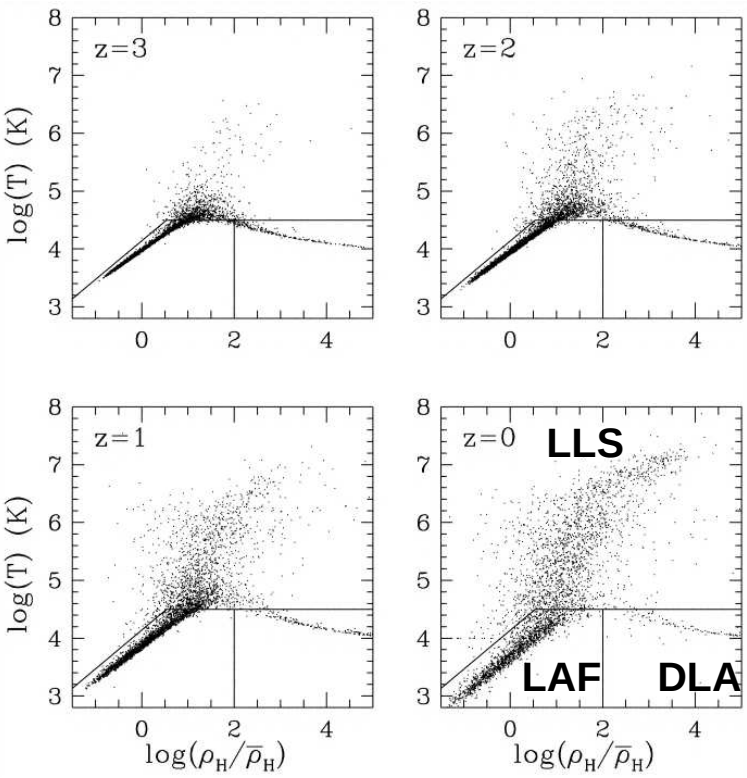

Figure 2.4: The redshift evolution of overdense regions in a numerical simulation showing the increasing mass fraction with time of gas in the range log(T) = 4.5 – 7, the so-called WHIM (from Dave et al. 1999). Also shown are the regimes of Damped Lyα, Lyman Limit system and Lyα forest absorber systems.

the cosmic evolution of intervening absorbers (e.g. Storrie-Lombardi 2000). Inter-galactic space has apparently become continuously tidier by about an order of magnitude from redshifts of several down to zero; with a decreasing cross-section of high column absorbers. At the current epoch we can now confidently predict that in going down from H I column densities of 10^{19} cm^{-2} (which define the current "edges" of well-studied nearby galaxies in

H I emission) to 10^{17} cm^{-2}, the surface area will increase by a factor of 30. The critical observational challenge is crossing the "H I desert", the range of log(N_{HI}) from about 19.5 down to 18, over which photo-ionization by the intergalactic radiation field produces an exponential decline in the neutral fraction from essentially unity down to a few percent (e.g. Dove & Shull 1994). Nature is kinder again to the H I observer below log(N_{HI}) = 18, where the neutral fraction decreases only very slowly with log(N_{HI}). The baryonic mass traced by this gas (with a 1% or less neutral fraction) is expected to be comparable to that within the galaxies, as noted above.

How are these diffuse systems distributed, what are their kinematics and under what conditions do "cold-mode" or "hot-mode" accretion dominate? These are questions which can not be addressed with the QSO absorption line data. The areal density of suitable background sources is far too low to allow "imaging" of the intervening low column density systems in absorption. Direct detection of the free-free continuum or recombination line emission from the ionized gas has also proven well beyond the capabilities of current X-ray and optical instrumentation. For example the expected Hα emission measure is only $\sim 5\times10^{-4}$ cm^{-6}pc. The very best current Hα imaging results reach down to emission measures of $\sim$0.1 cm^{-6}pc, which is still orders of magnitude removed from what would be needed.

Although conventional imaging in H I has not typically reached column densities below about 10^{19} cm^{-2}, this is not a fundamental limitation. Long integrations with an (almost-) filled aperture can achieve the required brightness sensitivity to permit direct imaging of the small neutral fraction within the Cosmic Web filaments between galaxies. The first detection of such diffuse filaments in the extended environment of M31 has just been made by Braun & Thilker (2004). This was accomplished by utilizing total power measurements made with the fourteen 25 m dishes of the WSRT. Although the angular resolution is low ($49'$ corresponding to 11 kpc at the M31 distance) the column density sensitivity is very high (rms of 4×10^{16} cm^{-2} over 17 kms^{-1}). A diffuse filament is detected connecting the systemic velocities of M31 to M33 (at a projected separation of 200 kpc) and also extending away from M31 in the anti-M33 direction as shown in Figure 2.5. This diffuse filament appears to be fueling denser gaseous streams and filaments in the outskirts of both galaxies. Peak neutral column densities within the filament only amount to some 3×10^{17} cm^{-2}.

The interaction zone of the diffuse filament with M31 has been studied in complementary surveys that permit calculation of the H I distribution function from H I emission measurements (rather than QSO absorption measurements) over an unprecedented range in log(N_{HI}) = 17.2 to log(N_{HI}) =

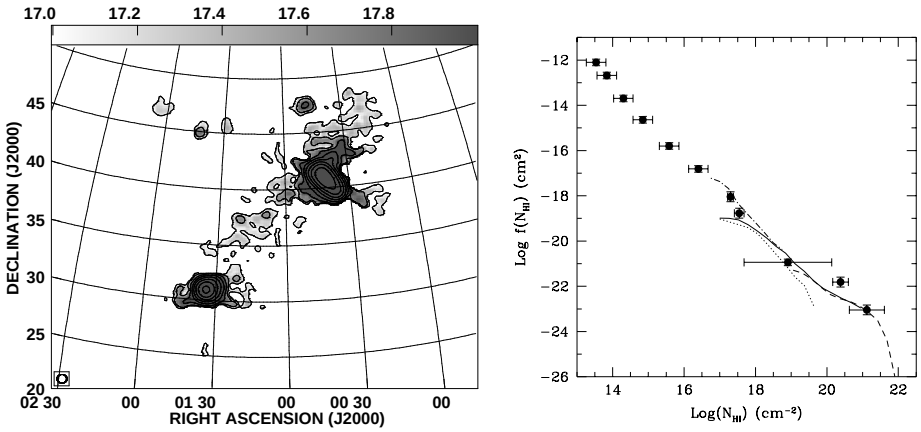

Figure 2.5: A Cosmic Web filament (left) of H I gas connecting the nearby galaxies M31 and M33 together with the corresponding H I distribution function (right) from Braun & Thilker (2004). The curves are the H I data, while the filled points represent QSO optical absorption line data. With sensitive H I observations the Lyman Limit absorption systems can be directly imaged in emission, despite their small neutral fraction, permitting direct study of the WHIM and its large reservoir of baryons.

21.9 as shown in Figure 2.5. The H I distribution function of these structures agrees very well with that of the low redshift QSO absorption lines which are also plotted in the figure as filled circles with error bars. The predicted factor of 30 increase in surface covering factor for low N_{HI} emission has been observationally verified. In so doing, it has been possible to provide the first image of a Lyman Limit absorption system. The morphology and kinematics are fully in keeping with the Cosmic Web hypothesis outlined above. We are now in a position to witness the continuing gaseous fuelling of normal galaxies with direct imaging. This gas represents the most effective tracer of the last 5 Gyr or so of galaxy interaction history. In combination with optical/UV absorption line observations of the ionization state and metallicity it then becomes possible to quantify the mass budget and enrichment history of this major baryon reservoir.

Efforts are now underway to extend the study of Lyman Limit Systems in HI emission beyond the Local Group. The deepest practical survey at this time (involving more than 1000 hours of observing time with the WSRT) will reach an rms of 2×10^{17} cm^{-2} over 20 kms^{-1} within a $35'\times3'$ beam. This should permit the environments of several hundred galaxies to be probed to

these depths for the first time. Some of the brightest Cosmic Web filaments can then be studied, when they fortuitously align with the elongated beam.

Similar surveys with an ultracompact MIRANdA configuration will be truly ground-breaking. For example, squeezing the nominal performance 30 antennas into a 200 m configuration provides a circular $5'$ beam, corresponding to better than 20 kpc physical resolution out to distances of 14 Mpc, with an rms sensitivity of $2{\times}10^{17}$ cm^{-2} over 20 kms^{-1} in a 12 hour integration over the entire 30 deg^2 FoV. A single 12 hour integration will thus be sufficient to detect the brightest knots within Cosmic Web filaments between major galaxies. Longer integrations, of 144 hours, will reach $5{\times}10^{16}$ cm^{-2} at this resolution, permitting routine detection of Lyman Limit System filaments throughout the Local Volume.

If higher sensitivity were available, for example with 45 antennas with 1.4 times better noise performance (35 rather than 50 K), then it would be possible to push Cosmic Web detection out to substantially larger distances. It would still be necessary to utilize an ultra-compact configuration, of say 300 m diameter, yielding a $3.5'$ beam, but this would probe the same low column densities noted above out to an effective distance of at least 20 Mpc, corresponding to a three times larger volume than accessible with the nominal MIRANdA specifications.

2.6 The Local Volume

The 'Local Volume' (the sphere of radius ∼10 Mpc centered on the Local Group) includes at least 500 known galaxies, many of which congregate in well-known groups like the Local Group, the relatively loose Sculptor Group and the more compact Centaurus A group. The fact that accurate distances (e.g. from TRGB measurements obtained with the HST) can now be obtained quite easily for the majority of these galaxies makes this volume and its research so special and timely. The combination of accurate galaxy positions, radial velocities and independent distances allows us to create a dynamic 3D view of the Local Universe. This in turn leads to a detailed understanding of the local flow field, ie. the Hubble flow and its dispersion. It also leads to a better understanding of the overall matter (dark and visible) distribution in and between galaxies as well as an accurate H I mass function at the low-mass end.

MIRANdA will enormously contribute to our understanding of the Local Volume by revealing all gas-rich galaxies in the surveyed sky down to an H I mass of $\sim 10^6$ M$_\odot$, vastly surpassing HIPASS in sensitivity and both angular

and velocity resolution. At the fringes of the Local Group, the sensitivity limit will be $\sim 10^4$ $M_\odot$. Thus, significant numbers of low-mass galaxies such as the recently discovered transition dwarf, Leo T (Irwin et al. 2007) will be found by MIRANdA.

2.7 Cosmology with MIRANdA

2.7.1 Galaxy Clustering

The clustering of galaxies encodes a wealth of cosmological and astrophysical information. In particular, the patterns of clustering reflect the manner in which a particular class of galaxies populates the underlying network of dark matter haloes, hence tracing its formation and evolution history. For example, it is well-known that optically-selected red galaxies possess a higher clustering amplitude or "bias" than blue galaxies. This reflects the tendency of red galaxies to reside in denser environments, or more massive dark matter haloes, which in turn reflects upon their formation mechanism. Furthermore, clustering strength also increases with optical luminosity.

These arguments have recently been quantified in the halo model for galaxy clustering. This model assumes that the mass function, clustering and radial profiles of the underlying dark matter haloes can be established accurately from N-body simulations. The clustering of the galaxies on top of these haloes is then described by the halo occupation distribution, $N(M)$, which specifies the average number N of galaxies residing in a halo of mass M. This function is parameterized in a simple way, and fit to the observations. The successful performance of this analysis depends on detecting deviations from a power-law in the clustering correlation function, which is only possible for large galaxy surveys such as the 2-degree Field Galaxy Redshift Survey (2dFGRS) and Sloan Digital Sky Survey.

First measurements of the clustering of H I-emission galaxies have been performed using the HIPASS survey (Ryan-Weber 2006, Meyer et al. 2007, Basilakos et al. 2007). The result (from a simple power-law fit) is that H I-selected galaxies possess a very low clustering bias. This is expected because H I galaxies appear to live in under-dense environments, given that as these galaxies enter the denser cluster environment, the gas is exhausted via star formation or stripped.

MIRANdA can perform an H I galaxy redshift survey on the scale of the 2dFGRS. This will yield extremely accurate measurements of the clustering pattern as a function of galaxy mass and environment, which will form a key part of MIRANdA's central portfolio of observations. The characteristic

"halo-model" deviation from a power-law clustering correlation function will be detected, enabling the dark matter halo occupation distribution to be inferred. These clustering measurements will reflect on where H I galaxies form, and how the gas is stripped or exhausted in the vicinity of dense environments. Various processes can remove H I from galaxies: gravitational tidal effects, ram pressure stripping, or strangulations. The cross-correlation of the H I galaxies with the distributions of clusters, groups and filaments will discriminate between these processes via the scales and densities at which they operate. The imprint of the redshift-space distortions will also be a key measurement, indicating how H I galaxies coherently flow into overdense regions. The work can be extended to higher redshifts ($z \approx 0.6$) through deeper MIRANdA pointings.

2.7.2 An SKA cosmology demonstrator

Future radio telescopes, culminating in the SKA, can potentially become the world's leading facilities for performing cosmological surveys. These advances are based on simple considerations of survey speed, which scales as $A^2\Omega$ for radio telescopes, where A is collecting area and Ω is field-of-view, as opposed to $A\Omega$ for optical telescopes. The scaling with A^2 ensures that the SKA (which provides a 2 order of magnitude increase in collecting area compared to existing radio telescopes) can detect H I emission-line galaxies to redshift $z \sim 3$ in just a few hours exposure. Such a redshift survey can be performed simultaneously with a deep continuum imaging survey, owing to the large telescope bandwidth. Furthermore, the goal for the SKA is a field-of-view $\Omega = 200$ deg^2 at 0.7 GHz, exceeding what is possible for an optical telescope by at least an order-of-magnitude.

Simple telescope and H I mass function models demonstrate that the SKA can achieve an all-sky H I emission-line galaxy redshift survey containing $\sim 10^9$ galaxies to a 5σ H I mass limit $\sim 5\times10^9 M_\odot$ out to redshift $z \sim 1.5$. Such a survey would map a cosmic volume exceeding what is possible today by a factor of 100. The dataset will allow transformational cosmological measurements, which form one of the Key Science Goals for the SKA. The patterns of galaxy clustering through this volume encode the properties of dark energy and dark matter haloes, the masses of neutrino species, and the physics of inflation. Baryon oscillations in the galaxy distribution can be used as a standard ruler to map out the cosmic expansion history.

MIRANdA has insufficient collecting area to perform any of this cosmological science. However, it can pave the way for these future SKA surveys by resolving key issues of survey design and analysis.

First, MIRANdA can measure the H I mass function with unprecedented accuracy, including how this function varies with redshift (to $z \approx 0.8$) and environment. The SKA project is entering a crucial phase of "system design" scheduled for the period 2008 – 2010. An essential question to be addressed is what combination of collecting area, angular resolution and bandwidth is required for performance of the key science projects. Unfortunately, current radio observations provide very weak guidance for these design studies, because almost nothing is known about the distribution of neutral hydrogen beyond the very local Universe. MIRANdA will provide a very significant step forward in this respect.

Secondly, MIRANdA can precisely measure the clustering properties of H I galaxies, which encode the main sources of systematic error for future baryon oscillation surveys with the SKA. Future cosmological measurements will be limited by systematic errors rather than statistical errors – quantifying and controlling these systematic errors is crucial for extracting robust cosmological conclusions. The leading sources of systematic error for baryon oscillation surveys are the poorly-modelled effects of redshift-space distortions, halo bias and the non-linear growth of structure. These processes all modify the underlying linear power spectrum which encodes the baryon oscillation signature, hampering our cosmological measurements. They can generically be described as "scale-dependent galaxy bias". MIRANdA can measure this function, including the "halo occupation distribution" of these galaxies with respect to the underlying dark matter fluctuations.

Chapter 3

Continuum Science

3.1 Summary

Understanding the formation and evolution of galaxies and active galactic nuclei (AGN) as a function of cosmic time is one of the most intensely investigated issues in contemporary astronomy, and is a key science driver for next-generation telescopes such as SKA, ALMA and ELTs. Today's instruments already give profound insights into the galaxy population at high redshifts, and a number of current surveys (e.g. ATLAS, ELAIS, GOODS, COSMOS) are asking questions such as: When did most stars form? How do AGN influence star formation? What is the spatial distribution of evolved galaxies, starbursts, and AGN at $0.5 < z < 3$? Are massive black holes a cause or a consequence of galaxy formation?

However, most of these surveys are primarily at optical and IR wavelengths, and can be significantly misled by dust extinction. Radio observations not only overcome dust extinction, but also provide data on AGN that are unavailable at other wavelengths. MIRANdA will be able to determine how galaxies formed and evolved through cosmic time, by penetrating the heavy dust extinction which is found in AGN at all redshifts, and studying the star formation activity and AGN buried within.

3.1.1 A deep southern sky survey

MIRANdA has the potential to have the enormous impact that the NRAO VLA Sky Survey (NVSS; Condon et al. 1998) had a decade ago, but at a factor of 50 better in sensitivity and 9 in angular resolution. This is particularly significant because of the growth in the number of ground-based telescopes (ALMA, VLT, Gemini, etc) that will operate in the southern

hemisphere. MIRANdA will survey the entire southern sky to a limit currently being reached only in tiny parts of the sky (e.g. in the HDF-N and HDF-S deep fields). To overcome instrumental confusion, these sensitivities can only be achieved with high angular resolution ($5''$ at 1400 MHz), which requires baselines to $\sim$8 km.

The instrumental continuum confusion limit at 1400 MHz with $5''$ angular resolution is $\sigma = 10\,\mu$Jy beam^{-1}. Assuming the strawman parameters, the southern sky can be surveyed to this confusion limit in a year. This is an amazing feat, and the following sections will describe a pick of the science programs that could be done with such a fast survey telescope. The $(T/N)^2$ dependence on both the point source and surface brightness sensitivity means that the extra dishes (N) and lower system temperatures (T) being proposed in the upgraded parameters would enable this confusion-limited southern sky survey in 1/5 of the time, or only 2 months. To this end, we also include a few more ambitious science programs in this chapter that require the faster survey speeds offered by the upgraded MIRANdA to make the project feasible.

It is worth emphasising that at $5''$ resolution, incompleteness becomes significant as emission extended on scales larger than $5''$ is resolved (see the discussion regarding the choice of angular resolution for the NVSS in Condon et al. 1998). This is a double-edged sword: higher angular resolution leads to a lower confusion limit (allowing a higher-sensitivity survey), but at the expense of completeness. However, this issue is likely to be less of a problem for the proposed MIRANdA survey than for NVSS for two reasons. First, at the extremely faint flux densities of the proposed MIRANdA survey, the source counts are dominated by distant star-forming galaxies with $\sim 1''$ angular sizes (see section 3.2 below), rather than the larger and more powerful radio galaxies which dominate the source counts in NVSS. Second, a continuum all-sky survey with short baselines will be available as a by-product of the proposed H I sky survey. While this compact continuum survey will be confusion-limited, the data can be sensibly combined with the longer-baseline $5''$ resolution southern sky survey to create a complete *and* confusion-limited high-resolution sky survey.

3.2 Star forming galaxies across the universe

With a flux density limit of $5\sigma = 50\,\mu$Jy beam^{-1}, typical starburst galaxies, with star formation rates (SFRs) around 100 $M_\odot$yr^{-1}, will be detectable to $z \approx 2$. The most extreme starbursts, with SFRs of a few 1000 $M_\odot$yr^{-1}, will

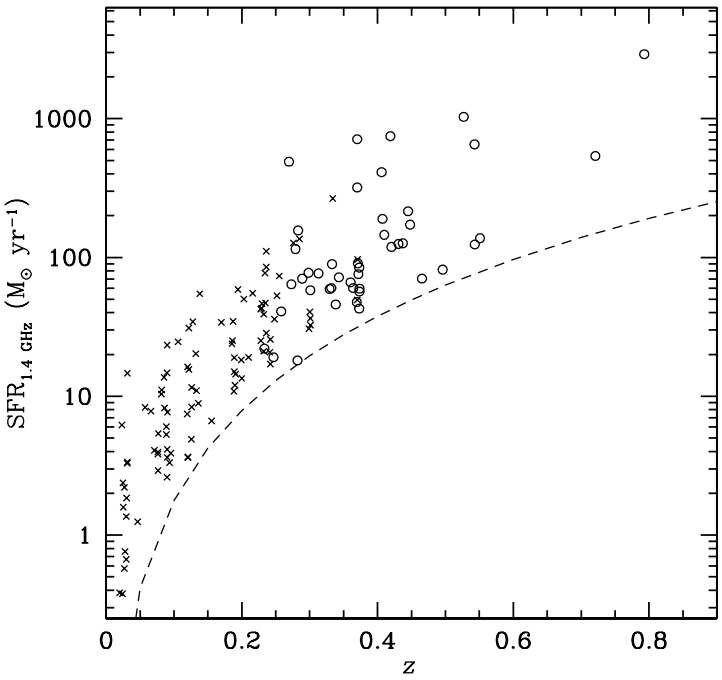

Figure 3.1: SFRs for star-forming galaxies in the Phoenix Deep Survey, as estimated from their radio luminosity. The dashed line indicates the 60 μJy detection limit of the radio observations. Figure reproduced from Afonso et al. (2003).

be visible well into the epoch of reionisation ($z \approx 6 - 10$) if indeed they exist then. Ordinary disk galaxies like the Milky Way, with SFRs of only a few $M_{\odot}yr^{-1}$, will be visible to $z \approx 0.3$ (see Figure 3.1). A confusion limited sky survey utilising the 8 km baseline configuration, obtained in addition to an ultra-compact H I survey, will make the star forming galaxy population accessible as never before. It will allow unprecedented exploration into how star formation in galaxies evolves with time, and how it depends on galaxy mass, galaxy environment, past star formation history, interaction/merger history, and more.

One of the most intriguing recent results in galaxy evolution is the mass dependence of galaxy star formation histories (Feulner et al. 2005; Juneau

Table 3.1: Predicted numbers of sources per square degree at 1400 MHz with a 10 μJy flux density limit, assuming standard cosmology. Table adapted from table 7 of Jackson (2005).

Redshift	N(FRI)	N(FRII)	N(SF)
z < 1	718	2	2556
z < 3	1145	21	6740
z < 5	1190	42	7584
z > 5	17	13	0

et al. 2005; Papovich et al. 2006). Evidence is growing that points towards a picture where massive galaxies form their stars early and quickly, and "turn off" at redshifts around $z \approx 2 - 3$, while progressively lower mass galaxies start to dominate the cosmic star formation history at progressively lower redshifts. This evidence comes not only from the mass-dependence but also from the impact of a galaxy's environment on its star formation rate (Lewis et al. 2002; Gomez et al. 2003), and its observed evolution (Poggianti et al. 2006). A recent measurement by Zheng et al. (2007) questions this picture, though, suggesting instead that the cosmic star formation history declines uniformly in galaxies of all masses at redshifts less than unity.

Resolving this question is fundamental for identifying how galaxies form and evolve through their star formation histories, the impact of their mass and their local environment, and the consequences on the resulting stellar populations and galaxy morphologies observed. This is only achievable with the large samples of strongly star forming galaxies made accessible by deep continuum surveys over large areas such as those planned for MIRANdA. The limiting factor affecting these studies will clearly be the resolution of MIRANdA. Apparent galaxy sizes at radio wavelengths steadily decrease with decreasing flux density (Windhorst 2003). This primarily reflects the intrinsically smaller sizes of high redshift galaxies in a hierarchically evolving universe. The median angular size at 1 mJy is about $2''$, and at 100 μJy is about $1''$. By 10 μJy the median angular size has dropped to about $0.4''$ (Windhorst et al. 1999; Windhorst 2003) With the proposed $5''$ resolution of MIRANdA, instrumental confusion will clearly be the limiting factor governing the sensitivity of continuum surveys, and this will remain the case until baselines spanning several tens up to hundreds of kilometres can be incorporated in the SKA. To mitigate the resolution limitations, it is highly desirable to match the proposed MIRANdA surveys with complementary

deep optical/near-infrared surveys, having much finer angular resolution. The southern sky surveys of SkyMapper (Keller et al. 2007) will be of vital importance here in the first instance.

3.3 The star formation / AGN fraction

Another important factor to consider is distinguishing the star forming population from the AGN population. Below 1 mJy starburst galaxies start to become a major component of the 1.4 GHz source counts, dominating below 0.5 mJy or so (Hopkins et al. 2000; Jackson 2005). Recent measurements, though, suggest that there may still be a significant proportion of low-luminosity AGN (Simpson et al. 2006) even at these levels. By 0.1 mJy existing AGN evolutionary models imply that starburst galaxies should be dominant, although normal star forming galaxies are not expected to dominate the counts until levels below $\approx 1\,\mu$Jy are reached (Windhorst et al. 1999; Hopkins et al. 2000).

Traditionally separate fields of astrophysical research, it is now becoming clear that AGN and star formation activity are intimately related. The question is how does galaxy formation influence the growth of the central black hole, or vice-versa? Many galaxy formation models now invoke feedback by supernovae, starbursts or AGN, while many others are now emphasising the importance of feedback due to powerful radio jets, which either push back and heat the infalling gas, reducing or even stopping the cooling flows building up the galaxy or shock heat and collapse the gas clouds and induce star-formation. There is no doubt that some feedback (positive or negative) between the AGN and the growth of the host galaxy is occuring, but it is hotly debated as to the nature of the feedback. A detailed study of the AGN and star formation activity in high redshift galaxies will help answer some questions. The sheer number of sources down to faint flux density limits that will be found with MIRANdA will go a long way in this regard. Optical and near-IR SEDs would allow us to identify starforming galaxies in the samples (as too would a comparison of the radio source flux density with the infra-red flux density and exploiting the radio-FIR correlation for star forming galaxies; see section 3.7) and a wide-field VLBI program between MIRANdA and telescopes on the east coast such as the Parkes 64 m, which will allow us to determine the fraction of radio emission in galaxies associated with a central, compact object (AGN). We already know that AGN with starforming host galaxies exist (see Figure 3.2), the question is how significant is this class of objects with respect to the overall population

of radio sources across cosmic time?

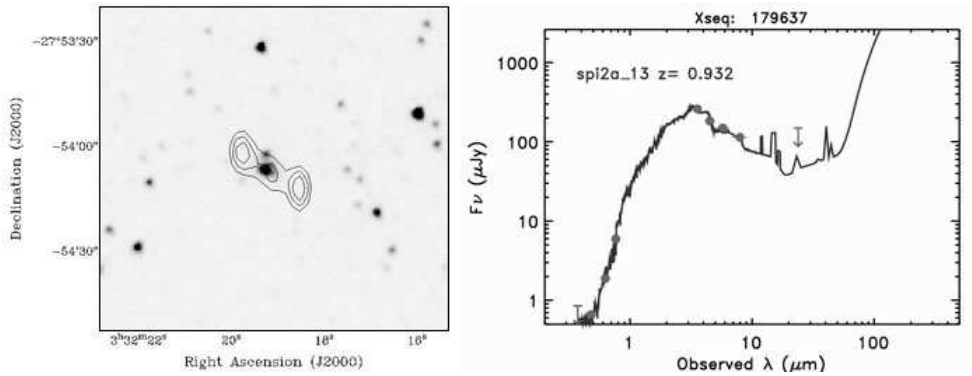

Figure 3.2: The composite source S425. The left image shows radio contours superimposed on a 3.6 μm SWIRE image, and the right image shows the SED. This source has the radio morphology of an AGN, but the SED of a star-forming galaxy.

3.4 Radio Galaxy evolution across cosmic time

There is an inevitable degeneracy between luminosity and redshift inherent in flux limited samples of classical (active) radio galaxies. This arises because only the most powerful sources are detected at the largest redshifts. In order to explore the physics of radio galaxies, and especially their evolution, large samples of radio galaxies of comparable luminosity across cosmic time are required. Most attempts to investigate changes in radio galaxy properties as a function of redshift have failed however because they are unable to properly separate luminosity-dependent effects from true cosmological evolution.

With the relatively slow survey speeds of existing radio telescopes, this degeneracy has in the past been broken by combining samples of radio sources selected at similar observing frequencies, but with different flux density limits (Blundell et al. 1999). However, we are still unable to say much about the global population of radio galaxies at redshifts above about 0.5 because our faint source counts are so limited. With current radio sky surveys we are simply unable to reach the luminosities required to find, if they exist, FRI radio galaxies at cosmologically significant distances. An FRI radio galaxy with a typical luminosity at 1400 MHz of 10^{24} W Hz^{-1} sr^{-1} (Figure 3.1) has an observed flux density of 2 mJy at $z = 1$ and 50 μJy

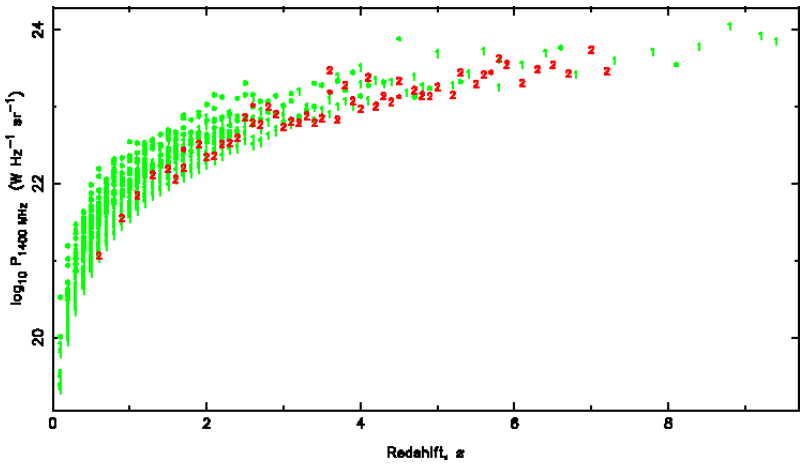

Figure 3.3: Power–redshift distribution, P–z, for FRI and FRII sources at 1400 MHz for a flux density limit of 10 μJy from Jackson (2005). Key: FRI radio galaxies (1), FRII radio galaxies (2), beamed sources (*).

at $z = 5$ for sources with a radio spectral index of -0.8. These low flux densities demonstrate why this experiment has not been possible in the past and why deep, large-FOV radio continuum surveys are essential if we are to understand active radio galaxy evolution in any detail. FRI type sources make up the vast majority of local radio sources and yet we know very little about their existence at higher redshifts; high redshift FRIs may even contribute up to 2/3 of the total source counts at sub-mJy levels (Padovani et al. 2007).

MIRANdA will detect radio sources down to $5\sigma = 50\,\mu$ Jy beam^{-1} with a dynamic range of 10^5 and essentially fill the luminosity-redshift plane (see Figure 3.3); assuming, of course, we obtain redshifts for the sources in the sample. The results of the proposed MIRANdA confusion limited survey contribute a wealth of knowledge in this field of research; a field which has stalled, waiting for the advent of big survey telescopes. Precise definition of the luminosity functions of FRI and FRII radio sources as a function of redshift is essential for us to understand the formation and evolution of active radio galaxies. This science should not be underestimated: radio galaxies represent the most massive galaxies at any redshift up to $z = 5.2$ and therefore represent our best chance to understand the formation and evolution of massive galaxies and their central supermassive black holes. In addition, they are likely also to provide the dominant source of energy in the

universe, and possibly even provide the dominant source of magnetic fields.

3.4.1 Searches for the highest redshift radio galaxies

Statistically large samples of high-redshift radio galaxies (HzRGs) are slowly being accumulated, with more than 30 known to date above $z = 3$. These samples are assembled by data mining existing radio sky surveys, and selecting sources with unusually steep radio spectral indices, taking advantage of the correlation between increasing redshift and steepening radio spectral index[1]. The need to data-mine large area radio sky surveys to define sufficiently large steep spectrum samples for optical follow-up is obvious: HzRGs are extremely rare. Between $3 < z < 4$, the minimum space density of powerful ($> 10^{26}\,\mathrm{W\,Hz^{-1}\,sr^{-1}}$) radio galaxies is $1.2 \pm 0.6 \times 10^{-9}\ \mathrm{Mpc^{-3}}$ and their minimum surface density is $63 \pm 29\ \mathrm{sr^{-1}}$ (De Breuck et al. 2006). By virtue of the flux density limits of existing sky surveys (several mJy at 1.4 GHz), the HzRGs detected to date are all amongst the most powerful radio galaxies (FRII class) that we observe at lower redshifts. For example, the HzRGs selected (De Breuck et al. 2006) by cross-matching the 1400 MHz NVSS survey with the 843 MHz Sydney University Sky Survey (SUMSS; Mauch et al. 2003), have radio luminosities of order $10^{26-27}\ \mathrm{W\,Hz^{-1}\ sr^{-1}}$, thus probing just the tip of the iceberg. Cygnus A, the most powerful radio galaxy in the nearby universe ($z = 0.056$) has a 1400 MHz radio luminosity of $\sim 10^{27}\ \mathrm{W\,Hz^{-1}\ sr^{-1}}$. To date, little to nothing is known about the lower luminosity (e.g. FRI) population of sources at high redshift. This is a major shortfall with current studies of high redshift radio source populations.

Two surveys, done at widely separated frequencies down to the confusion limit would be a huge improvement on existing capabilities to find HzRGs using the steep-spectrum selection technique. The surveys could be done at, for example, 700 MHz and at 1800 MHz, but the 700 MHz confusion limit at $5''$ resolution is $\sim 500\,\mu$Jy/beam! Instead, surveys done at 1400 MHz and 2700 MHz would be far more valuable in terms of reaching FR I-class radio galaxies at high-redshift. This program would benefit hugely from the 1/5 survey speed offered by the upgraded MIRANdA parameters because the two southern sky-surveys will take only 4 months, instead of 2 years. Most importantly, MIRANdA will reach sensitivities a factor of 300 times fainter

[1] Although this technique increases the likelihood of finding radio galaxies at high redshift, it severely biases the resultant samples to only those with unusually steep spectral indices. As a result, we currently know very little any population of normal spectral index radio galaxies at high redshift

than existing steep spectrum samples [2], thereby sensitive to a lower luminosity radio galaxies. Another benefit of the MIRANdA steep spectrum sample over current samples is that a single telescope producing two sky surveys at different frequencies removes systematic errors inherent in cross-matching surveys made with different telescopes, sometimes with vastly different angular resolutions. The fast survey speeds offered by MIRANdA also reduces the number of spurious spectral indices caused by source variability on time scales of the two surveys. This could be further reduced by doing the two surveys in parallel, rather than contiguously.

Once the steep spectrum samples have been selected, optical (from SkyMapper) and then deep near-IR imaging would be required to identify the host galaxy. Spectroscopy on the faintest near-IR hosts would be required to secure their redshifts.

3.4.2 Why should we archive the calibrated visibility data?

To avoid confusion, this science program described above requires baselines out to 8 km (angular resolution of $5''$ at 1400 MHz). The spatial resolution offered with an 8 km baseline would not allow us to image the radio sources (most HzRGs have angular sizes $< 5''$) but if the visibility data were retained we would be able to measure source sizes to better than $1''$. There is a strong negative correlation between the linear size of the radio source and redshift, but presently we cannot say much more about this because we are constrained by Malmquist bias. MIRANdA will produce sufficient numbers of HzRGs at low enough radio luminosities that we will be able to explore this linear size-redshift correlation and separate out radio luminosity dependent effects from cosmological evolution. We can only do this, however, if we have the visibility data and can measure radio source sizes down to $1''$ or better for the high signal-to-noise sources.

3.4.3 Radio spectral energy distributions

The sample of HzRGs known to date (biased heavily by the steep spectrum selection technique) have radio spectral energy distributions (SEDs) very well characterised by single power laws (Klamer et al. 2006). This appears in stark contrast to the majority of known radio galaxies that have curved SEDs, steepening toward higher frequencies. However, aside from a handful of studies, very little is known about the global/statistical properties of radio

[2]The SUMSS-NVSS USS sample was selected with a 15mJy flux density limit imposed at 843 MHz

galaxy SEDs. MIRANdA can contribute enormously in this regard. One thing it will do very well is to produce uniform sky surveys at a number of frequencies across its available band, each with well-defined and uniform systematics, and accurate flux densities. This will allow an investigation into the shapes of radio SEDs as a function of various radio source parameters (linear size, redshift, luminosity, average spectral index). We would therefore advocate for as large a frequency coverage as possible for MIRANdA; but even 6 surveys each separated by 300 MHz in frequency between 700 and 2700 MHz, would open up an new region of radio source parameter space that we currently know little about.

3.5 Polarisation properties of galaxies

The confusion limited southern-sky survey will detect of order 500,000 polarised sources (Gaensler et al. 2004). The resultant catalogue of polarised sources will have two important applications. First, these data will allow us to produce a "$\log N - \log L$" distribution for polarization from extragalactic radio sources down to polarized fluxes as low as 50μJy beam^{-1}. Such a distribution has never been calculated at such levels (cf Mesa et al. 2002; Tucci et al. 2004), but will prove vital for providing an observational underpinning for the much deeper "rotation measure grid" that will be seen by the SKA (Gaensler et al. 2004). Secondly, there are hints at much higher flux levels that the fractional polarization gets larger for increasingly fainter radio sources (Mesa et al. 2002). This is not understood, but may be indicative of a slightly different population emerging at lower flux levels. The much deeper data-set to be obtained here will be able to resolve this issue.

3.6 A Low Surface Brightness Survey

3.6.1 Low surface brightness galaxies

The NVSS has a 5σ surface brightness sensitivity of 0.7 K (4.5 mJy arcmin^{-2} within the $45''$ synthesised beam). An ultra-compact MIRANdA survey will be sensitive to sources with up to 100 times lower surface brightnesses. This is unchartered territory: we really have no clue what sources we will find at these low surface brightness levels. In addition, whilst not quite as good as the continuous uv-coverage offered by the SKAMP survey, for example, a compact (baselines out to 1 km) MIRANdA survey will be far superior to the NVSS in terms of sensitivity to large scale structure: in the snapshot

mode which the NVSS was produced, the VLA is sensitive to largest angular sizes of 8 arcmin whereas the MIRANdA survey will be sensitive to largest angular scales of about 50 arcmin. A survey to find low surface brightness sources could be done as follows:
1. Complete a confusion limited survey to $\sigma_{rms} = 10\mu\mathrm{Jy\,beam}^{-1}$ with baselines out to 8 km. Proper source counts can then be made and a catalogue of sources on the sky will be derived. Ideally, this survey would only take 2 months by utilising the upgraded MIRANdA parameters.

2. Complete a second continuum survey in the HI-optimised compact configuration (which we assume to be 1 km; angular resolution $40''$) down to the same limit as above. This survey would be very confused but this does not matter at all for the science proposed.

3. The confusion-limited (8 km configuration) survey would then be smoothed to the resolution of the HI-optimised survey and subtracted, leaving only the sources which have surface brightnesses below the limit of the confusion-limited survey.

Sources whose emission is dominated by large scale structure will be left behind and we will, for the first time, be able to probe a parameter space that no past or existing radio sky survey has been able to probe. Dead radio galaxies? Diffuse cluster halos and relics? Diffuse halos containing the missing Dark Matter (see section 3.6.2)? Who knows what else lurks below the current sensitivities of today's surveys.

3.6.2 Thomson scattering off Dark Matter

A plausible repository for the 90% of missing baryons (dark matter) is in a diffuse intergalactic medium (IGM). Gunn & Peterson (1965) showed that any such IGM must be ionised. One way to test for its presence is to search for halos around strong high-redshift radio galaxies caused by radio emission that has been Thomson-scattered by the ionised IGM (Sholomitskii & Yaskovitch 1990; Geller et al. 2000). The brightness of the halo relative to the central source is a measure of the density of the IGM and thus a direct measure of Ω_{IGM}. Heroic efforts with existing telescopes to do this have resulted in 2σ detections of a non-zero Ω_{IGM}; providing plausibility of concept rather than any detection of the diffuse IGM. Halos are expected to be 1/3 tangentially polarised with halo sizes decreasing in surface brightness as 1/r, limited only by the age of the central radio emitting source and the

speed of light. Therefore, for a quasar emission age of 10^8 years at $z = 3$, halos in principle could extend out to 1°. In addition, if the radio emission is intermittent then the halo would show a ring-like pattern.

The crucial thing for an electron scattering experiment is sensitivity to low surface brightness structure, high dynamic range (10^5) and good polarisation purity, since searches for halos should be done through their polarised signature to reduce confusion. The experiment requires surveys with both high and low spatial resolutions in order to properly remove (subtract) the bright confusing (point) sources from the field to be left with the diffuse, large scale faint halos. The high dynamic range, polarisation purity and clean, uniform visibility data that is expected from this telescope makes it an ideal telescope to do this experiment.

3.7 The radio−FIR correlation

One of the tightest correlations in extragalactic astronomy exists between the radio continuum (RC) and far-infrared (FIR) emission from low-redshift non-AGN galaxies (Condon 1992); even if the actual mechanisms driving the correlation are not absolutely clear. But to what flux level and what redshift does this correlation continue to hold?

Appleton et al. (2004) have shown a good correlation between the 24 μm and 20 cm flux densities for objects with a median $z = 0.3$ extending out to z $\sim$ 1, and Beswick et al. (2006) show that the luminosities of all identified 24 μm sources in their extremely deep radio field still follow the correlation for sources with 24 μm flux densities $\geq$ 80 μJy. Exploration of the radio-FIR correlation at even fainter levels can only be obtained at present by the technique of stacking, and (Boyle et al. 2007) have stacked ATLAS (Norris et al. 2006) radio data to show that, indeed, the radio-FIR correlation extends down to μJy levels.

Figure 3.4 shows all ATLAS sources, in both the CDFS and ELAIS-S1 fields, which have measured 20 cm and 24 μm flux densities. These sources include both star-forming galaxies, which presumably follow the radio-FIR correlation, and AGN, which are expected to lie above it. As a result, a lower bound is clearly visible, presumably corresponding to the radio-FIR correlation. Also shown are the stacked data from Boyle et al. (2007). Although the stacked data roughly follow the correlation, it is clear from Figure 3.4 that their extrapolation lies below the lower bound to the data. This is probably caused by a systematic error in the stacking procedure, however it is possible that the weak radio sources represent a different population

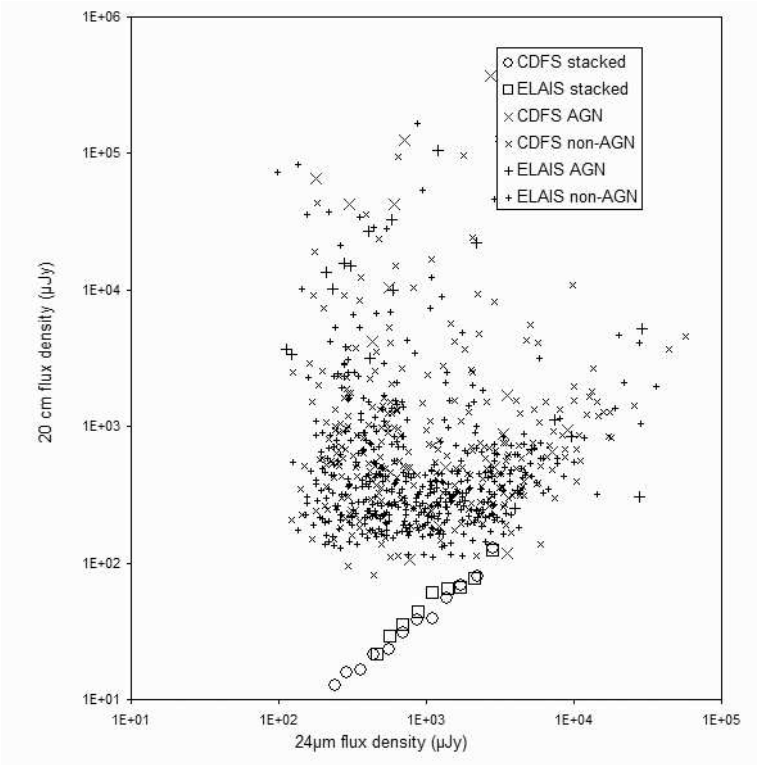

Figure 3.4: The observed flux densities of all detected sources in the two ATLAS fields, together with the stacked data from (Boyle et al. 2007). The *AGN* classification is determined by morphology or spectroscopic classification, while *non-AGN* means that the source has not been classified as an AGN, but may still be either an AGN or star-forming galaxy.

of objects, or objects with an intrinsically different value of the FIR-radio continuum correlation coefficient (at 24 μm), from objects seen in the local Universe. The MIRANdA survey data will help to resolve the issue, without stacking down to 50 μJy, and with stacking down even lower flux densities still.

3.8 The Integrated Sachs-Wolf Effect

MIRANdA may be able to answer the question of whether dark energy exists at $z \sim 1$ and if so on what scale. The test of its existence is in the

predicted correlation between the CMB anisotropies and mass structure at $z \sim 1$; such a correlation would only be seen if the CMB photons have been redshifted by the low-redshift structure as it collapses, and only occurs if the current expansion of the Universe is NOT matter dominated. It may be possible to detect this so called Integrated Sachs-Wolf effect by cross-correlating fluctuations detected in the CMB with large scale fluctuations in the mass distribution at $z \sim 1$ as probed by radio galaxies. Cross-correlation of the NVSS radio galaxies with the CMB anisotropies gave a tentative detection of the ISW effect, but at significance of only 2σ (Boughn & Crittenden 2004). An extremely deep survey with MIRANdA would provide a much more stringent test of the correlation; this test has a much lower confusion limit than the traditional limit for source counts etc because we are looking for a statistical result on size scales of order the scales of the CMB anisotropies.

3.9 A weak lensing demonstrator

Future radio telescopes, culminating in the SKA, can potentially become the world's leading facilities for performing cosmological surveys. In particular, the web of cosmic structure imprints a coherent shape distortion in the distribution of distant galaxies. This weak gravitational lensing is a powerful probe of the characteristics of dark energy and dark matter. The SKA continuum survey can be used to construct such a lensing map featuring excellent image quality, a high source density to limit statistical noise, and a wide survey area to reduce cosmic variance. We note two key advantages compared to optical imaging surveys. Firstly, the point-spread function of a radio telescope is well-determined and stable (being simply derived from the interferometer baseline distribution). Secondly, distance measurements in optical imaging surveys are derived from photometric redshifts, which suffer from systematic uncertainties, whereas the H I survey provides precise redshifts for a subset of galaxies at $z < 1.5$.

MIRANdA has insufficient collecting area and resolution to perform the weak-lensing experiment. However, it will pave the way for the SKA surveys by resolving key issues of survey design and analysis. This requires a MIRANdA survey with at least $5''$ resolution in order to avoid confusion down to $\sigma = 10$ μJy beam^{-1} and in order to map the angular sizes of the faint radio population down to $1''$. MIRANdA will contribute by refining our knowledge in the following ways:

1. Measurement of the faint radio source counts over large areas. Future lensing surveys in radio wavebands will target star-forming disk galaxies, owing to the complex morphologies and low angular density of powerful FRI and FRII radio galaxies (see Table 3.1). The number density of these disk galaxies determines the future accuracy of dark energy measurements, and is an important parameter for designing the corresponding SKA survey.

2. Measurement of the size and ellipticity distributions of star-forming disk galaxies as a function of flux density and redshift. Lensing can only measure shapes of resolved galaxies; the size distribution is therefore a crucial ingredient in designing future surveys. We need to assess the degree of overlap and confusion in the faint source population, and measure the "covering factor" of the FR I galaxies which will be masked out of the lensing analysis.

3. The refinement of shape measurement techniques in Fourier space, which must proceed in parallel with the location of the sources in the image plane.

4. The effect of image processing (cleaning and calibration) on correlated noise in the radio images.

The imprint of gravitational lensing has been detected in the FIRST radio survey with a significance level of 3-σ (Chang et al. 2004). MIRANdA should allow lensing measurements at roughly the same level as the current leading optical imaging surveys: covering hundreds of deg^2 with perhaps one resolved source per arcmin^2. Although MIRANdA will not be competitive with the next generation of optical lensing surveys such as Dark Energy Survey and PanStarrs, MIRANdA will pave the way for successful lensing experiments in the radio wavebands.

Chapter 4

Extragalactic Faraday Rotation

4.1 Summary

The presence of coherent magnetic fields on large scales points to a powerful and ubiquitous process which organises random motions into highly-ordered structures. Galaxies and clusters are likely formed from collisions of smaller constituents, and then are continually energised by galaxy mergers, stellar winds and supernovae — it is thus remarkable that the magnetic fields produced by the resulting complicated gas flows and electrical currents are some of the largest organised structures in the Universe.

MIRANdA can provide a major contribution to our understanding of how large-scale magnetic fields are generated and maintained. This will be realised through a deep wide-field 1.4-GHz continuum survey, which will yield an all-sky grid of closely spaced ($\sim 10'$) polarized extragalactic sources. For each such source, Faraday rotation can be measured and a corresponding foreground rotation measure (RM) extracted. The resulting RMs will provide a definitive three-dimensional map of the ordered and turbulent components of the Milky Way's magnetic field, against which dynamo and other models for cosmic magnetic field generation can be tested. These data will also provide an observational underpinning for the much more densely packed RM grid eventually planned for the (SKA).

4.2 Introduction

The Milky Way and many other nearby spiral galaxies all show well-organized, large-scale magnetic fields (Beck et al. 1996). These fields play a crucial role in disk stability, the confinement of cosmic rays and the global turbulent cascade in the interstellar medium, and possibly also regulate galaxy formation and evolution. The presence of this coherent magnetism on large scales demonstrates the existence of physical processes which gradually organise random motions into highly-ordered structures. The dynamo mechanism is the favoured explanation (Ruzmaikin et al. 1988). However, dynamos are not yet well understood and still face theoretical difficulties, especially in light of recent results which show that field amplification in galaxies can be extremely rapid (e.g. Gaensler et al. 2005).

Our own Milky Way is an excellent test-bed to address these issues, because a huge ensemble of background RMs can be used to probe its three-dimensional magnetic field structure. RMs from both pulsars and extra-galactic sources (EGS) can be used in such studies. However, until recently there had been comparatively few EGS RMs available, and studies utilising pulsar RMs alone have been constrained both by the comparatively sparse sampling of pulsars on the sky and by uncertainties in pulsar distances. These limitations have all made it difficult to map the three-dimensional field distribution, especially in complicated regions.

4.2.1 The Magnetic Field in the Galactic Disk

The Galactic magnetic field is primarily concentrated in the disk, with the large-scale field having both radial and azimuthal components. Recent surveys of the Galactic plane at high resolution and at multiple wavelengths have assisted greatly in the study of the field in the disk by providing 1–2 EGS RMs per deg^2 at low Galactic latitudes (e.g. Brown & Taylor 2001, Brown et al. 2007).

New data-sets such as that shown in Figure 4.1 strikingly confirm the presence of a large-scale coherent field. However, the statistics of such RM data are insufficient to derive unique solutions for the field geometry, and usually rely on pre-imposed assumptions regarding the geometry of the spiral arms and the thickness of the disk. Furthermore, the latitude coverage of these surveys is substantially incomplete, with currently very limited RM coverage in the first and third quadrants. Finally, these data lack the sample sizes needed to complicated small-scale features, and to separate the magnetic field in arm vs. inter-arm regions. The order-of-magnitude im-

provement in the size of RM samples offered by MIRANdA will allow us to overcome these current limitations in our understanding.

4.2.2 The Galactic Magnetic Field at High Latitudes

Even less attention has been given to the Galactic magnetic field at high latitudes (see Han & Qiao 1994), because of the sparse sampling of RMs over most of the rest of the sky (1 RM per ~ 40 deg^2). As a corollary, the scale-height of the magneto-ionic medium is only vaguely understood.

There are two important motivations for trying to obtain a better understanding of the high-latitude field. First, because this part of the sky is free from turbulent and tangled fields as are seen in the plane, overall patterns in RM are easy to identify (e.g. Frick et al. 2001). Second, unique insights on Galactic magnetism, and on the mechanisms which maintain it, can be provided by studying the *parity* of the field across the Galactic plane. Specific issues which can be addressed by such studies are as follows.

- The symmetry of the vertical (B_z), azimuthal (B_ϕ) and radial (B_r) components of the field above vs. below the plane discriminate between overall field geometries, and hence between various primordial field and dynamo models. For example, a reversal in B_ϕ, but not in B_z, between positive and negative Galactic latitudes would indicate either a primordial vertical field, or an A0 mode (antisymmetric field with a dipolar structure) as would result from weak differential rotation (Ferrière 2005). Alternatively, a reversal in B_z across the plane, but not in B_ϕ or B_r, corresponds to a quadrupolar field, as results from strong shear (Zweibel & Heiles 1997).

- The strength of B_z is a diagnostic of the origin of the magnetic field. For a Galactic disk of diameter $2R$ and thickness $2h$, kinematic dynamo models predict $B_z/B_r \approx \sqrt{h/R} \approx 0.3$. However, if $B_z \ll B_r$, this can indicate that there is a significant primordial component to the magnetic field (Ruzmaikin et al. 1998).

- The strength of B_z compared to the horizontal component regulates the efficiency with which cosmic rays flow from the disk into the halo and then into the intergalactic medium (IGM) (e.g. Carilli et al. 1992). Conversely, vertical magnetic fields of fluctuating sign may result from Parker instabilities or galactic winds. In a few edge-on galaxies, polarization data suggest strong vertical fields (e.g. Tüllmann et al. 2000), but the situation for our Galaxy is unclear.

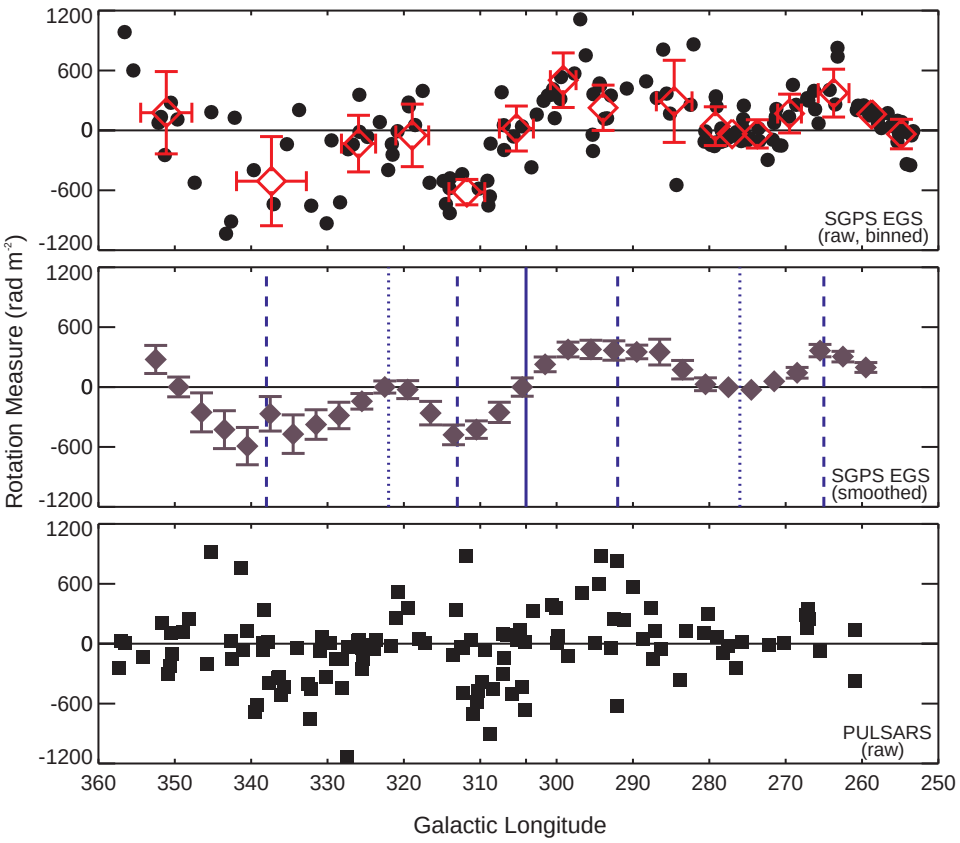

Figure 4.1: RM versus Galactic longitude for EGS and pulsar RMs in the Southern Galactic Plane Survey (SGPS), from Brown et al. (2007). Top panel: circles represent the individual SGPS EGS RMs (errors are smaller than the symbol size), while open diamonds represent data averaged into independent longitude bins containing nine sources each. Where symbol size permits, the error bars are the standard deviation in longitude and RM for each bin. Middle panel: diamonds represent boxcar-averaged SGPS EGS data over 9 degrees in longitude with a step size of 3 degrees. In contrast to the binned data in the top panel, the error bars are the standard error of the mean. The solid line marks the approximate longitude of transition from predominantly positive RMs to negative RMs ($\ell \sim 304°$). Dotted (dashed) lines mark approximate longitudes of minimum (maximum) |RM| in SGPS data. Bottom panel: squares represent individual pulsars with known RMs in the SGPS region (errors are smaller than the symbol sizes).

As explained in Section 4.3, MIRANdA can provide the densely sampled RM grids at high latitude needed to address these issues.

4.3 A Rotation Measure Grid With MIRANdA

The key experiment for studying magnetic fields with MIRANdA will be to image the entire southern sky at 1.4 GHz to a 1-σ sensitivity of 50 μJy in full-Stokes continuum emission. For MIRANdA, this would be achieved in a one-hour integration per pointing, which for a field of view of 30 deg^2 implies a total survey time of 5–6 weeks.[1]

Such a survey will detect many millions of background radio galaxies and AGN in total intensity (see Chapter 3), and many of these sources will have detectable linear polarization. By measuring the polarization position angle in many contiguous channels spread across the MIRANdA observing bandwidth, foreground RMs can be extracted toward a vast number of polarized sources. Such an "RM grid" can provide an incredible probe of ordered and turbulent magnetic fields as a continuous function of Galactic longitude and latitude.

To predict what the polarized sky at these flux levels will look like, we turn to the "$\log N - \log P$" predictions of Gaensler et al. (2004), and the subsequent refinements of this model by Stil et al. (in preparation). Assuming that, under typical conditions, a signal-to-noise ratio of $\approx$10 is needed in linear polarization in order to extract an accurate RM (Beck & Gaensler 2004), we predict that the proposed MIRANdA all-sky polarization survey would yield RMs toward $\sim 5 \times 10^5$ extragalactic sources, with an average spacing between RM points of $\lesssim 10'$. (In comparison, the typical spacing at high Galactic latitudes between data-points in current RM catalogues is $\gtrsim 10^\circ$.)

Broadly speaking, the Milky Way's magnetic field has two components: a large-scale, coherent, magnetic field, tied to the overall structure of the spiral arms, disk and halo, and a small-scale, fluctuating field which traces individual regions such as supernova remnants (SNRs) and H II regions, as well as diffuse turbulence in the ionized ISM. The effective angular resolution with which a grid of background RMs can probe the Galaxy's magnetic field is determined by the need to be able to separate large-scale and small-

[1] Obviously much deeper surveys could be reached in longer integrations, but the resulting Stokes I images would be heavily confused. Also, an initial RM grid from MIRANdA would provide such a large leap forward in our understanding of the polarized sky, that we would need to properly digest these new data before knowing how best to survey deeper.

scale fields in the data. The large-scale Galactic magnetic field is traced by RM *gradients*: typically $\sim 20 - 30$ rad m^{-2} deg^{-1} (e.g. Clegg et al. 1992), although in regions of high magnetic fields and gas densities, gradients more than an order of magnitude higher can be observed. In contrast, the small-scale field is traced by random RM fluctuations, which have a typical dispersion $\sigma_{\rm RM} \approx 30$ rad m^{-2} on degree scales (Minter & Spangler 1996). Averaging over an ensemble of RMs in a region can separate out these two contributions at scales larger than the effective smoothing size.

Separation of the smooth and fluctuating components of the magnetic field has required binning of current RM data-sets at intervals of ~ 10 deg^2. Such an analysis begins to beautifully reveal the overall structure associated with field reversals and spiral arms, as shown in Figure 4.1. However, MIRANdA can greatly improve current RM yields, providing a source density over the entire sky of ~ 20 RMs per deg^2. With such a data-set, we can successfully distinguish between the behaviours of the smooth and fluctuating components of the field (at a signal-to-noise ratio of $\sim 4 - 5$) down to a resolution of ~ 1 deg^2. One square degree turns out not to be some arbitrary scale, but represents an approximate dividing line between the sizes of individual SNRs and H II regions, and the larger scale structure of spiral arms, super-bubbles and fountains. Polarimetry with MIRANdA will thus provide our first complete view of the magnetic geometry of the Milky Way, on scales ranging from sub-parsec turbulence up to the global structure of the disc and spiral arms.

Of course, other RM surveys will be carried out before those planned for MIRANdA. An example is shown in Figure 4.2, illustrating a forthcoming analysis of 500 RMs measured with the ATCA covering the South Galactic Cap. The 200 hours of observing time that underlie this data-set should provide some important first constraints on the vertical field geometry of our Galaxy. However, in just 80 hours, MIRANdA will measure $\sim 10^4$ RMs in this same region, clearly providing a colossal improvement in the effective sensitivity and angular resolution of a smoothed Galactic RM map at these latitudes.

Also notable amongst forthcoming RM surveys is the GALFACTS survey at Arecibo, to begin in 2007–2008. However, while GALFACTS data will certainly improve our understanding of both large-scale structure and small-scale turbulence in the Galactic magnetic field, GALFACTS will cover only a limited longitude range both above and below the disk in the first quadrant and at the anti-centre (see Figure 4.3). In contrast, MIRANdA will allow for the possibility of continuous probing in longitude for three of the four Galactic quadrants. With such longitude coverage, it should

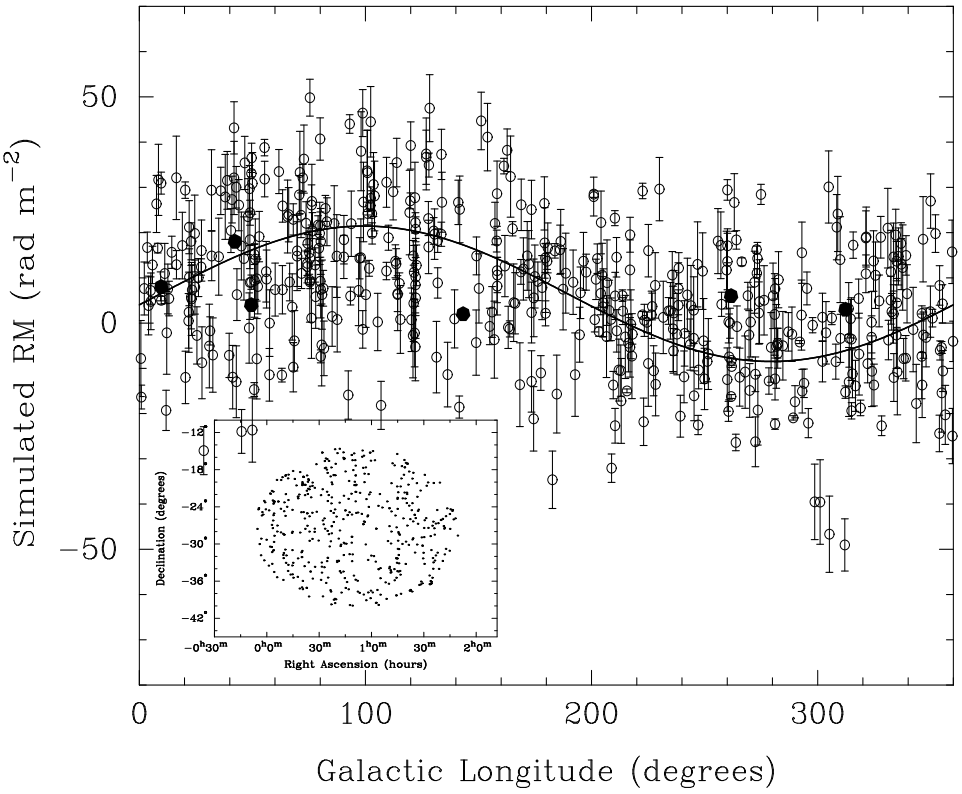

Figure 4.2: The distribution in ℓ of 500 highly polarized NVSS sources covering the South Galactic Cap, the RM of each of which has recently been measured with the ATCA (Mao et al., in preparation). For each source, a simulated RM value is plotted, assuming a simple three-dimensional magnetic field geometry for the disk and halo; the filled circles show the six previously known RMs in this region of the sky. In the simulation, the field parallel to the disk reveals itself as a sinusoidal dependence of RM vs. ℓ, while the constant offset in RM is the signature of a non-zero value for B_z. The phase and amplitude of the sinusoid then yield the pitch angle and strength, respectively, of the horizontal field above the disk. **Inset:** The distribution of the 500 NVSS sources on the sky.

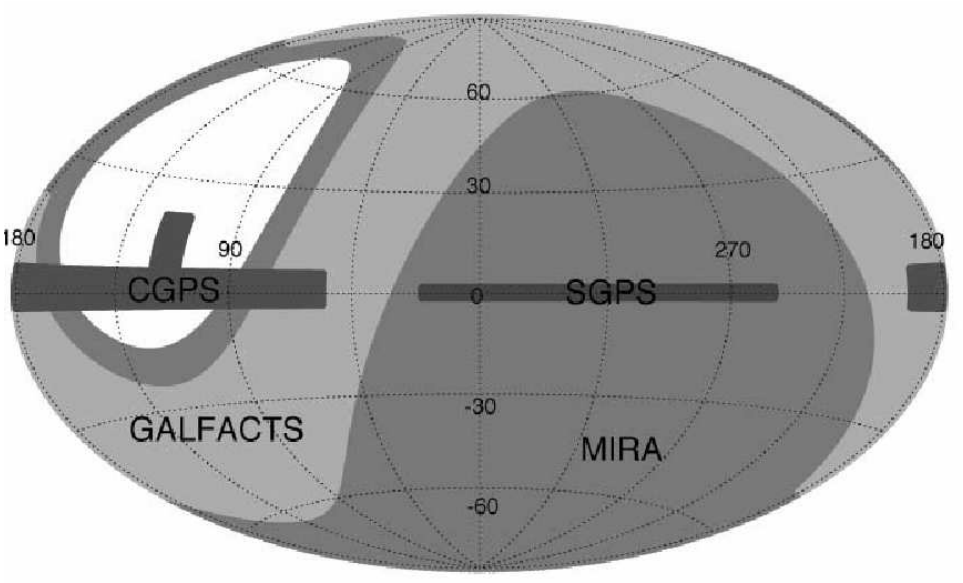

Figure 4.3: Comparative sky coverage of MIRANdA, GALFACTS, and of the recent Galactic plane polarization surveys, projected in Galactic coordinates (image courtesy of the Canadian MIRANdA science team).

be possible to fully map the magneto-ionic disk, to reveal the signature of the warp (should it exist in the magneto-ionized medium), and to provide insight into how the transition between the disk and halo occurs. In this sense, GALFACTS and other such surveys will serve us "practice runs" for MIRANdA, whose much larger sample of RM measurements will be coupled with more complex distributions associated with the multiple reversals and high levels of turbulence expected for the inner Galaxy.

4.4 Specifications for Polarimetry with MIRANdA

The accuracy of the RMs from a polarization survey is set by the total bandwidth and the signal-to-noise. For an RM grid survey that uses a 300 MHz bandwidth centred on 1.4 GHz, a signal-to-noise ratio of 10, will provide an uncertainty in RM of ± 5 rad m^{-2}. This level of precision is needed to detect the small levels of Faraday rotation expected at high Galactic latitudes, but higher precision is problematic due to systematic effects such as ionospheric Faraday rotation. The maximum RM to which a survey is sensitive is set by the width of individual channels: for 1-MHz channels (i.e., 300 channels

across the band), the maximal signal will be $|\mathrm{RM}| \approx 22\,000$ rad m^{-2}, which will be more than enough for most experiments.

For typical AGN spectra and a fixed total bandwidth, the precision in RM is proportional to $\nu^{3.5}$, so that higher frequency surveys give much larger RM uncertainties. Conversely, depolarization effects become severe at low frequencies, such that although RM measurements are accurate, most sources are not polarized. Considering both these effects, a centre frequency of 1.4 GHz seems to be a "sweet spot" for EGS RM surveys.

An EGS RM survey does not set strong constraints on the array configuration for MIRANdA, since the target fields will primarily be point sources. Furthermore, there will be minimal source confusion in Stokes Q and U, so that long baselines are not required. However, there is another sweet spot, in resolution, at angular scales of $\approx 30'' - 60''$, because at higher resolution, sources tend to be resolved out, while at lower resolution, many sources are depolarized. Thus a concentration of collecting area within a central ~ 1 km core would be ideal.

For accurate polarization calibration, good parallactic angle coverage of each field is highly desirable. Thus even if the snapshot $u - v$ coverage of MIRANdA is very good, each image needs to be constructed from multiple cuts. However, any long-term source variability in polarization will make it difficult to measure RMs. Thus the multiple cuts on each field are best spread over a single 12-hour track, perhaps appropriate for commensal observing with H I galaxy surveys. Continuum polarization observations are best carried out at night, and continuous GPS monitoring of the total electron content will be needed to correct for ionospheric Faraday rotation. Since most faint EGS will have a fractional linear polarization of $\sim 10\%$, the final images will require a polarization purity of at least –20 dB across the entire field.

The survey data that will need to emerge from the reduction pipeline will be all-sky maps of Stokes I, Q, U and V in 1-MHz channels, corresponding to a total size for the final data cube of ~ 12 TB. However, the high-level end product will be much smaller, simply consisting of a catalogue of position, flux, fractional polarization and RM for each of the sources in the RM grid (total catalogue size ~ 15 MB).

4.5 The Faraday Signature of the IGM

Beyond individual galaxies and clusters, all of "empty" space may be magnetized, either by outflows from galaxies, by relic lobes of radio galaxies, or

as part of the large-scale structure of the cosmic web. Such a field has not yet been detected, but its role as the likely seed field for galaxies and clusters, plus the prospect that the IGM field might trace and regulate structure formation in the early Universe, places considerable importance on its discovery. Once the magnetic field of the IGM is detected, a measurement of the characteristic size scales of its fluctuations can allow us to differentiate between the wide variety of mechanisms proposed for magnetic field generation in the IGM (see Gaensler et al. 2004 and references therein). While RMs of distant EGS are potentially a useful probe of the IGM, to date there has been no detection of magnetic fields in the IGM; current upper limits on the strength of any such field are model dependent, but suggest $|B_{\rm IGM}| \lesssim 10^{-8} - 10^{-9}$ G (Kronberg 1994, Blasi et al. 1999).

With a sufficiently large RM sample, this all-pervading cosmic magnetic field may eventually be identified. Just as the correlation function of galaxies yields the power spectrum of matter, the analogous correlation function of this RM distribution can provide the magnetic power spectrum of the IGM as a function of cosmic epoch and over a wide range of spatial scales. Such measurements will allow us to develop a detailed model of the magnetic field geometry of the IGM and of the overall Universe.

For Faraday rotation occurring at a redshift z, the observed RM is reduced by a factor $(1+z)^2$ over its intrinsic value. However, a simplistic assumption is that the comoving magnetic flux and electron density are both constant, so that electron density evolves as $(1+z)^3$, while the magnetic field evolves as $(1+z)^2$ (e.g. Widrow 2002). In this case, we expect the observed RM to be proportional to $(1+z)^3$. While this is a naive calculation, it demonstrates the general principle that RM signatures from distant objects can be quite large, even if the foreground IGM has a relatively small magnetic field. More robust treatments are presented by Kolatt (1998) and Blasi (1999), who demonstrate in detail how the statistics of RM measurements as a function of redshift can be used to remove the foreground Galactic contribution, and then to extract the strength and power spectrum of magnetic fields in the IGM.

These studies require a very large sample of RMs from sources at known redshifts, and thus are probably more likely to be addressed with the SKA rather than with MIRANdA. However, recent results such as those shown in Figure 4.4 show that at least in certain specific regions, it may be possible to identify very weak magnetic fields over scales > 1 Mpc with more modest RM samples. If MIRANdA can be expanded so that it can push down even further in continuum sensitivity, its large sky coverage and dense RM sampling might make the first such studies possible, especially for fields

which have already been well-studied at other wavelengths. In any case, MIRANdA data will act as a crucial pathfinder for SKA studies of the IGM, by identifying the likely source statistics and survey yields, and by allowing us to quantify the accuracy with which foreground RMs will be able to be modelled and then removed.

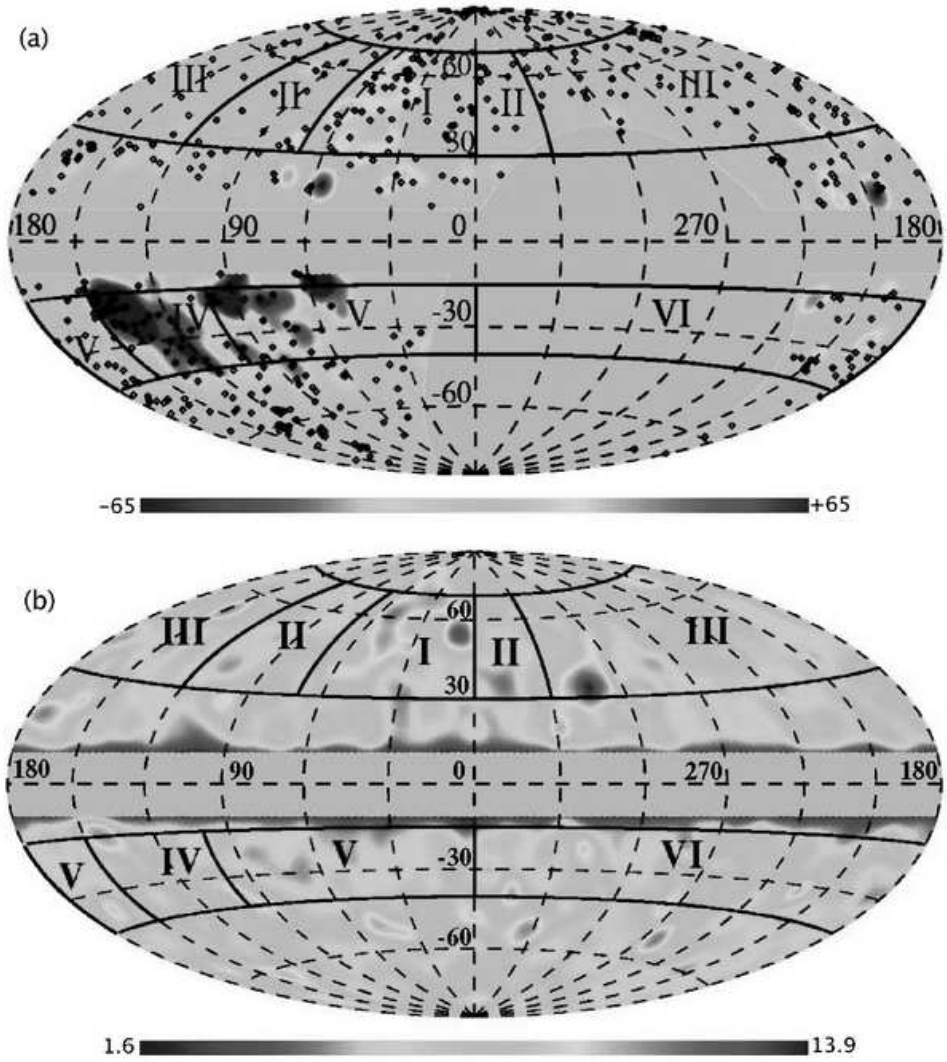

Figure 4.4: (a) An all-sky plot of the smoothed distribution of EGS RMs. The black squares show the positions of individual EGS RM measurements. The colour map shows RM variations, smoothed to 7° resolution in an Aitoff projection of Galactic coordinates. The colour range from blue to red signifies RMs ranging from -65 rad m^{-2} to $+65$ rad m^{-2}. (b) The 2MASS galaxy column density similarly smoothed to 7° resolution. The Hercules supercluster, lying in the high density region labelled I, shows an RM distribution which is possibly correlated with the galaxy distribution. This suggests the presence of a large-scale coherent magnetic field in this supercluster, with strength ~ 0.3 μG on scales ~ 0.5 Mpc. Figure reproduced from Xu et al. (2006).

Chapter 5

Galactic and Magellanic Science

5.1 Summary

The rebirth of observational studies of the Milky Way and Magellanic System over the past decade has raised new and profound questions about the evolution of the interstellar medium (ISM). The community has transitioned from studying small-scale aspects of the ISM to a more wholistic approach, which seeks to combine information about a variety of ISM phases with information about magnetic fields. With MIRANdA we can make significant and unique inroads into understanding the evolution of the ISM and through that the evolution of Milky Way. These are crucial steps along the path to understanding the evolution galaxies.

The Milky Way and Magellanic System because of their very large sky coverage can only be observed in survey mode. As such, they present themselves as ideal targets for MIRANdA. Here we discuss how MIRANdA can be used to achieve superb advances in our understanding of the evolution of the Milky Way, its ISM and its magnetic field. To achieve these advances we propose several large-scale projects, these include: accounting for and studying the structure of all H I associated with the Milky Way and Magellanic System to unprecedented column density limits and angular resolution; constraining the large-scale Galactic magnetic field in the inner Galaxy with *in situ* measurements of H I Zeeman splitting; exploring the growth of molecular clouds using diffuse OH mapping of the Galactic plane; probing the turbulent magneto-ionic medium of the Galactic halo with diffuse continuum polarization mapping of the whole sky. The unifying technological require-

ment for all aspects of the Galactic and Magellanic science presented herein is the demand for low-surface brightness sensitivities achieved by compact configurations.

5.2 The Milky Way as a Laboratory for Galaxy Evolution

Galaxy evolution is one of the great puzzles in current astrophysics, incorporating how galaxies assemble and evolve from the beginning of the universe to the present day. Unfortunately, our knowledge of the fundamental processes of galaxy evolution is blocked because we do not understand the evolutionary cycle of interstellar matter in our own Galaxy. We know that the life cycle of the Milky Way, and of most spiral other galaxies, involves a constant process of stars ejecting matter and energy into the interstellar mix, from which new stars then condense. Somehow matter makes the transition from hot, ionised stellar by-products to become the cold molecular clouds from which stars are formed. The circulation of matter between the Galaxy's disk and its surrounding halo further complicates this cycle. ISM studies in our Galaxy probe the evolutionary cycle with sensitivity and resolution unattainable in external galaxies; it is only in the Milky Way that we can observe the evolution of the interstellar medium on scales ranging from sub-parsec to kiloparsecs. Furthermore, the evolution of the Galaxy is controlled by the Galactic and local magnetic fields, yet these components are largely unknown. The Milky Way is thus an ideal laboratory for studying galaxy evolution.

In recent years there has been a renaissance in Galactic ISM surveys. This has largely been driven by advances with the Canadian and Southern Galactic Plane Surveys, which used a combination of single antenna and aperture synthesis telescopes to map the Galactic plane in atomic hydrogen (H I) and polarized continuum emission at an unprecedented resolution of $\sim 1'$. From these surveys have followed a number of Galactic Plane projects at comparable or better resolution such as the FCRAO and Boston University surveys of ^{12}CO and ^{13}CO and the Spitzer GLIMPSE survey of infrared emission. These surveys have revised the way we think about ISM studies, revealing structure on all size scales, a remarkable agreement between ISM phases, and a wide variety of new polarization structures. More recently there has been a push to improve the all-sky H I and radio continuum atlases from the $\sim 1^\circ$ resolution of the past 15 years to $\sim 15'$.

The future of Galactic and Magellanic ISM studies lie in low-surface

brightness observations. For the Milky Way, the drive is to extend the arcminute resolution work pioneered in the Galactic plane to the Galactic halo and the disk-halo interface. These regimes will allow us to better understand how the Milky Way interacts with its environment, how matter is expelled from the disk and how the Galaxy has evolved. Here we describe a number of projects which will use MIRANdA to revolutionise our understanding of the Milky Way and its ISM. The observational tools for these projects include H I and OH emission, H I Zeeman splitting and diffuse polarized emission.

5.3 H I Associated with the Milky Way and Magellanic System

5.3.1 High Velocity Clouds and the Galactic Halo

High and intermediate velocity clouds (HVCs and IVCs) are believed to play important roles in both the formation and the evolution of the Galaxy. Some HVCs may be related to the Galactic Fountain; some are tidal debris connected to the Magellanic Stream (Putman et al. 2003) or other satellites; some may be infalling intergalactic gas, and some may be associated with dark matter halos and be the remnants of the formation of the Local Group. The structure and distribution of high velocity gas probes tidal streams and the building blocks of galaxies providing critical information on the evolution of the Milky Way system. One problem that has long plagued HVC studies is the almost complete lack of distances to these objects, which has traditionally sparked debates about whether HVCs are Galactic or extragalactic. Although the distance problem is improving somewhat with increased number of distances using absorption towards halo stars, the problem remains. Regardless, the consensus now is that there are probably a variety of HVC origins.

Nearby HVCs can be used as probes of the thermal and density structure of the Galactic halo. HVCs have, in general, a high velocity relative to their ambient medium which results in a ram pressure interaction between the cloud and medium. Recent H I observations have indeed shown that a significant fraction of the HVC population have head-tail or bow-shock structure (Brüns et al. 2000, Brüns et al. 2001). By comparing the observed structures and thermal distributions within them to numerical simulations it is possible to determine basic physical parameters of the Galactic halo such as density, pressure, and temperature. In situations where the density and pressure of the ambient medium are known by independent methods the

problem can be turned around to determine the distance to the observed clouds (Peek et al. 2007).

The recent Galactic All-Sky Survey (GASS; McClure-Griffiths et al., in prep) has imaged the sky south of declination zero at $15'$ resolution to a 1-σ brightness temperature limit of 70 mK per km s^{-1}, or a column density limit of $N_H \approx 8 \times 10^{17}$ cm^{-2} over 20 km s^{-1}. The angular resolution of this survey offers a factor four improvement over previous all-sky surveys (IAR-LDS) and the 1 km s^{-1} velocity resolution offers a factor of 15 improvement in spectral resolution over HIPASS. With these improvements we are beginning to resolve the structure of some of the mid-sized HVCs. However, we do not yet have the sensitivity or resolution necessary to study the detailed physical and thermal structure over a large number of HVCs. It seems that the structure that we do see is just the tip of the iceberg.

GASS is also revealing a wealth of tenuous filaments connecting HVCs to the Galactic Plane at column densities of $N_H \sim 10^{18}$ cm^{-2}. An example is shown in Figure 5.1, which shows that the HVCs in Complex L are interconnected by a thin, low column density filament and that this filament appears to extend to the Galactic disk. Filaments of HVCs such as these may be related to the "cosmic web" predicted in cosmological simulations. Recent observations of the M31-M33 system (Braun & Thilker 2004) have revealed the local analogue of the cosmic web, showing that very low column density gas ($N_H \sim 10^{16-17}$ cm^{-2}) connects the two galaxies. The current generation of Milky Way H I surveys do not reach the column density limits needed to explore this fascinating web of structure in the entirity of the Local Group. An H I survey with MIRANdA to a brightness limit of 100 mK per km s^{-1} at $2'$ resolution could be smoothed to reach an unprecedented column density limit of $N_H \sim 2 \times 10^{16}$ cm^{-2} at $15'$ resolution over the entire sky. This survey would reveal the majority of the cosmic web in the Local Group and provide important constraints for models of the formation of structure in the Local Group.

5.3.2 Disk-halo Interaction

We know that the evolution of the Milky Way is significantly impacted by the two-way flow of gas and energy between the disk and halo. Although we can now detect enormous amounts of structure in the atomic component of the Milky Way halo, we are far from understanding its origin and its relationship to the processes that dominate in the disk. There are a number of important unanswered questions about the transfer of matter between the disk and halo. For example, the range of metallicities and stellar ages

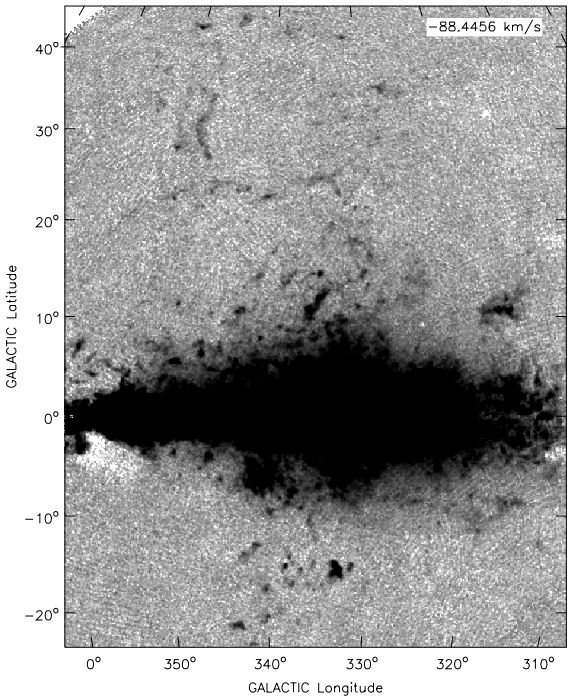

Figure 5.1: H I emission from the Galactic All-Sky Survey at -88.5 km s^{-1} showing the tenuous structure connecting the clouds of Complex L to the Galactic Plane (McClure-Griffiths et al., in prep).

observed in the Milky Way suggests that it must continually receive fresh fuel for star formation but how does the Galaxy receive the fresh fuel for star formation? What happens to matter expelled from the disk? Does it cool and return to disk and if so how long does the process take? Alternately, does expelled matter remain in the halo? Finally, what are the physical conditions of the halo? Our ability to answer these questions is significantly hampered by our inability to image the detailed physical structure of the H I in the halo.

Recent work by Lockman (2002) and Ford et al. (in prep) has shown that a significant amount of mass in the lower halo is contained in small clumps of H I, such as those shown in Figure 5.2. The nature and origin of these cloudlets, which participate in Galactic rotation and are only tens of parsecs in size, are at present unknown. Do they originate from outflow

from the Galactic disk or are they related to inflow for extragalactic space? The one thing that we do know is that small, mostly unresolved, cloudlets are ubiquitous throughout the inner Galaxy (See Figure 5.2).

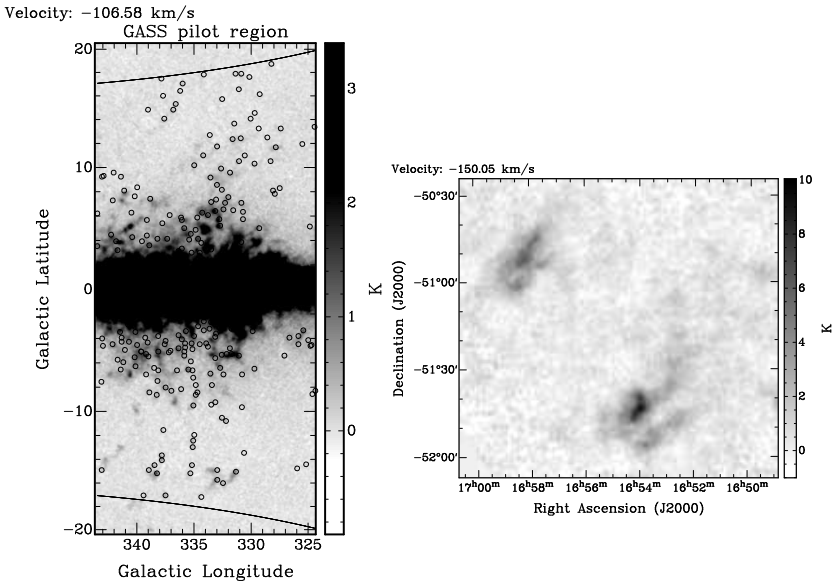

Figure 5.2: H I emission from the Galactic All-Sky Survey showing a plethora of halo cloudlets believed to be the result of significant explosive events in the Galactic disk (Ford et al., in prep).

With the present generation of surveys at 15′ resolution it is not possible to explore the thermal and physical structure of these cloudlets, which may contain information about their origin, motion and evolution. Follow-up observations on several individual cloudlets, such as those shown in the right panel of Figure 5.2, show a tantalising glimpse of possible head-tail structure and other evidence of interaction. These observations may offer the opportunity to resolve a directional ambiguity with these clouds. In general we can measure only the absolute value of the z component of the cloud velocity with respect to the Galactic Plane, i.e. we cannot determine whether the clouds are moving towards or away from the Galactic Plane. Finding head-tail structure in the clouds can help resolve this ambiguity by showing the direction of motion. At present these follow-up observations are prohibitive, requiring hundreds of hours with the ATCA to reach 100 mK at arcminute scales.

Ideally we would like to apply the same techniques that we use with

HVCs to halo cloudlets and use the clouds' structure to probe the temperature and density structure of the lower halo. The temperature and density structure of the Galaxy's lower halo is very poorly constrained with values for nT ranging from 10 to 1000 K cm^{-3}. Although diffuse X-ray emission and ultraviolet spectral lines, such as OVI, can help constrain the properties of the hot ionised medium in the lower halo, the filling factor of the warm neutral medium, and its properties are very poorly constrained. Halo cloudlets can provide unique insight into this important transition region from Galactic disk to halo.

5.3.3 H I in the Magellanic System

At a distance of 65 kpc, the gas-rich irregular dwarf galaxies, the Large and Small Magellanic Clouds form an interacting triad with the Milky Way. Located at approximately $-70°$ declination an uninterrupted view of almost the entire system is achievable. Evidence of the three-way interaction is in the form of the three tidal features associated with the system (Putman 2000). The Bridge forms an apparently contiguous H I filament connecting the SMC and LMC. A very extended halo of H I gas, the Magellanic Stream, trails the clouds and subtends an area over 1000 deg^2. The Leading Arm is the tidal counterpart of the Magellanic Stream, preceding the motion of the clouds around the galaxy.

Observations of the entire Magellanic System have only been obtained with the relatively low resolution of the Parkes telescope ($\sim 14'$). High-resolution observations of the higher H I column-density regions of the LMC, SMC and Bridge exist with resolutions down to $\sim 1'$ and sensitivities of 10^{18} cm^{-2}. Recently the ATCA was used to map the Magellanic Stream from its origin to 0 declination achieving resolutions of $\sim 7'$ and column densities down to $\sim 10^{19}$cm^{-2}.

In order to fully understand the structure, formation processes and turbulence characteristics of the entire Magellanic System, higher resolution images are required. Such data would enable the study of the turbulent ISM, and signatures of the interactions between the galaxies such as head-tail features, the compression of the LMC disk and the stripping of matter by the Galactic H I halo. An understanding of the extent of H I around the System to better sensitivity would increase the sophistication of numerical simulations.

The large field of view of MIRANdA makes it ideal for an investigation of the entire Magellanic System (over 2500 deg^2). However deep imaging of the low column density extended H I would be required to obtain the target

sensitivities ($\sim 10^{17}$ cm^{-2}). If it proves impossible to reach these sensitivity limits, studies of the Magellanic Stream and Leading Arm could still greatly benefit from MIRANdA. An area of ~ 1000 deg^2 could be observed to $\sim 1'$ resolution at a column density limit of 10^{18} cm^{-2}. Such an investigation would reveal structures down to scales not yet observed, increasing the knowledge base on the organisation of structure in the Stream. Comparisons with existing and new results from other areas of the System would create a much more complete picture of the Magellanic ISM. The improved spatial resolution would also enable searches for morphological signature of H I infall into the Galactic Halo. A deep survey of the Eastern Magellanic Bridge (~ 50 deg^2) would complement existing ISM turbulence studies of the western Bridge.

5.3.4 An All-Sky Galactic H I survey

MIRANdA is undoubtedly a survey instrument. The Milky Way and Magellanic Systems, because they fully surround us, demand large area surveys. An all-sky Galactic H I survey with MIRANdA would build on the Galactic All-Sky Survey and current Magellanic surveys to provide a full census of all H I associated with the Milky Way and the Magellanic System at arcminute resolution. This survey would provide essential information about the physical and thermal structure of HVCs and their interaction with the halo; the role and origin of halo cloudlets and the physical structure of the Magellanic Stream and Leading Arm.

In order to study Galactic and Magellanic H I we require an all sky survey with $\sim 2'$ angular resolution and ~ 1 km s^{-1} velocity resolution (5 kHz). HVCs and the structures that connect them are typically very low column density, $N_H \sim 10^{18}$ cm^{-2}. Over a typical velocity width of ~ 20 km s^{-1}, this requires rms sensitivities at the 100 mK level or below. Galactic H I at high latitudes is also very low surface brightness. Ford et al (in prep) have found that the distribution of halo cloudlets peaks at ~ 0.5 K. In addition to low surface brightness sensitivity, the halo structures of interest can cover large areas of the sky and therefore require good short baseline coverage.

To achieve the goals of these projects we need to reach a low surface brightness temperature sensitivity limit of ~ 100 mK over a $\sim 2'$ synthesised beam. The important figure of merit here is the surface brightness limited mapping speed given in Chapter 1. From equation 1.3 it is clear that the filling factor of the array, f, is crucial to achieving a reasonable mapping speed for surface brightness sensitivity limited surveys. We re-

write equation 1.4 in the form

$$f = \frac{A\,\epsilon_a\,N}{\pi/4L^2}, \tag{5.1}$$

where L is the maximum baseline length. For surface brightness sensitivity limited surveys the mapping speed goes as L^{-4} so for a fixed collecting area the surface brightness sensitivity achieved is strongly dependent on the resolution of the survey. Therefore, in order to survey the entire southern sky to a 100 mK sensitivity limit in a reasonable ($\sim$ 1 yr) time MIRANdA would need to be configured with a maximum baseline of $\sim$ 500 m, or equivalently the filling factor needs to be > 0.01.

An additional consideration for this survey is the need to include single dish data for sensitivity to structure on the largest scales. Fortunately the Galactic All-Sky Survey already exists with comparable sensitivity and spectral resolution to the proposed survey and can be combined with the MIRANdA survey.

5.4 Magnetic Fields in the Galaxy: H I spectropolarimetry

One of the key science drivers for the Square Kilometre Array is understanding the magnetic universe. For the Milky Way, rotation measures of extragalactic point sources as described in Chapter 4 will yield information about the line of sight averaged magnetic field weighted to regions of ionised gas. To fully understand the Galactic field and its effect on the evolution of the Galaxy we require *in situ* measurements of the field throughout the Galaxy. One technique for obtaining *in situ* measurements is Zeeman splitting of the H I line (e.g. Heiles & Troland 2003, 2005). Using the kinematic information in the H I line and its relationship with Galactic distance gives information about the third dimension that is not available with rotation measures.

There are three types of measurements that can be made with H I spectropolarimetry: H I Zeeman measurements of absorption towards background continuum sources, H I Zeeman measurements of emission at the tangent point and H I absorption of the polarized continuum background. Of these, H I Zeeman measurements of emission at the tangent point is the most novel and provides the most information about the value of the magnetic field across a wide strip in the inner Galaxy. Measuring H I Zeeman is not trivial; the intrinsic velocity separation induced by Zeeman splitting of the H I

line is extremely narrow, only 2.8 Hz per μG. To detect Zeeman splitting we measure the difference between the right and left circular polarizations, Stokes V, which is proportional to the velocity derivative of the Stokes I profile, $V = 2.8 B_{los} dI_\nu/d\nu$ Hz $\mu\mathrm{G}^{-1}$.

Each line of sight in the Milky Way interior to the Solar circle passes a point where its projection on the Galactic plane is tangent to a circular orbit around the Galactic centre and the distance is geometrically determined. This locus of tangent points is shown with a thick white line in Figure 5.3 overlaid on a recent model of the Galactic magnetic field (Brown et al. 2007). At the tangent point the H I emission reaches its most extreme velocity, the terminal velocity, beyond which the H I profile drops off steeply. Because of the steep drop beyond the terminal velocity it is possible to measure the Zeeman effect. This method will yield an in situ measurement of the magnetic field at every point along the locus of tangent points, which will tie down the Galactic magnetic field models in a way that is not possible with any other measurement.

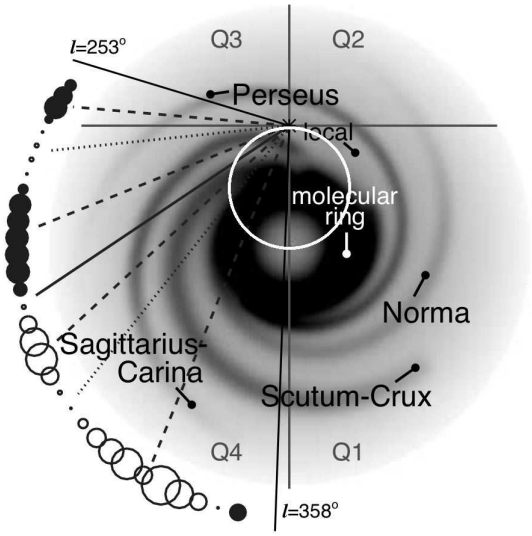

Figure 5.3: A model of the Galactic spiral structure overlaid with point source rotation measures from from Brown et al. (2007). The thick white circle at the centre of the image shows the locus of tangent points.

5.4.1 A Galactic Plane survey of H I Zeeman in emission

The ideal survey to conduct this tangent point Zeeman experiment would cover as much of the area $-90^\circ \leq l \leq +90^\circ$ as possible. A small, but significant latitude coverage of $\sim 5^\circ$ is needed to ensure that our measurements reflect the global Milky Way magnetic field, rather than being subject to individual clouds. We therefore propose a survey of the area $270^\circ \leq l \leq 45^\circ$, $|b| \leq 2.5^\circ$: ~ 700 deg^2. For a typical magnetic field strength of ~ 5 μG and a velocity width of 5 km s^{-1}, we expect the amplitude of the Stokes V spectrum to be 70 mK. We require that the derivative of the line be very well sampled in velocity space, so for a typical derivative line width of 5 km s^{-1}, we require $\Delta v \approx 0.25$ km s^{-1}or $\Delta\nu \approx 1$ kHz. This survey requires a 1-σ sensitivity limit of ~ 20 mK in each polarization. In order to reach these low surface brightness limits we once again require that the telescope have a high filling factor. Because resolution is not a stringent demand on this project, an ultra-compact configuration with most of the collecting area inside a maximum baseline of ~ 200 m would be preferred. Measuring H I Zeeman in emission requires both low sensitivity limits and good polarization properties of the telescope. Interferometers are well suited to this experiment because polarization calibration can be achieved to better accuracy than with a single dish. With such a compact configuration MIRANdA would be uniquely positioned to measure the magnetic field along the tangent point and contribute directly to constraining models for the Milky Way magnetic field.

The H I spectropolarimetric dataset will have several other important uses. It can be used to obtain measurements of H I Zeeman in absorption towards continuum sources in the Galactic Plane. This will provide hundreds of measurements of the magnetic field contained in cold H I clouds. We know that the magnetic field is important in determining the structure and evolution of molecular clouds, which must evolve out of cold atomic clouds. The dataset can also be used to measure H I absorption against the Galactic polarized background (Dickey 1997), which will give kinematic distances to the polarized background throughout the inner Galaxy.

5.5 Probing the Evolution of Cold Gas in the Milky Way: OH emission and H I self-absorption

A significant hurdle in our understanding of the evolution of the ISM and the formation of stars is how molecular clouds form from cold atomic gas. The

process by which previously atomic clouds become molecular is believed to involve compression of the cloud so that the column density of the atomic material becomes significant enough to self-shield and thereby reduce the photo-dissociation of H_2 (Elmegreen 1991). The timescale required for this process is predicted by various theoretical calculations but there are virtually no observational constraints. Recent work by Goldsmith & Li (2005) and Goldsmith et al. (2007) has shown that measurements of residual cold atomic gas fraction within a molecular cloud may provide a means for dating the molecular cloud itself. The formation time for molecular clouds and the star formation timescale within a given cloud has important implications for the global star formation rate in galaxies and the evolution of the Galaxy. As a molecular cloud condenses there is a time-dependent relationship of the molecular to atomic fraction. This molecular cloud dating technique, however, requires knowledge about the fraction of atomic to molecular gas as well as the temperature and density within the cloud. To obtain information about the molecular content of the gas, and to constrain the temperature and density of the cloud it is possible to use diffuse OH emission.

It has long been recognised that OH emission is a good tracer of cold gas in the Galaxy (e.g. Dickey et al. 1981). Whereas H I is a poor tracer in cold dense clouds because its thermal line width tends to be the same as the internal velocity structure of diffuse clouds, the intrinsic linewidth of OH is very narrow and it can be easily distinguished in the interior of diffuse clouds. Li & Goldsmith (2003) have used the combination of narrow line H I self-absorption and OH measurements to probe the atomic to molecular fraction of molecular clouds. Their work has shown that OH emission is an excellent tracer of the so-called transition clouds, which appear to bridge the gap between cold, neutral clouds and fully molecular clouds. OH emission has the added advantage that the Λ doubling of lines at 1665 and 1667 MHz gives more direct information about the excitation temperature and column density than is available with H I. Furthermore, OH unlike high frequency molecular gas tracers, such as CO, can be observed on the same spatial scales as the atomic gas. Unfortunately, OH like CO, is typically sub-thermal in diffuse clouds and so the emission is very weak. The peak brightness temperatures in Li & Goldsmith (2003) are only ~ 0.5 K.

5.5.1 An OH survey of the Galactic Plane

To-date H I self-absorption and OH studies of transition clouds have been pointed observations towards a small number of relatively nearby clouds. We have learned from the H I Galactic Plane Surveys (e.g SGPS; McClure-

Griffiths et al. 2005) that H I self-absorption is present along almost all lines of sight in the inner Galaxy. We have also found that the H I spectral resolution of these surveys is insufficient to fully resolve the linewidth of many of the coldest self-absorption features. The prevalence of self-absorbing clouds in the Galactic Plane suggests that a blind survey of OH emission would reveal hundreds to thousands of transition clouds at a variety of distances and evolutionary states. This large statistical sample would be invaluable to understanding how molecular clouds form. Combined with information about infrared dark clouds and starless cores, as revealed by MSX and GLIMPSE, we may finally be able to answer how quickly do molecular clouds form? which clouds form stars and at what point in a molecular cloud's evolution does star formation begin?

We therefore propose a simultaneous survey of H I and 1665 MHz and 1667 MHz OH emission in the Galactic Plane. For each spectral line we require ~ 5 MHz total bandwidth divided over $\sim 10{,}000$ channels for spectral resolution of ~ 0.1 km s^{-1}. The survey should cover the area $270^\circ \leq l \leq 45^\circ$, $|b| \leq 2.5^\circ$: ~ 700 deg^2 with an angular resolution of $\sim 2 - 3'$. To detect OH emission we require a 1-σ sensitivity limit of ~ 0.1 K in a 0.2 km s^{-1} velocity width. This sensitivity limit will also be more than sufficient to detect H I self-absorption.

5.6 Diffuse Polarization in the Milky Way

The Galactic magnetic field plays a major role in most physical processes in the ISM such as turbulence, energy balance, cosmic ray propagation and gas dynamics. Study of the Galactic magnetic field has significantly increased since high resolution polarimetric radio surveys have become feasible. However most of these studies have focused on the Galactic Plane and almost nothing is known about the magnetic field strength and structure in the Galactic halo and the transition region from the disk to the halo.

The transition between the disk and the halo is an active region containing unique physics. Hydrostatic equilibrium modeling predicts a more or less quiescent magnetic field in the halo, transforming to a turbulent field in the disk at a transition height of about 500 - 1000 pc (Kalberla & Kerp 1998). A change in the character of the magnetic field is indeed seen in external galaxies (Dumke et al. 1995) and also in the Milky Way there is evidence that the polarization characteristics change at $|b| \approx 30^\circ$ (Wolleben et al. 2006; see Figure 5.4). At intermediate latitudes, 'Galactic chimneys' are thought to transfer ionising photons from the OB stars in the disk to

the halo, providing a major part of the ionization of the halo (Reynolds 1985). Numerical simulations indeed show that supernova explosions in the disk cause large scale gas streams into the halo, where ram pressure dominates over magnetic pressure and the magnetic field is swept into magnetic bubbles (de Avillez et al. 2004). The imprints in the Galactic magnetic field left by these processes give us unique knowledge about the magnetism and gas dynamics in a bubble or chimney. External galaxies often show magnetic field structures inclined or even perpendicular to the plane (Beck 2001). However, in only one Galactic superbubble (in the Northern sky) has the magnetic field been studied (West et al. 2007).

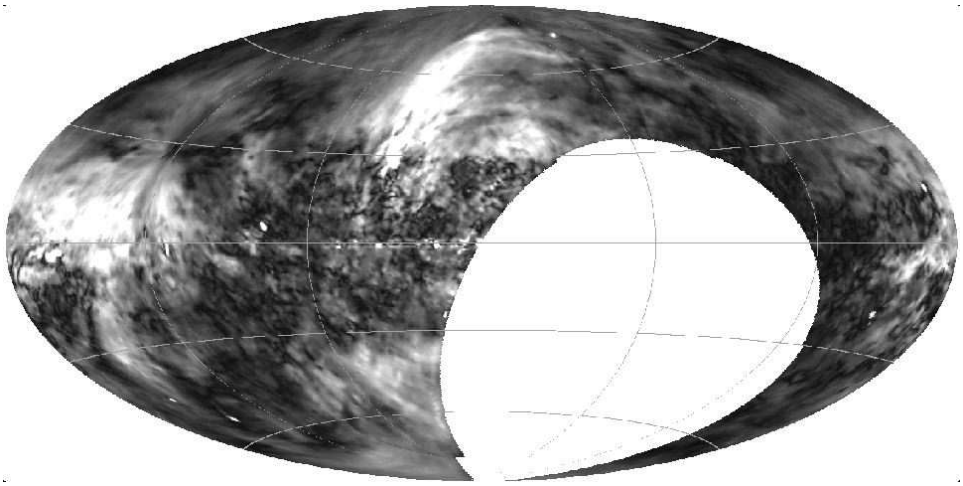

Figure 5.4: All sky diffuse polarization at 1.4 GHz from the survey of Wolleben et al. (2006). The image is in Galactic coordinates with $l = 0°$, $b = 0°$ at the centre.

Unique insights on Galactic magnetism and the mechanisms required to create and maintain it can only be obtained from study of the magnetic field in the halo. The widely observed uniform large-scale magnetic field components are thought to be the result of dynamo action, although this mechanism is not yet fully understood. Observations of the magnetic field at high latitude will be an important constraint to distinguish among the many dynamo models. Measurements of the rotation measure grid (see Chapter 4) will constrain the large-scale field structure but in order to understand the turbulent properties of the magnetic field structure we also require information about the diffuse polarization. Only measurements of diffuse polarization can confirm whether the halo magnetic field is quies-

cent or if not, on what scales it is turbulent. Similarly, diffuse polarization measurements are necessary to determine where the field transitions to the turbulent disk field and the properties of the transition region.

The magnetic field structure is not easily observed in the Milky Way because of the abundance of small-scale structure obscuring the larger-scale order. To overcome this we can apply a technique known as Faraday synthesis, which makes use of a large observing bandwidth to separate structures according to their rotation measure. The idea behind this is that for each pixel and each frequency observed the polarization vector is derotated so that we have a cube of total polarized emission as a function of rotation measure. This can effectively separate multiple polarized emission layers along the line of sight. The resolution in rotation measure space is determined by the total bandwidth observed, therefore to apply this technique most effectively we seek to achieve the widest bandwidths possible. Furthermore, the maximum observable Faraday depth is related to the inverse square of the channel width.

5.6.1 An All-sky survey of Diffuse Polarization

To probe the turbulent magnetoionic medium in the Galactic halo and disk-halo interface we propose an all-sky survey of diffuse polarization utilising the full frequency range available to MIRANdA. From Wolleben et al. (2006) we know that polarised structure exists at 1.4 GHz down to at least the $\sim$ 12 mK sensitivity limit of their survey. Average rotation measure fluctuations in the Milky Way are expected to be a few tens of rad m^{-2}. The RM resolution achieved depends on the bandwidth used $d\phi \approx 2\sqrt{3}\Delta\lambda^{-2}$ (Brentjens & de Bruyn 2005), such that 500 - 1800 MHz would give us $d\phi \approx 18$ rad m^{-2}, which is marginally sufficient. To ensure that we do not suffer from bandwidth depolarization in regions of high rotation measure that can be found in the Galactic plane we need modest channel widths of $\sim$ 4 MHz. Finally, in order to correctly interpret rotation measures it is crucial that we combine the interferometric survey data with total power information from a single dish. This survey, therefore, will require a survey of comparable sensitivity and frequency coverage conducted with Parkes.

Chapter 6

VLBI Science

6.1 Summary

We describe possible areas of science that can be addressed using VLBI and MIRANdA. A number of scientific programs present themselves when considering the use of MIRANdA as part of the Australian Long Baseline Array (LBA) and the global VLBI array. Better angular resolution at L-band, better sensitivity, and better (u,v) coverage will aid standard VLBI observations of OH masers, pulsars, and AGN. An innovative additional capability for MIRANdA is multibeaming. If this can be harnessed for VLBI in the form of multiple phased array beams, a number of wide-field survey observations become feasible.

In time, MIRANdA should also become a part of the recently developed Australian e-VLBI network, currently called PAMHELA. An interesting possibility is to not use MIRANdA as part of the LBA, but use it as a source of trigger information for radio transients, as part of MIRANdA survey work. These triggers could be transmitted to PAMHELA, and the candidate sources targeted at high angular resolution in rapid follow-up observations. The combination of MIRANdA and PAMHELA would be unique and powerful. PAMHELA would add great scientific value to the low resolution detection of transients by MIRANdA.

At this point the VLBI community support the extension of the MIRANdA frequency range to S-band but recognise several alternatives to this that may be more cost effective, such as the upgrade of the Ceduna antenna to L-band and/or the use of one of the AuScope geodetic antennas in WA at S-band. All these options should be studied a greater length. The addition of antennas to MIRANdA beyond the current plans will make for a more

sensitive VLBI array but will not materially open up new areas of science for VLBI.

6.2 Introduction

MIRANdA consists of an array of 30 antennas of 12 m diameter, with a maximum baseline of up to 8 km, with a frequency range of perhaps 0.8−2.4 GHz. Used as a phased array, MIRANdA would have a sensitivity approaching that of Parkes. Good sensitivity, plus its location on the west coast of Australia means that MIRANdA can potentially provide substantial gains for Australian and global VLBI in at least the frequency range 1.4−1.7 GHz (L-band).

Within L-band, a number of VLBI science applications are possible, using MIRANdA as an additional element in the LBA. Given the phased array field of view of approximately 5 arcseconds, the following observations could be usefully made:

- Pulsar proper motion and parallax observations benefit from good sensitivity on long baselines in order to do the best possible astrometry. The relatively low frequency of MIRANdA is optimal for pulsars;
- OH Maser observations benefit from good sensitivity on long baselines, important to resolve individual maser spots;
- Active galactic nuclei (AGN) only require a narrow field of view. The addition of long, sensitive east-west baselines is critical for performing high dynamic range imaging of the often complex mas-scale jet radio sources. Further, use of MIRANdA along with RadioAstron observations will be possible, examining AGN on the longest possible baselines to investigate brightness temperature limits in AGN.

If it is feasible (given the multi-beaming capabilities of MIRANdA) to form multiple, independent phased arrays beams, it will be possible to undertake some forms of wide-field imaging, whereby different beams are pointed to different sources, which all lie within the much larger primary beams (compared to the phased array beam width) of the other Australian telescopes. In this way, MIRANdA will be capable of participating in in-beam phase referenced observations (as are important in pulsar VLBI) to gain extra sensitivity. For observations which are not sensitivity limited but require a large FoV and the (u,v) coverage of MIRANdA, the option exists to

tie a subset of more closely spaced antennas, sacrificing a small portion of collecting area to increase FoV.

Finally, interesting science is possible with MIRANdA if we consider it as a complementary facility to the recently developed Australian e-VLBI capabilities. In particular, some of the most significant work MIRANdA will undertake will come from fast, sensitive, high resolution surveys of the entire radio sky. These surveys will uncover radio transient sources in the mJy regime, which should ideally be rapidly followed up at VLBI resolution to examine the details of their structure and evolution. In this case, MIRANdA can provide trigger information for real-time e-VLBI observations.

On the question of extending the upper frequency of MIRANdA to a frequency of 2.4 GHz, this would be greatly beneficial to the Australian VLBI array, since Ceduna does not have a L-band system and the best (u,v) coverage requires Ceduna and MIRANdA, and because S-band is a sweet spot in terms of sensitivity across the LBA. As such, for VLBI, extending the MIRANdA frequency range to include S-band is strongly encouraged by the Australian VLBI community.

However, an alternative option could be an L-band upgrade of Ceduna in the medium term, to achieve the best (u,v) coverage at L-band, rather than extend the MIRANdA frequency range for the best (u,v) coverage at S-band. It is also recognised that the AuScope geodetic VLBI antennas funded through NCRIS 5.13 will operate at S-band and one will be sited in Western Australia. It is possible that this antenna could be used at S-band for LBA observations if available. This antenna would not have the sensitivity of MIRANdA, but would provide filling of the (u,v) plane and satisfy a number of science requirements for the applications listed in this document.

We recommend that further work be done to characterise the costs and benefits of a) extending MIRANdA to S-band for VLBI; b) upgrading the Ceduna antenna for L-band; c) using the AuScope antenna in WA for astronomical VLBI.

6.3 MIRANdA as a component of the LBA

MIRANdA will be an additional antenna in the LBA and will also be capable of participating in global VLBI experiments, at frequencies of 1.4 and 1.6 GHz. Using a single phased array beam from MIRANdA with the existing Australian LBA will allow many VLBI experiments to be performed, those that do not require a field of view larger than a few arcseconds in diameter

(due to the phased array field of view limitations of maximum baseline lengths of 8 km). These experiments include observations of AGN and of pulsars.

6.3.1 (u,v) coverage

Figure 6.1 shows the improvement in the (u,v) coverage by including MIRANdA in the LBA at 1.6 GHz. The maximum baseline is greatly increased and east-west baselines are formed to complement the north-south baselines of the east coast antennas.

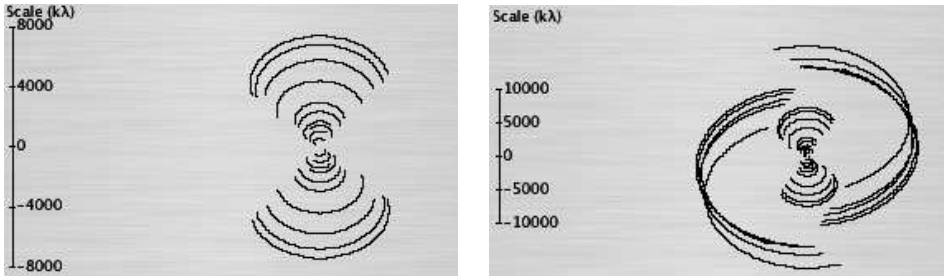

Figure 6.1: LEFT: (u,v) coverage of the LBA at a frequency of 1.6 GHz (ATCA, Parkes, Mopra, Hobart, Tidbinbilla) for a source at $\delta - 45$ degrees observed for 12 hours. RIGHT: The (u,v) coverage from an identical observation but including MIRANdA in the LBA.

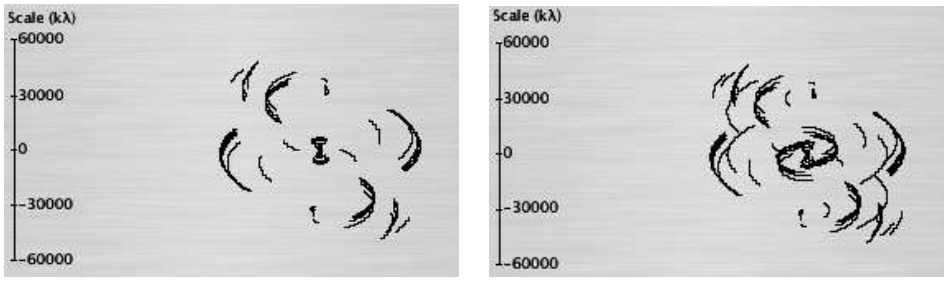

Figure 6.2: LEFT: (u,v) coverage of a global VLBI array at a frequency of 1.6 GHz (ATCA, Parkes, Mopra, Hobart, Tidbinbilla, Kashima, Hartebeesthoek, VLBA_OV, VLBA_MK) for a source at $\delta - 30$ degrees observed for 12 hours. RIGHT: The (u,v) coverage from an identical observation but including MIRANdA in the global array.

Significant gains are also apparent for global VLBI observations that

use MIRANdA. Figure 6.2 shows the improvement in (u,v) coverage by the addition of MIRANdA into an array of antennas in Australia, Japan, South Africa, and the USA. MIRANdA significantly closes a number of holes in the (u,v) coverage.

6.3.2 Sensitivity

For the observational cases shown above in Figure 6.1, the sensitivity (1σ image rms) of the LBA alone is 25 μJy/beam (assuming a bandwidth of 128 MHz, dual polarisation at ATCA, Parkes, Mopra and 64 MHz, dual polarisation at Hobart and Tidbinbilla). Along with three times the angular resolution, the inclusion of MIRANdA (at 128 MHz dual polarisation) improves the sensitivity of the array to 18 μJy/beam.

For the observational cases shown in Figure 6.2, the sensitivity of the global VLBI array is 22 μJy/beam. Although the inclusion of MIRANdA does not add longer baselines to the global array, it significantly improves the (u,v) coverage, particularly on intermediate baselines and improves the sensitivity to 17 μJy/beam.

6.3.3 Potential observational programs

OH Masers

The ground-state lines for the hydroxyl radical (OH) occur at a frequency of about 1650 MHz. OH is a common molecule and has been observed to undergo maser action in a variety of astrophysical environments. Maser emission from the main-lines at 1665 and 1667 MHz are commonly observed towards high-mass star formation regions, while emission from the satellite line at 1612 MHz is common towards late-type stars and 1720 MHz masers are observed in regions where supernova remnants are interacting with molecular gas.

High resolution observations from long baseline arrays show highly complex and varied structures for the various maser species associated with high-mass star formation regions, with spherical expansion, bipolar outflows, disks and rings, bow-shocks and infall. The different maser species typically trace different parts of the star forming regions. Combining high-resolution OH imaging with observations of methanol and water masers, and the high velocity resolution dynamical information it is possible to image and interpret the three-dimensional distribution of masers in great detail, and in some cases to obtain proper motions and accurate distance estimates. The inclusion of MIRANdA as an element of the LBA will significantly increase

the resolution of OH maser observations and make them comparable to that which can be achieved for the higher frequency methanol and water maser observations using only the existing LBA.

Magnetic fields play a critical role in star birth and star death. OH masers provide an excellent means of studying the magnetic fields in the regions where they are located, as strong polarization is observed from the Zeeman effect with line-splitting that is often significantly larger than the line width. Magnetic fields of several mG are typically measured in both star-formation regions and stellar winds. Multiple spectral components and variations in the magnetic field strength within a region means that VLBI observations are required in order to unambiguously identify Zeeman pairs and hence obtain accurate magnetic field estimates.

OH masers (strongest in the 1667 MHz transition) have also been detected towards late-stage mergers which are ultra-luminous infrared galaxies (ULIRGs). Much of the maser emission in these sources is diffuse and resolved out on long baselines, however, compact emission is observed where the masing gas amplifies compact background sources such as supernovae in the host galaxies. Through observing the changes in the compact emission over time it is possible to investigate the supernova rate in these starburst regions, which cannot be done through other means.

Pulsar parallaxes and proper motions

VLBI astrometry of pulsars is crucial for obtaining model-independent distances and transverse velocities, and thus calibrating the pulsar distance scale, luminosity function and Galactic electron distribution (see e.g. Brisken et al. 2002). However, pulsars are difficult targets for VLBI. Many are comparatively weak, requiring sensitive VLBI arrays, and their steep spectral indices force observations to be undertaken at low frequencies, typically L-band. Observing at low frequencies both decreases angular resolution, requiring higher signal to noise detections and better control of systematic errors to obtain a given positional accuracy, while simultaneously increasing systematic uncertainties due to larger phase errors from rapidly changing ionospheric gradients.

The LBA is the only existing Southern VLBI array that is sensitive enough to undertake astrometry studies of faint pulsars. However, the existing LBA is limited in its capabilities for L-band astrometry. This is primarily because the Ceduna 30m telescope in South Australia does not possess an L-band receiver, due to its beam waveguide construction. Without Ceduna, the LBA is reduced to a roughly north-south arrangement of telescopes,

with a detrimental effect on (u,v) coverage. The Ceduna baselines are the longest in the LBA, and their removal roughly doubles the extent of the synthesised beam in the east-west direction. Finally, the reduction to 5 antennas (or 4 when, as is common, the NASA DSN antenna at Tidbinbilla is unavailable) reduces the number of available baselines from 15 to 10 (or 6), making control of systematic uncertainties more difficult.

The addition of the phased MIRANdA to the LBA essentially offsets the loss of Ceduna at L-band, but with two additional benefits:

1. Being located approximately 1600 km further west than Ceduna, MIRANdA offers a further doubling of resolution in one axis (i.e. four times the existing L-band resolution); and

2. MIRANdA is much more sensitive than Ceduna, being a 64m equivalent compared to a 30m. Moreover, this sensitivity contributes to the longest baselines whereas currently with the LBA at L-band the longest baselines are to the less sensitive 26m dish at Hobart. When uniform weighting is used (which is typically the case for astrometry), the improvement in image sensitivity is striking: 43 μJy with MIRANdA compared to 98 μJy without, while if Tidbinbilla is unavailable 56 μJy can still be obtained, compared to 140 μJy without MIRANdA. These calculations assume a 10 hour phase referenced observation with a 50% calibrator/target duty cycle.

The combination of these benefits would allow the LBA to target a much wider range of pulsars for astrometry than is presently feasible. Pulsars, kicked by the SN explosion, have high and easily detected proper motions. These have been found to lie along the spin axes (Johnston et al. 2005), and therefore can be used to provide insights into the initial blast of the SN and the pulsar characteristics.

As pulsar astrometry is driven by angular resolution and baseline sensitivity, an S-band capability for MIRANdA would be very useful for proper motion and parallax observations, giving high sensitivity on the longest baselines.

Imaging over wide fields

Adding MIRANdA to the LBA offers a number of interesting opportunities for wide-field VLBI science. The full potential of such an array will depend greatly on the configuration of MIRANdA itself, since the overall field-of-view will be almost completely constrained by its synthesised primary beam.

At L-Band this equates to a field-of-view of $\sim 6''$ FWHM with the entire 8 km array. While this is not useful for large-scale survey work, the combined increase in sensitivity and resolution of this array could be used to survey and monitor supernova remnants in starburst regions as far as 20 Mpc with sub-parsec spatial resolution. Such surveys can be used to determine limits on the star-formation rate and supernova rate in the local Universe (Lenc & Tingay 2006).

For more general VLBI surveys a greater FoV to increase the survey speed would be beneficial. Since the available FoV is inversely proportional to the maximum baseline length an increase in FoV can be achieved by utilising a smaller subset of MIRANdA. For example, if a 1 km diameter core of MIRANdA is utilised as part of the LBA then the available field-of-view can approach $\sim 1'$ FWHM. This of course comes at the cost of reduced sensitivity since only a fraction of MIRANdA would be utilised. To minimise the impact on the sensitivity, the array could be designed with a denser population of antennas in the inner 1 km core. Such an array could be used to survey and study the morphology and population of galaxies in the early Universe (Jackson 2004). Combined with observations at other wavelengths, this would improve our understanding of the evolution of galaxies in the early Universe.

The Focal Plane Array (FPA) receivers on MIRANdA allow a further method to increase field of view. The currently proposed 200 element FPAs have the potential to form up to 50 independent phased array beams, increasing the observable field of view by a factor of 50 in angular area and thus increasing the survey speed by the same factor. When combined with the 1 km subset array a field-of-view as wide as $\sim 7'$ (comparable to the field of view of the Tidbinbilla 70 m antenna at L-band) may be achieved increasing the overall survey speed by a factor of 350. Operating MIRANdA in this way will introduce some technical challenges for VLBI.

Space VLBI and AGN

The nuclei of AGN are structurally, kinematically, and spectrally complex, involving relativistic jets of material on parsec (mas) scales that evolve with time and frequency (e.g. as seen in AGN such as in Centaurus A; see Figure 6.3). VLBI is the only direct method with which AGN and these jets can be probed on mas scales. Of prime importance for AGN VLBI are length of baseline, sensitivity of array, and uniformity of (u,v) coverage. The addition of MIRANdA to the LBA and global VLBI array makes substantial improvements in these regards, as seen in earlier sections.

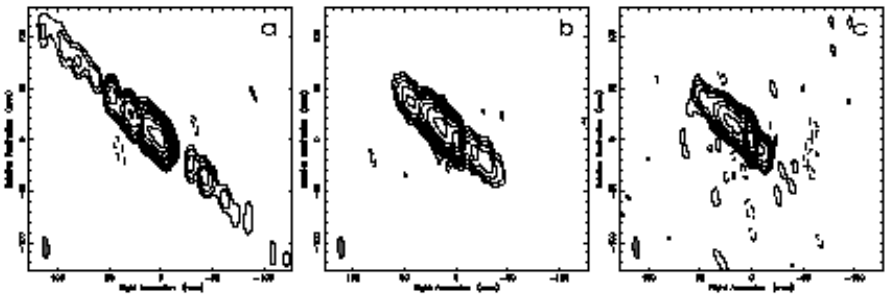

Figure 6.3: Images at 2.3, 4.8 and 8.6 GHz (left to right, respectively) of the AGN jet in Centaurus A, showing the frequency dependent structure on mas scales (Tingay & Murphy 2001).

As well as for complicated radio AGN structures, the inclusion of MIRANdA will add extra sensitivity for the detection and study of weak AGN, at the mJy level. Recent results from the LBA show the value of VLBI follow-up of large area radio surveys such as AT large Area Survey (ATLAS: Norris et al. 2007). A detection of one of these ATLAS sources indicates a radio bright, but infrared faint object. The study of more sources in these radio deep fields with VLBI allows investigation of the importance of star formation vs AGN activity in the early formation of galaxies.

The Russian space VLBI mission RadioAstron is making progress toward launch in 2008 and will operate at 18 cm, within the MIRANdA frequency band. The use of Parkes/Tidbinbilla on the east coast and MIRANdA on the west coast will allow sensitive coverage for Southern Hemisphere RadioAstron observations. The long baselines provided by space VLBI will explore the high brightness temperature limits of AGN. This work carries on from the results obtained from the LBA in conjunction with the VSOP space VLBI mission (Horiuchi et al. 2004; Tingay et al. 2002) which found a large fraction of unresolved nuclei in bright AGN, and intra-day variability work which has found evidence for structures of 10 μas in 56% of flat-spectrum AGN (Lovell et al. 2003, 2007). RadioAstron will be capable of directly resolving these sources for the first time.

Finally, the next generation gamma-ray telescope, the Gamma-ray Large Area Space Telescope (GLAST), will be flying when MIRANdA starts operation. There will be a significant collaborative effort between the GLAST mission and ground-based VLBI arrays in monitoring GLAST AGN targets. As the Southern Hemisphere VLBI array, the LBA would benefit from the

use of MIRANdA for monitoring gamma-ray AGN, both in the detection of weak sources and the study of their high resolution structures. Previous work in the Southern Hemisphere targeting the bright gamma-ray AGN discovered by the EGRET instrument aboard the Compton Gamma-Ray Observatory (CGRO) has been conducted using the LBA (Tingay et al. 1996).

As with pulsar astrometry, AGN observations would greatly benefit from the higher angular resolution and sensitivity possible if MIRANdA had an S-band capability.

6.4 MIRANdA and PAMHELA for rapid transient science

A significant part of the MIRANdA science case involves the rapid survey capability of the instrument and its ability to detect rapid transients in continuum emission. The types of transient that MIRANdA will likely detect include galactic X-ray binaries, gamma-ray bursts (GRB), flaring stellar systems, and possibly supernovae in nearby galaxies. The event rate and detection limits required for each of these transient types varies significantly. Chapter 8 of this document deals with the details of transient surveys with MIRANdA.

In the case of the known and yet to be discovered transients, it is likely that the objects is question will be compact and will have structures that evolve rapidly. This is certainly true of the known transient sources such as X-ray binaries, GRBs, and supernovae. Following detection with MIRANdA, very useful observations could be made with a VLBI array. For example, is compact structure present in the transient source? What is the morphology of the compact structures and how do they evolve with time? What are the multi-frequency characteristics of the transient source above 1.7 GHz? These questions will allow the underlying source of the radio emission (supernova, black hole binary, GRB) to be investigated, determining the emission mechanism at radio wavelengths in combination with possible multi-wavelength observations from high energy and optical observatories.

We propose using MIRANdA in stand-alone mode for transient detection. We propose that transients that satisfy certain criteria trigger rapid follow-up observations with PAMHELA, the Parkes, ATCA, Mopra, Hobart Electronic Long-baseline Array. Example (u,v) coverages for PAMHELA are shown in Figure 6.4.

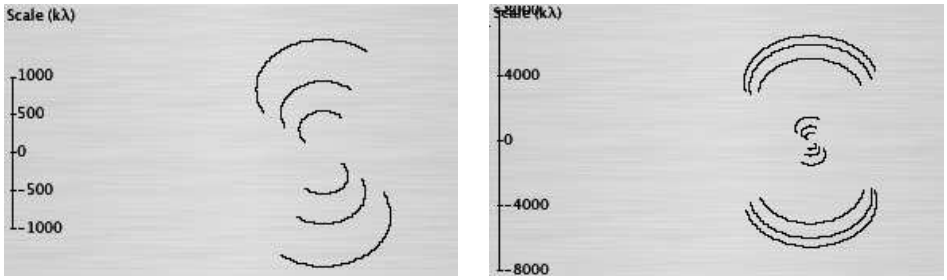

Figure 6.4: LEFT: (u,v) coverage of PAMHELA at a frequency of 1.6 GHz (ATCA, Parkes, Mopra only) for a source at $\delta - 45$ degrees observed for 12 hours. RIGHT: Full PAMHELA (ATCA, Parkes, Mopra, Hobart).

6.4.1 Transient detection with MIRANdA and trigger criteria for PAMHELA

Given uncertainties regarding the transient detection rate from surveys with MIRANdA (see Chapter 8), the definition of trigger criteria at this stage is premature. However, some approximate guidelines can be derived from the capabilities of MIRANdA, the capabilities of the VLBI array, and practical considerations of dynamically scheduled VLBI observations.

Since transients will occur at random times and follow-up VLBI observations would potentially disrupt observers on the Parkes, ATCA, Mopra, and Hobart telescopes, we should adopt strategies that limit the disruption to ATNF users. Given the MIRANdA $1 - \sigma$ sensitivity in a 60 second pointing of 0.3 mJy and assuming five sigma is required for a transient detection (1.5 mJy), an observation with Parkes, the phased ATCA, and Mopra would require an integration time of approximately 160 seconds to detect such a source at the same significance (assuming it to be unresolved) on the ATCA-Parkes baseline.

We envisage a system in which transient detections greater than 2 mJy trigger a PAMHELA observation of approximately 15 minutes, under certain circumstances. The trigger criteria for PAMHELA observation could therefore look something like:

- Is transient detection by MIRANdA > 2 mJy at 1.6 GHz?
- Is the transient at an hour angle that can be observed by PAMHELA for > 1 hr?
- Is a suitable phase reference source nearby on the sky?

- Is a 1.6 GHz observation currently possible at all antennas? Is PAMHELA follow-up possible at another frequency?
- Are scientific programs at the PAMHELA antennas highly ranked enough that disruption should not occur?

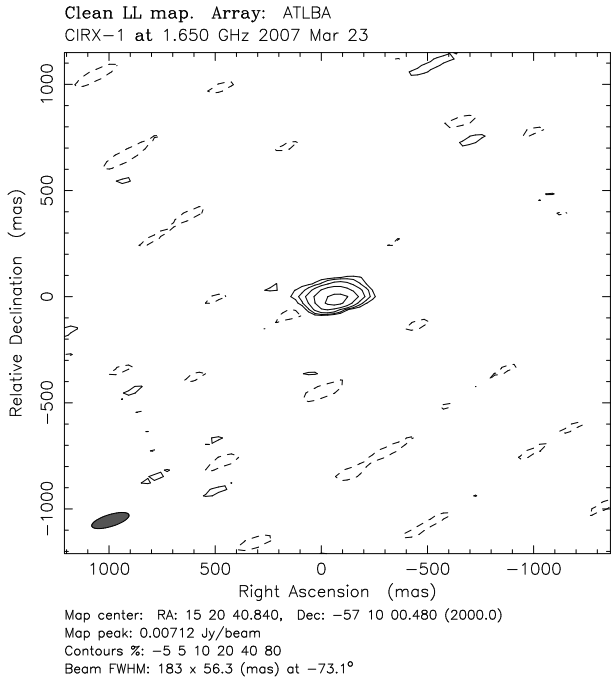

Figure 6.5: An e-VLBI image of Circinus X-1 from March 2007, realised with PAMHELA running at 256 Mbps. The total flux of the compact component is approximately 10 mJy. Observations were approximately 3 hrs in duration over 2 nights.

6.4.2 e-VLBI capabilities and example science

The capabilities for e-VLBI in the form of PAMHELA, are currently under development as a collaboration between ATNF and the Swinburne University of Technology, who provide a software correlator (Deller et al. 2007a). Recently (March 2007) the first PAMHELA observation of the X-ray transient Circinus X-1 was conducted at a data rate of 256 Mbps on Parkes, the ATCA, and Mopra and at 128 Mbps on Hobart (Phillips et al. 2007;

see Figure 6.5; Deller et al. 2007b). These successful PAMHELA tests lay the basis for rapid VLBI follow-ups of MIRANdA transient detections. As PAMHELA, as an e-VLBI instrument, is demonstrating technologies relevant to the SKA (long haul data transmission via fibre and real-time correlation), it is important to aim to include MIRANdA as an extension to PAMHELA as soon as is practically possible.

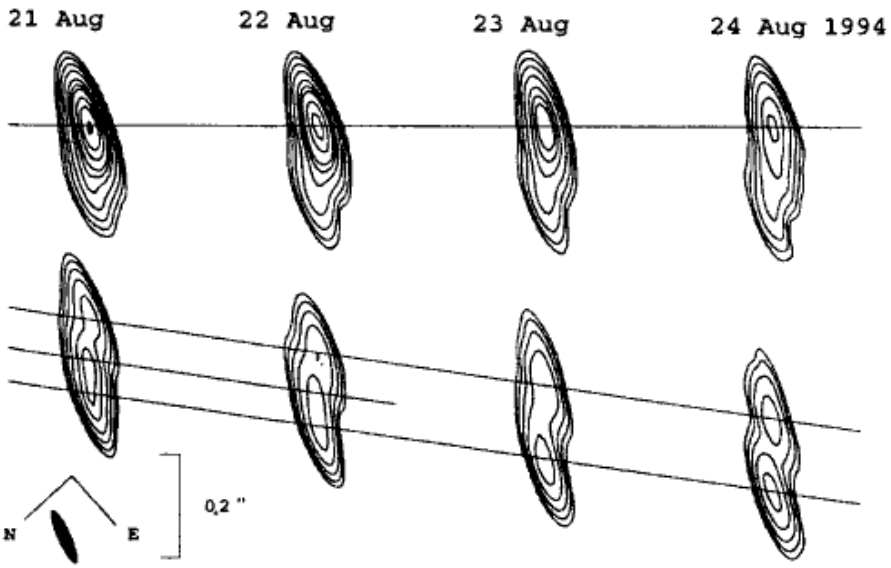

Figure 6.6: Discovered with MOST, using a trigger instrument analog to MIRANdA, GRO J1655−40 was observed with rapid turnaround using the Parkes-Tidbinbilla interferometer (PTI) to determine compact structure. This montage made from four LBA observations planned and executed based on the rapid PTI results (Tingay et al. 1995).

X-ray binary systems such as Circinus X-1 are a major target for PAMHELA observations triggered by MIRANdA. The X-ray binary GRO J1655-40 was studied 10 years ago using a similar system (see Figure 6.6). GRO J1655-40 was an X-ray binary with multi-Jy radio emission which revealed apparent superluminal motions in the compact jet components (Tingay et al. 1995). The goal of the transient studies would be to investigate the properties of the X-ray transient population up to two orders of magnitude weaker in radio emission, at the mJy level.

6.4.3 Issues

The dynamic scheduling of PAMHELA to respond to MIRANdA transient detections would likely require a significant software effort to implement, and a high level of coordination between the ATNF observatories. The advantage of such a system is that every interesting transient can potentially be followed up with PAMHELA observations.

It may turn out that such a system is impractical, however. A logistically simpler but scientifically perhaps less useful approach would be to schedule dedicated PAMHELA time periodically during MIRANdA transient surveys. In this way, perhaps 12 hours per week could be scheduled for PAMHELA to observe all MIRANdA transients detected over the period of the previous week.

Chapter 7

Pulsar Science

7.1 Summary

Since the discovery of pulsars (Hewish et al. 1968), Australian telescopes have played a major part in the discovery of new pulsars, using pulsars as tools for the study of gravitational physics and the interstellar medium and for investigating the properties of neutron stars. The commissioning of MIRANdA will provide the transition between the use of large single-dish instruments (such as Parkes) to using large numbers of small antennas with a wide field-of-view (FoV) as is likely in the final mid to high frequency SKA design.

Historically it has been common to carry out pulsar research using large single dish instruments. MIRANdA provides a pathway between the current systems and the full-scale SKA. MIRANdA will be ideal for carrying out relatively fast all-sky surveys that will allow ~ 1000 pulsars to be discovered. It will be possible for MIRANdA to continue to observe these (and previously known) pulsars in order to determine their astrometric, spin and orbital parameters. MIRANdA will, for a few millisecond pulsars, be able to provide data suitable for integration into a global timing array project which aims to detect low-frequency gravitational wave sources. The proposed extension to MIRANdA will allow a significant increase in the number of pulsars discovered during surveys and will improve the ability of the instrument to time millisecond pulsars with high accuracy.

The pulsar survey proposed here is severely computational limited and this becomes worse as the square of the maximum baseline length. It is therefore necessary that as many short baselines as possible be present in the configuration of MIRANdA. For pulsar timing, there is no such requirement;

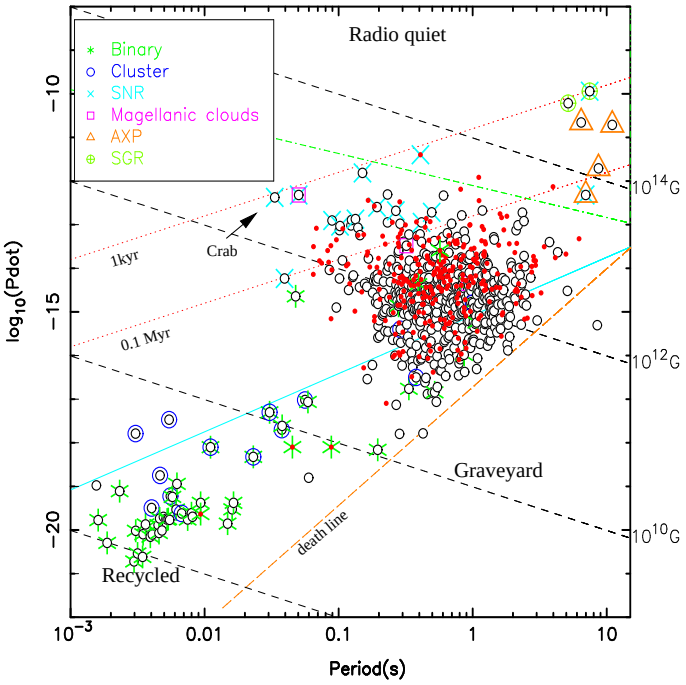

Figure 7.1: The Period-Period derivative plane for the currently known pulsars.

any configuration is adequate. The proposed expansion of MIRANdA is good for two reasons. First, it should ensure more short baselines are present in the array. Secondly, the reduction in the system temperature increases the instantaneous sensitivity, vital for timing and crucial for reducing the computational load in the survey.

7.2 Searching for pulsars

The current pulsar catalogue lists 1772 known pulsars (Manchester et al. 2005). Approximately 880 of these were discovered using the Parkes 20 cm multibeam receiver (e.g. Manchester et al. 2001). Pulsar surveys need to take into account that 1) a typical pulsar only radiates strongly for a small percentage of its period, 2) post-detection filtering and the propagation of the signal through the interstellar medium broaden the observed pulse widths, 3) the pulsar signal is also dispersed as a function of frequency

due the interstellar medium, 4) pulsars have a wide range of periods from $\sim$1 ms to 10 s, and 5) pulsars are usually intrinsically weak radio sources. We highlight the different types of known pulsars and their range in pulse periods and spin-down rates in Figure 7.1.

Pulsar surveys are clearly designed to maximise the number of new pulsars discovered which leads to a choice between observing frequency, back-end systems and sampling time within the instrumental constraints. The observing frequency of $\sim$1 GHz, the on- and off-line processing power and the large FoV makes MIRANdA a powerful instrument for carrying out a new pulsar survey. It is essential to continue undertaking pulsar surveys to detect weaker pulsars and objects missed in previous surveys. Pulsars may not have been found in previous surveys due to interference in the data, the pulsar being "switched off" for long time periods or the neutron star precessing and moving the radio beam into and out of our line of sight. The science case for detecting new pulsars is wide-ranging and includes:

- The ability to improve models of the pulsar population and hence determine birth rates and the Galactic distribution (e.g. Vranesevic et al. 2004.)

- The discovery of unique objects, particularly highly relativistic binary systems including pulsar-black hole binary systems. Many unexpected discoveries will be made in future surveys.

- The discovery of pulsars useful for specific topics of research. These include young pulsars for probing the neutron-star interior and highly stable millisecond pulsars for inclusion in pulsar timing array projects (see Section 7.3.2).

- Mapping the electron density distribution of the Galaxy. Any pulsar survey provides an estimate of a pulsar's dispersion measure. Combining this measurement with an estimate for the pulsar's distance (obtainable using timing, VLBI or HI absorption studies) allows the mean electron density in the direction of the pulsar to be determined (e.g. Cordes & Lazio 2002.)

- Determining the Galactic magnetic field. Combining measurements of pulsar rotation measures and dispersion measures provides a measurement of the magnetic field strength along the line of sight to the pulsar. Combining these values with estimates of the pulsar distances allows the Galactic magnetic field to be mapped (e.g. Han et al. 2006).

- Understanding the pulse emission mechanism. As the number of known pulsars increases so does the variety in pulse profiles, polarisation and fluctuation properties. A more complete understanding of the pulse emission mechanism will only occur from the careful analysis of these properties for a large sample of pulsars at multiple observing frequencies (e.g. Karastergiou & Johnston 2006).

MIRANdA will be able to perform sensitive all sky pulsar surveys. A straight-forward survey described below would be 10 times more sensitive than previous all-sky pulsar surveys carried out in the Southern hemisphere and could detect up to 1600 new pulsars.

7.2.1 An example all-sky survey

The unique capability of MIRANdA that enhances pulsar surveys is the simultaneous availability of multiple beams covering a large FoV allowing the rapid survey of large areas of the sky. The survey speed of the telescope, given in equation 1.2 suggests that MIRANdA will be 13× faster than the Parkes Multi-beam Pulsar Survey that detected 750 new pulsars in a 10°-strip of the Galactic plane (Manchester et al. 2001) and ∼ 350× faster than the previous Parkes all-sky survey (Lyne et al. 1998) carried out 436 MHz. However, the caveat here is that we need to able to record and process (coherently) the gigantic data requirements such a survey entails. We return to this below.

We suggest a survey with MIRANdA which occupies ∼100 days of observing time and covers the 30,000 square degrees of visible sky. Each 30 square degree single pointing therefore is observed for ∼150 min. Such a survey, with the strawman MIRANdA parameters, would equal the sensitivity of the Parkes Multi-beam Pulsar Survey and would be 10 times more sensitive than the previous Parkes all-sky survey.

Simulations (Lorimer; private communication) show that such a survey would detect 1600 pulsars with periods greater than ∼ 40 ms, about half of which would be new discoveries. Many of the new detections would be low-luminosity objects; a large sample of low-luminosity pulsars is important in defining pulsar birthrates and evolution. Furthermore, even though this proposed survey would not be sensitive to millisecond pulsars, many exotic objects have longer periods including the original binary pulsar PSR B1913+16 (Hulse & Taylor 1975), pulsars with high-mass companions and relativistic systems such as PSR J1141−6545. It is likely that any pulsar companion to a black hole would be slow spinning and the survey described here might

find such an object. Finally this survey would be sensitive to transients with pulse widths greater than 10 ms or so.

Requirements

The computing requirements for the pulsar survey are very large. The rate at which the data must be collected is given by

$$\mathrm{DR} = \tau \times c \times b \times M \times B \tag{7.1}$$

where τ is the sampling rate, c is the number of channels across the band, b is the number of bits, M is number of beams and B the number of baselines. For the MIRANdA parameters, a survey for millisecond pulsars with $b = 8$, $c = 512$, $\tau = 10000$ gives a data rate of $\sim$65 Gbytes/sec, much too large by a factor of at least 100. Therefore, we are forced abandon a search for MSPs and rather settle for parameters like $b = 2$, $c = 64$, $\tau = 200$ which yields a data rate of $\sim$40 Mbytes/sec and single pointing requires $\sim$450 Gbytes of disk storage. This sort of data rate implies that the data can be sent down the optical fibre to the processing centre in Geraldton/Perth.

Data processing involves first forming a time series for a given pixel within each primary beam (computationally cheap) and then using standard pulsar search techniques. The amount of processing power need scales as

$$\mathrm{PP} \propto L^2 D^{-2} M \tag{7.2}$$

where L is the maximum baseline length and D the dish diameter. This equation implies that minimising L is vital for data processing. For the survey described above, if L is of order $\sim$1 km the survey processing (assuming a 100 node cluster) will take a factor 10x more than observing time.

7.3 Timing pulsars

The assumption that a pulsar is a regular rotator that follows a predictable slow-down model forms the basis of a powerful technique for finding its rotational, positional and orbital properties. Pulsars are commonly divided into three categories:

- The millisecond pulsars are fast spinning and have small spin-down rates. These pulsars are extremely stable and their signals can be used for testing relativistic orbital mechanics, probing structures in the interstellar medium and even for detecting a background of gravitational waves.

- The normal pulsars have much stronger magnetic fields than the millisecond pulsars, are younger and often exhibit large and often unpredictable variations in their periods. Timing analyses of young pulsars have allowed their astrometric, binary and spin-down parameters to be determined leading to improved formation and evolution models. Sudden increases in the pulsar's spin rate (known as glitches) are the only probe of the superfluid interior structure of neutron stars and lead to fundamental insights into the behaviour of matter under extreme densities and pressures.

- The unusual pulsars. These include the recently discovered rotating radio transient objects (RRATs) in which only a single pulse of radiation is detected over observations spanning ~ 30 minutes (McLaughlin et al. 2006). A new class of pulsar has also recently been identified in which the pulse shape suddenly changes, or in extreme cases, the pulsar turns off for long periods of time (Kramer et al. 2006). Long-term timing analyses help to elucidate such phenomena. Almost since the discovery of pulsars it has been known that the pulse emission can sometimes switch off for short periods of time. Even with more than thirty years of pulsar observations the physical mechanisms causing these "switching-off" phenomena is still not understood.

There are numerous pulsar timing programs currently being carried out world-wide. Compared to many of the telescopes involved in these projects, the first stage of MIRANdA has a relatively small collecting area, has restricted frequency coverage, high system temperature and small bandwidths. However, MIRANdA has three main advantages: 1) it is sited in the southern hemisphere providing the opportunity to observe pulsars that only one major pulsar-timing telescope (Parkes) can currently see, 2) it is located in the world's most radio-quiet site, which greatly benefits pulsar observations that are very sensitive to radio frequency interference, and 3) the large FoV means that multiple pulsars can be observed simultaneously.

7.3.1 Normal pulsars

Approximately 1800 normal pulsars are currently known. It is likely that this number will significantly increase with the new surveys being undertaken world-wide (and with MIRANdA). In order to achieve maximum science from these discoveries it is necessary to repeatedly observe each pulsar over a data span of approximately one year. After this initial observing period, the basic astrometric and rotational parameters are known and a decision can be

made whether the pulsar is of sufficient interest for continued observations.

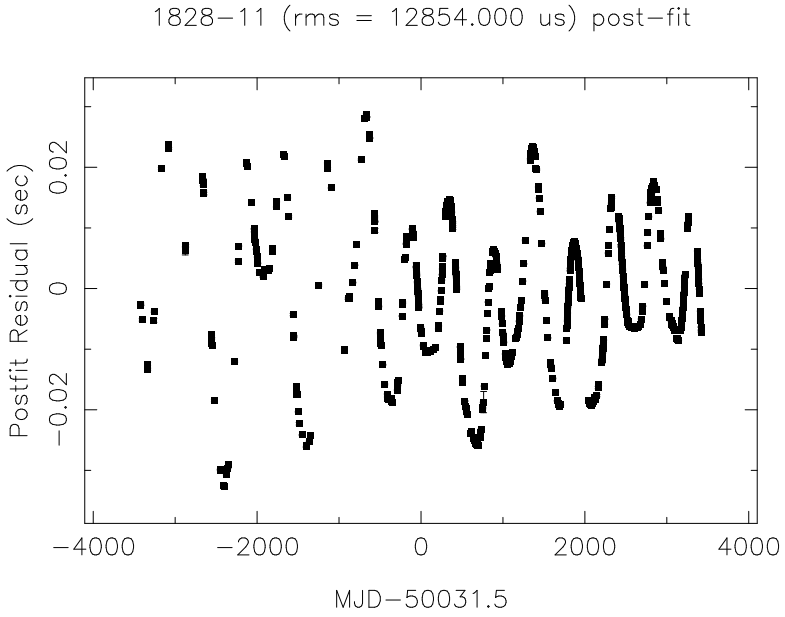

Figure 7.2: The timing residuals for PSR B1828−11 obtained using the Jodrell Bank Lovell telescope. The sinusoidal signal is explained as the neutron star undergoing free-precession.

MIRANdA will be able to monitor all the pulsars discovered during the surveys described above. This would consist of approximately fortnightly monitoring over 12 months with observations typically lasting between $\sim$ 10 min and 1 hr. This will allow the pulsar parameters to be determined and the existence of any interesting binary systems, glitching pulsars or other unusual phenomena to be identified. For instance, we plot the timing residuals for PSR B1828−11 in Figure 7.2. The sinusoidal signal seen in the timing residuals for this pulsar is explained as the neutron star undergoing free precession (Stairs et al. 2000). As MIRANdA can also be used as an imaging interferometer it will be possible to obtain accurate pulsar positions almost immediately. This in turn will allow quicker determination of the other pulsar parameters than would be possible without knowledge of the pulsar's position.

Long-term monitoring of a subset of "interesting" pulsars will be desirable. Observations made every few weeks over the period of a few years

would allow, for example, the determination of proper motions, orbital effects and the careful study of glitch events.

The timing capabilities of MIRANdA will provide the essential ephemerides for southern hemisphere pulsars for the GLAST mission. New discoveries from GLAST can be rapidly timed without disruption at other telescopes, or even at MIRANdA since there can be multiple beams within the large FoV. Large telescopes, such as Parkes, are currently observing many normal pulsars. MIRANdA would be able to reduce the observing load at such telescopes by monitoring multiple pulsars simultaneously.

Requirements

The requirements for the timing of normal pulsars are not stringent. However, it does require that MIRANdA produces a phased-array beam. It is likely that the large FoV will provide the opportunity to observe multiple pulsars simultaneously, thereby reducing the total time required to observe all the requested pulsars. Therefore the creation of multiple phased-array beams within the FoV would be useful, especially if they can be formed independently (simultaneously) with the standard imaging correlator operations. This could allow pulsar timing to be carried out in "piggy-back" mode with other observations. A moderately powerful pulsar backend system is required for each phased array beam and observing frequencies close to 700 MHz would be ideal.

7.3.2 Millisecond pulsars

One of the most exciting modern-day applications of millisecond pulsar timing is to combine data from multiple pulsars to form a global timing array (Hobbs 2005). The aims of such a project are many-fold with the main goal of making a detection of the gravitational wave (GW) background at nano-Hertz frequencies. In brief, GW backgrounds are predicted to occur due to cosmological (e.g. due to inflation, cosmic strings or phase transitions), or astrophysical (e.g. due to coalescing massive black hole binary systems that result from the mergers of their host galaxies) processes (e.g. Maggiore 2000). The background is detected by looking for correlations between the timing residuals of pulsars that have a wide range of angular separations (Jenet et al. 2005).

The initial design for MIRANdA does not provide enough frequency coverage, low enough system temperatures nor a large enough aperture to compete with the precise timing data sets being obtained using the Parkes

and other telescopes. However, with careful choice of observing systems, it will be possible for MIRANdA to provide data on a few pulsars that will be useful for a global timing array project. This will reduce the observing requirements at other telescopes. One of the major science drivers for the SKA is to carry out pulsar timing array research. As at least part of the SKA is likely to be built using large numbers of small antennas it is essential that the techniques required to carry out high precision timing using such antennas have been developed and tested. MIRANdA will be the ideal instrument for such studies.

Requirements

The requirements for high precision pulsar timing are many-fold. The observations require high polarisation purity (0.1%), large bandwidths (300 MHz at 1400 MHz a minimum), observing frequencies close to 1.4 GHz (simultaneous observations at both higher and lower frequencies would be advantageous), backends that support on-line pulsar folding (with at least 2048 phase bins and 2048 frequency channels with 8-bit sampling) and on-line coherent dedispersion systems. For this project there are no requirements for long baselines between the antennas, nor for a large FoV, because the number of pulsars useful for high precision timing is small.

7.3.3 Unusual pulsars

The Parkes multibeam pulsar survey has recently discovered rotating transient sources (RRATs) that are thought to be an unusual type of pulsar (see Figure 7.3). MIRANdA provides an excellent instrument for the discovery of more such sources (see Section 7.4). It will also be possible to monitor already known RRATs in a similar fashion to the observations of normal pulsars described above. Similarly, it has recently been realised that some pulsars are undetectable for long times, often many weeks, before "switching-on" and behaving as a normal pulsar for some time, typically a week or two. These pulsars are difficult to study using existing telescopes and with current observing techniques. The large FoV provided by MIRANdA will allow long-term monitoring of these objects (possibly piggy-backing on other uses).

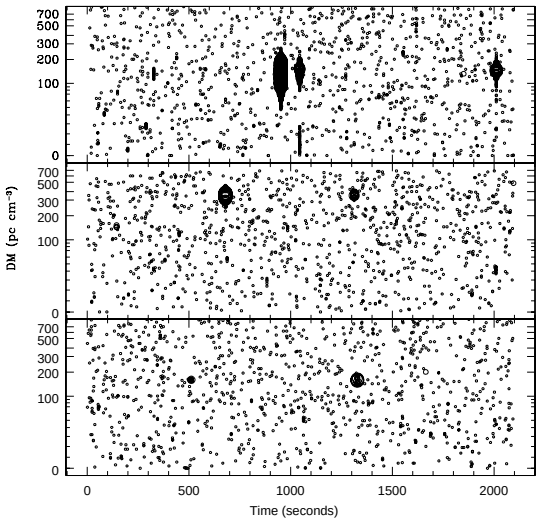

Figure 7.3: Discovery plots of rotating radio transient sources discovered during the Parkes Multibeam Pulsar Survey. Figure reproduced from McLaughlin et al. (2006).

7.4 Fast transients

Fast radio transients, those with periods of 1 s or less, are generally associated with coherent emission processes. Examples of known fast transients include the giant pulse emission from radio pulsars (Johnston & Romani 2003) and flares on the Sun and other active stars. Speculation abounds in the literature as to other putative sources of fast radio transients. Possibilities include the explosions of primordial black holes (Phinney & Taylor 1979) and emission from merging neutron stars (Hansen & Lyutikov 2001). Detecting fast transients is difficult; first because the volume of data necessary to sift through is large and secondly because the effects of dispersion through the inter-stellar and galactic media broadens the pulse. A comprehensive review of fast radio transients and search techniques is given in Cordes & McLaughlin (2003).

MIRANdA potentially opens up new parameter space to fast transients because of its large FoV and interference free environment. A transient search would involve the acquisition, storage and processing of large quantities of data. All these factors scale as the square of the baseline length, so it is only feasible to search for fast transients using extremely short baselines

(likely less than 300 m or so). A very compact configuration is therefore desirable, and even then ultra-fast sampling will be challenging.

It seems likely, at least initially, that fast transients are best detected as part of the pulsar survey with ∼ms type sampling rates. Such a survey would certainly detect RRATs, possibly giant pulses, and retains a possibility of detecting unknown once-off events such as exotic mergers. Targeted observations of selected sources at ultra-fast rates may also be possible, e.g. for searching for giant pulse emission from the nearest galaxies.

Consideration should also be given to establishing a circular transient buffer of duration a few tens of seconds. This would hold data taken at the fastest possible rate. If any external trigger (e.g. a gamma-ray burst) were to arise in the correct part of sky, the buffer could be saved for subsequent analysis.

7.5 Pulsar VLBI

Pulsar VLBI using MIRANdA is covered in detail in Chapter 6 of this document. In brief, the existence of a large interferometry system in the southern hemisphere, with the ability to carry out VLBI between the east and west coasts of Australia will allow many pulsar positions, proper motions and parallaxes to be determined. A single long baseline is adequate for such experiments.

Compared to the northern hemisphere, there are currently few interferometric pulsar parallaxes measured in the south, mostly because they are difficult to obtain using available instrumentation. Currently the baselines (Parkes - ATCA - Mopra - Hobart) are primarily north-south, and Tidbinbilla offers limited availability. With MIRANdA one gets a long east-west baseline, a high-sensitivity station and an immediate improvement in uv coverage. The focal plane arrays potentially allow observations with multiple beams allowing simultaneous observation of calibrator sources. Even though MIRANdA has limited frequency coverage, the specified range is suitable for pulsar VLBI experiments.

7.6 Expansion of MIRANdA

The expansion option of MIRANdA allows for greater collecting area and lower system temperature. The decrease in system temperature is particularly beneficial for the pulsar survey. The same survey outlined above could be done in half the time (even without the increase in collecting area)

which reduces for the total data volume and the processing requirements of the survey. Pulsar timing will improve with high signal-to-noise pulse profiles leading to improved timing precision. The extended MIRANdA could provide high precision timing data sets of millisecond pulsars comparable with other telescopes if a wide enough frequency coverage is available (an ideal system would be to simultaneously observe at three frequencies close to 600 MHz, 1.4 GHz and 3 GHz).

Chapter 8

The Transient Radio Sky

8.1 Summary

The good sensitivity and large field-of-view make MIRANdA a unique instrument for studying radio transient emission. We strongly expect that MIRANdA will make a unique discovery in the transient parameter space, although it is naturally hard to predict the nature of a new class of transients.

The key to a successful transient instrument is that it have high sensitivity, large field-of-view, good dynamic range and high resolution. MIRANdA fulfills these criteria with its ability to achieve sub mJy sensitivity across the entire sky in a single day observing. Nearly all transients arise from point source objects; high resolution is ideal for obtaining accurate positions necessary for follow-up at other wavebands. It is important also that a wide range of timescales from seconds to months are covered by the transient detector. This implies a careful search strategy for uncovering rare objects.

MIRANdA will most likely suffer from a surfeit of transient sources. This will pose challenges both for imaging and for determining which sources are most interesting and worthy of follow-up observations on other facilities.

8.2 Introduction

It has been the general trend in radio astronomy to move from dipole-like antennas towards parabolic dishes which have much larger forward gain at the expense of a much smaller field-of-view. Consequently, this severely limits the possibility of detecting (random) transient events and the transient sky in the radio is only poorly characterised. At the same time, many

classes of objects are known to be variable radio sources including the Sun, the planets, cool stars, stellar binary systems, pulsars, supernovae (SN), gamma-ray bursts (GRBs) and active galactic nuclei (AGN).

Since the 1990s, large scale, blind surveys for transients in the radio have been performed by a number of groups. Amy et al. (1989) built a transient detector used in parallel with normal observing on the Molonglo Observatory Synthesis Telescope. Although they had good sensitivity and covered a significant fraction of the southern sky in more than 4000 hr observing, they detected only known pulsars. Katz et al. (2003) used detectors in three locations across the USA and observed the entire visible sky over a period of 18 months with a sensitivity of $\sim$27 kJy to transients with periods longer than 0.1 s. The widely separated antenna locations allowed rejection of interference and the only astronomical sources they detected were solar bursts. Matsumura et al. (2007) observed the sky at a declination of 41.5 degrees for 27 continuous days. They detected two transient sources with flux densities in excess of 1 Jy which were only present on a single day. The origin of these transients is unclear.

Transients can be conveniently divided into fast (1 second or less) and slow transients; fast transients are dealt with in Chapter 7 and will not be considered further here. Detection of fast transients involves a significant computational load in contrast to slow transients which can be detected directly in the u-v plane using the normal data flow through the imaging correlator. In this chapter we consider the known classes of transients and their likely detection rate by MIRANdA. We then speculate on what new classes of transient sources MIRANdA might detect in a blind survey.

8.3 Gamma-ray bursts

Gamma-ray bursts (GRBs) are associated with the most explosive events in the Universe. In the gamma-ray band, they occur approximately twice per day and are visible out to redshifts in excess of 6. The afterglow of the GRB fades over time and is detected in X-ray, optical and radio bands. In the radio, the power-law decay of the light curve can be modified by the effects of interstellar scintillation causing fast time variability. The high rate of GRBs means it is not practical to follow them all in the radio band using conventional interferometers like the VLA and the ATCA.

There are about 600 GRBs per year and, in the radio, some 25% are expected to remain visible above 0.1 mJy for $\sim$30 days (Carilli et al. 2003). This implies some 75 GRBs per year would be visible by MIRANdA in the

southern hemisphere and the study of their light curves would thus provide a large increase in our knowledge in the evolution of these sources at late times.

GRBs are almost certainly beamed in gamma-rays; this implies that we only detect some fraction of the total population. However, it may be possible to detect so-called orphan GRBs without the initial gamma-ray trigger by looking for variable radio sources. Levinson et al. (2002) performed such a search by using data taken with the VLA for the NVSS and FIRST surveys. They detected 9 transients sources present in one data set but not the other. They conclude that several hundred radio afterglows of GRBs should be present in the sky at any one time above a level of 1 mJy, similar to predictions made by Totani & Panaitescu (2002).

8.4 Supernovae

MIRANdA could provide a census of radio-loud supernovae in the nearby Universe. These sources have variability timescales of days or weeks, and a MIRANdA survey which reached 1 mJy detection levels over this period of time could probe out to at least 50 Mpc (Gal-Yam et al. 2006) for this type of event. Furthermore, detection in the radio does not have the biases inherent in optical surveys such as dust absorption in the host galaxy.

8.5 Active Galactic Nuclei

It has become clear over the last decade that AGN variability falls into two categories. Many, indeed most, AGN are intrinsically variable with slow modulations in flux with timescales of months to years. In contrast, some AGN show deep flux modulations in less than a day. These are now known to be caused by scintillation in the interstellar medium of our Galaxy.

8.5.1 Intrinsic Variability

Fiedler et al. (1987a) observed a set of 33 AGN, with flux densities of a few Jy, every day for more than 6 years. All sources were variable over this time span with typically smooth variations in flux with quasi-periods of months to years. It is clear that MIRANdA will see this sort of variability over the whole sky as a matter of course and be able to produce light curves for a large number of AGN sources. Indeed, this intrinsic variability may be problematic for calibration as MIRANdA will use a global sky model as an

initial approximation used to calibrate a particular field. Strong variable sources need to be tracked in order to ensure the viability of the calibration process.

8.5.2 Intra-day variable sources

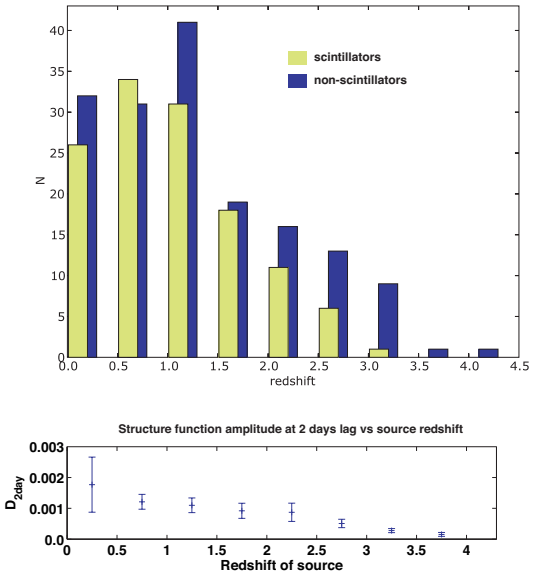

Figure 8.1: The redshift dependence of scintillation observed in the MASIV survey. The top panel compares the redshift distributions of sources that showed significant variability and those that did not. The bottom panel shows the drop-off in scintillation amplitude with redshift, using the amplitude of the structure function as a measure of the variability amplitude on timescales up to 2 days.

A subset of compact quasars show variability on timescales of less than a day; the intra-day variable (IDV) sources (Kedziora-Chudczer et al. 1997). IDVs are of astrophysical interest because the small angular sizes ($< 50\,\mu$as) that they must possess in order to exhibit interstellar scintillation require them to possess brightness temperatures near or, in many cases, several orders of magnitude in excess of the 10^{12} K inverse Compton limit for incoherent synchrotron radiation. The cm-wavelength variations observed in AGN on timescales < 3 days are dominated by interstellar scintillation (ISS), rather than intrinsic variability. Two key observations support this: (a) a delay of 1–8 min in the arrival times of the variations at telescopes on different continents as the scintillation pattern sweeps across the Earth (Dennett-Thorpe & de Bruyn 2002, Bignall et al. 2006); and (b) annual cycles in the variability due to the (orbital) motion of the Earth relative to the scattering material (e.g. Bignall et al. 2003). The MASIV survey confirmed the dominance of ISS as the mechanism of cm-wavelength IDV by showing a strong

correlation between H-α intensity (as measured by the WHAM survey) and IDV variability properties (Lovell et al. 2003; Lovell et al. 2007).

A survey with MIRANdA could cover the sky every day to a 5σ limit of 2 mJy, which would detect variability at the 2% level for 100 mJy sources and at the 20% level for 10 mJy sources on a daily basis. This is similar to levels achieved in the (targeted) MASIV survey (Lovell et al. 2003) which found that more than 50% of the sources in the sample were variable. With 17 sources per square degree above 10 mJy in the sky (Jackson 2005), MIRANdA would usefully survey some 350 000 AGN each day. It is useful to ensure that the baselines of the MIRANdA configuration be long enough to exceed the confusion limit, however the stability of the confusing structure in each field from one day to the next would enable variable sources to be identified beyond the confusion limit.

An IDV survey would be most usefully conducted near the upper edge of MIRANdA's frequency band. Studies of IDV at 2 GHz show that the variability timescales for most sources are in the range 2–14 days at an anticipated survey frequency of 1.6 GHz. These timescales are ideally suited to a survey which visits each field once per day. Ultra-fast IDVs can be identified as those whose fluctuations are unresolved on <1 day timescales and followed up with the ATCA and the VLA. The dominant mechanism of variability for IDV quasars at 1.6 GHz is refractive scintillation. The modulation indices of IDVs at 1.6 GHz are expected to be within a factor of two of those at 5 GHz, where most previous IDV surveys have been conducted (and where the scintillation amplitude peaks) for two reasons: (i) in the regime of refractive scintillation the expected magnitude of the scintillations scales only weakly, as $\lambda^{-17/30}$, and (ii) the sources are expected to be smaller relative to the size of the scattering disk. IDV sources display variations at 5 GHz that indicate that their intrinsic angular sizes exceed the Fresnel angular scale and thus that the scintillations are partially quenched. The angular size criterion for unquenched scintillation at 1.6 GHz is 2.5–9 times less stringent than at 5 GHz.

MIRANdA stands to answer several fundamental questions about the super-Compton AGN emission exhibited by IDVs.

- IDVs as probes of the intergalactic medium (IGM). IDVs may provide the first **direct** detection of the ionized baryons in the IGM at $1 < z < 6$ through angular broadening induced by turbulence in the IGM.

  The MASIV survey (Lovell et al. 2007) has shown that few sources above a redshift of 2 are variable (see Figure 8.1). This suppression of ISS as a function of redshift is most likely caused by scattering in

the turbulent ionized IGM, as illustrated in Figure 8.2. The increased scattering experienced by more distant sources as their radiation propagates through more of the IGM causes them possess larger apparently angular sizes and thus to show lower levels of ISS as their radiation propagates through our own Galaxy. The abundant amount of turbulent, ionized material in the IGM at these redshifts is likely the result of injection into the IGM from recently formed AGN and remnants of the epoch of reionization. Energy injected into the IGM at large scales is expected to cascade through turbulence until it eventually dissipates at some small inner scale. Such a process is evident in nearly all astrophysical processes, notably in the interstellar and interplanetary medium (Armstrong et al. 1995, Spangler & Gwinn 1990).

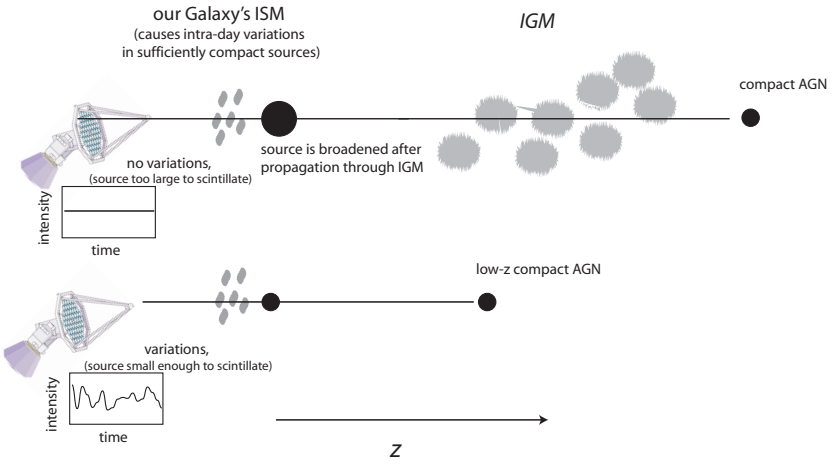

Figure 8.2: An illustration of how intergalactic scattering affects the redshift distribution of the variable sources. Intrinsically compact sources at high redshift are subject to more scattering by the intergalactic medium, which broadens their apparent sizes to a point that they no longer appear compact enough to exhibit ISS.

IGM angular broadening detects of all baryons in the ionized IGM; this is because the process of scatter broadening is caused by phase delays associated with the change in refractive index of the ionized plasma. This is starkly different from the other main probe of the IGM, the Ly-α forest, which is sensitive to a miniscule fraction of the total IGM baryon content; there are estimated to be $\sim 10^5$ ionized

atoms for every Ly-α absorbing atom detected. This technique is sensitive to turbulence on scales from 10^8–10^{11} m, just above the expected turbulence dissipation scale, and can provide a measure of the total energy involved in the turbulent cascade.

The sheer number of sources MIRANdA can monitor would enable us to finely probe the evolution of structure in the ionized IGM as a function of redshift. We could thus probe the evolution of most of the baryonic content of the IGM. However, to make such a contribution, the survey would need to be complemented by optical follow-up to determine the redshifts of the radio sources surveyed.

- IDV is observed to be a highly intermittent phenomenon in most sources. What fraction of IDVs are intermittent, and what is the duty cycle of their IDV? The four-epoch MASIV survey detected variability in 56% of the 482 sources it surveyed. However, most exhibited IDV only over one or two epochs instead of all four. By continuously observing a large sample over a long period (say 30 days) MIRANdA, could comprehensively determine the intermittency properties of IDVs. An intriguing possibility consistent with the MASIV data is that nearly *all* compact AGN exhibit IDV at one time or another.

- MIRANdA could determine whether IDV intermittency is source- or ISM-related. The intermittency could be caused either by fluctuations in the turbulent properties of the intervening ISM or by the emergence of bright μas structure within the source necessary for the source to exhibit ISS. If the intermittency is ISM-related, the character of any polarization fluctuations associated with the IDV should evolve in the same way as the total intensity fluctuations. However, if the intermittency is source-related one expects the polarization variations to evolve in a manner different to those in the unpolarized intensity (e.g. due to reconfiguration of magnetic fields internal to the source).

  A further complication arises because annual cycles in the variability timescale need to be distinguished from true IDV intermittency. However, these two phenomena can be separated by making a number of observations at identical epochs separated by exactly one year. The variations should be dissimilar between epochs if the source variability is intermittent.

- The brightening and fading of IDV in intermittent sources, which MIRANdA could automatically measure in hundreds of thousands

of IDVs, would then address the physics that originates the bright emission in the first place. The survey cadence is sufficiently high for studying intermittency in the IDV, which seems to occur on timescales > 14 days (Kedziora-Chudczer 2006). There is already substantial evidence that IDV intermittency is source-related in several objects (e.g. Macquart & de Bruyn 2007; Senkbeil et al. in prep.). In this case, the rise and fade times of fast variations in IDVs would address the longevity of μas components associated with IDV: the rate at which the AGN supplies energy to power the bright emission to originate the IDV, and the rate at which energy losses cause its eventual decay. These rates can then be compared with specific AGN processes to identify the mechanism associated with the super-Compton radio emission.

8.6 Extreme Scattering Events

Extreme Scattering Events (ESEs) are a type of transient in which the flux variations are not intrinsic to the source but are caused by variations in refraction along the line-of-sight (Fiedler et al 1987b; Romani et al. 1987). In other words ESEs are a lensing phenomenon; not gravitational lensing, but refraction of radio waves in ionised gas. It has long been recognised that the lenses which cause ESEs must be Galactic, probably within a few kiloparsecs, but in the 20 years since the phenomenon was discovered there has emerged no satisfactory physical model for the ESE phenomenon. In part this is a reflection of the difficulty of explaining the existing data using established ideas about the interstellar medium. But another reason for the lack of progress is that there has been very little new data on the phenomenon since the early work (Fiedler et al 1987a, 1994; see Figure 8.3) and the field has stagnated; MIRANdA will address this problem in a comprehensive way.

Why study ESEs? after all the ESE phenomenon is a bit of an oddity which doesn't have any obvious connection with other major areas of current astrophysical activity. Analysis of existing data suggests (Walker 2006) that ESEs are caused by dense gas clouds which are unlike any other catalogued component of the interstellar medium. The data suggest that the individual lenses are spherical, and must therefore be associated with neutral, self-gravitating gas clouds, and that they are present in vast numbers in the Galaxy — probably dominating its total mass. In short the ESE data appear to be revealing the Galaxy's dark matter. Conventional wisdom has it that the dark matter is composed predominantly of weakly interacting elementary

particles, not baryons, so the ESE data offer a direct challenge to one of the prevailing ideas in cosmology.

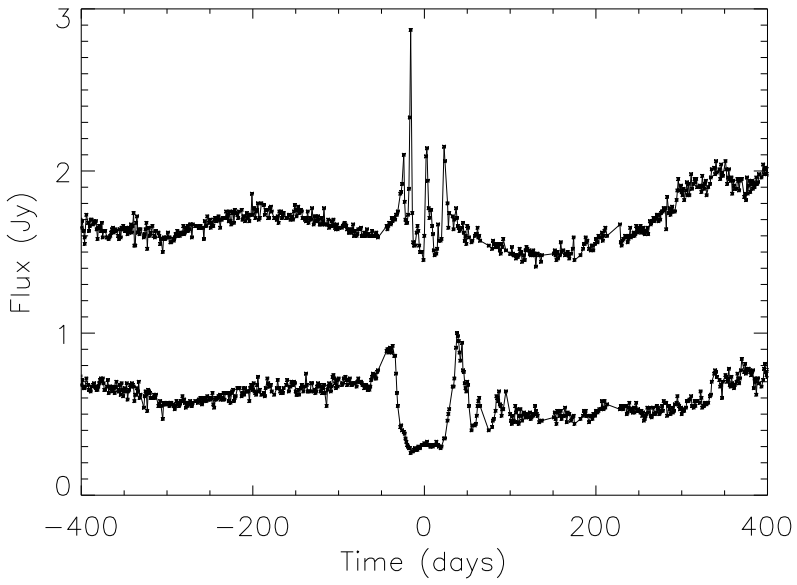

Figure 8.3: The Extreme Scattering Event in Q0954+658, at 8.1 GHz (top curve) and 2.7 GHz (lower curve), from Fiedler et al (1987). An offset of +1 Jy has been added to the high-frequency data for clarity. The mid-point (symmetry point) of the event at Time = 0 corresponds to MJD44650.00. These data were obtained from `http://ese.nrl.navy.mil/`.

Is this a credible challenge given that the data on ESEs are relatively limited, whereas existing data on the Cosmic Microwave Background (CMB) are extensive and of high quality? The challenge is stronger than one might imagine at first. Analysis of the data on CMB fluctuations leads to constraints on the baryonic content of the Universe which are usually stated in the form "the baryonic content of the universe is $\Omega_b = 0.04$" with an error bar (e.g. `http://map.gsfc.nasa.gov`). However, this number is really only a measure of the baryons which are tightly coupled to the radiation field, i.e. diffuse baryons, around the time of recombination — the total baryonic content of the Universe could be much greater than this if most of the baryons are locked up in dense lumps which are only weakly coupled to the radiation field. A similar degree of care is required in interpreting the

abundances of the light elements in the context of Big Bang Nucleosynthesis (BBN) – nobody has measured abundance patterns in the dark matter – and in the context of the present discussion the basic constraint coming from light element abundances is that the dense clouds responsible for ESEs must have formed prior to the BBN epoch. Whether this can be understood in the context of the physics of the early Universe is an open question; but the key point here is that the issue is indeed open: the insight offered by the ESEs is not necessarily in conflict with the CMB and BBN data.

Clearly ESEs merit further study. MIRANdA is a great instrument for this purpose as can be seen by considering the possibilities for monitoring large numbers of compact radio sources. For a nominal FOV of 30 $\deg^2$, with a 20 sec integration and 10 sec of overhead (slewing and settling time), an area of $15,000$ $\deg^2$ can be surveyed in approximately 4 hours, so it is feasible to do this every day. In a 20 sec integration the noise level in a continuum image (300 MHz bandwidth) should be roughly 0.7 mJy at the upper end of the frequency range for MIRANdA (around 1.8 GHz). A 50% flux change can therefore be detected as significant in sources brighter than about 10 mJy, and to this depth there should be 2.2×10^5 radio sources in the survey area (Wall 1994). Roughly 20% of these sources are expected to be "compact" based on the models constructed by Jackson & Wall (1999); here we take "compact" to mean that the source is small enough in angular dimension to be able to exhibit an ESE, so that there are ~ 45000 sources in the survey area which have the potential to exhibit an ESE. (Clearly this is not the meaning originally intended by Jackson & Wall (1999), but we lack the information necessary to make a better estimate ourselves.)

The existing data (Fiedler et al. 1994) have a total coverage of approximately 600 source-years, a four-year ESE survey with MIRANdA will improve on this by a factor of roughly 300. There will be a number of benefits which follow immediately from the increased coverage, namely: better definition of the light-curves of ESEs; information on the number and distribution of lenses in the Galaxy; and measures of the clustering of the lenses. What is even more important, however, is the possibility of discovering ESEs in real time, while the events are in progress, and studying them in detail with instruments other than MIRANdA. Events like those seen by Fiedler et al. (1994) in Q0954+658 and Q1749+096 should be seen at the rate of roughly 60 per year, with 10 in progress at any gven moment. We could study individual events with full polarisation information, good temporal sampling and good frequency coverage (e.g. complete sampling of the 1 to 9 GHz interval); and all this at high signal-to-noise ratio. Such data would be of tremendous value. We would do better still if we could also obtain high

resolution (VLBI) images of the evolving source structure during the events, showing how the lenses distort the appearance of the source at various times. Multiple imaging is expected and the various images are expected to rotate on the sky, change in brightness, appear and disappear over the course of an event. At present it is not clear whether it will be possible to resolve the image distortions caused by an ESE, and even attempting the observations will be difficult because the VLBI network has to be scheduled in real time, but if these effects can be measured then the data will be place strong constraints on the electron column-density profile of the lenses, their distances and transverse velocities. Finally there are some key measurements which could be made at higher frequencies – i.e. the optical to X-ray band – which should directly reveal the dense neutral gas clouds responsible for ESEs via scattering, absorption and perhaps refraction (Draine 1998).

8.7 Stars

8.7.1 Flare stars

A surprisingly large fraction of cool stars, with spectral types of M and later are known to flare in the radio (Berger 2006). These flares can be used to measure the magnetic field strengths of the stars, and indeed Berger (2006) argues that radio observations are the best way to obtain these values. Burgasser & Putman (2005) show an example of a spectacular flare from an M dwarf which peaks at 30 mJy and lasts for a few minutes. The numbers of such events potentially detectable by MIRANdA is unclear, but one could imagine taking a census of such stars in the local (10 pc) neighbourhood.

8.7.2 Catacylismic variables

Catacylismic variables (CVs) are binary stars consisting of a white dwarf and a red dwarf in orbit about each other with a period of a few hours. The systems are generally divided into two classes depending on the magnetic field strength of the white dwarf. CVs are variable over all wavelengths and a wide variety of timescales. However, only the nearby magnetic CVs are persistent (weak) radio sources. Nova from CVs are occasionally seen in the radio with flux densities in excess of 10 mJy (Dulk et al. 1983). Examination of overlapping fields in the VLA FIRST survey for variable radio sources, and subsequent optical follow-up, led Bond et al. (2002) to claim the first radio selected CV. With a total galactic population in excess of 10^6, any

deep radio survey for variability is certain to detect many radio flares from these objects.

8.7.3 Neutron stars, black holes and microquasars

Compact stellar objects such as neutron stars or black holes in orbit with periods of a few days about a normal star can accrete material from their binary companion. This accretion produces X-ray emission and the systems are generally known as X-ray binaries. The systems give off relativistic jets and the jet emission is detectable in the radio band. Several hundred of these X-ray systems are known out of a likely galactic population of tens of thousands.

There is a rich radio phenomenology associated with these objects, both in the quiescent and outburst states (see e.g. Fender 2004). In a small handful of objects, the jet is seen expanding at superluminal speeds into the interstellar medium. These observations give an insight into the disk/jet interaction and the formation of accretion disks in general. There are obvious links, both observationally and theoretically to the AGN disk/jet structures seen in the distant Universe. For example, there appears to be a scaling between X-ray and radio power in black holes of all sizes (Merloni et al. 2003).

Currently a few tens of objects have significant radio outbursts lasting ten days and which repeat on a timescale of a year or so. These sources tend to be bright and easy to monitor. There must surely be an underlying, dimmer population of these objects about which we have little information. A regular sky survey, such as MIRANdA will do, should provide more information on these objects, especially when coupled with X-ray observations.

8.8 New classes of transients

The most interesting transient sources detected with MIRANdA will undoubtedly be objects which we currently know nothing about. One of the advantages of an all-sky survey is that it is tailor-made for detecting the unknown. It has become clear recently that the radio sky contains many transient objects, the indentification of which remains mysterious. For example, Hyman et al. (2005) discovered a bursting transient towards the Galactic Centre which lasted for only a few minutes but had a flux density in excess of 2 Jy. The bursts repeat at irregular intervals and the identification of this source remains unclear. Bower et al. (unpublished) examined archival VLA data of the same field spanning 22 years with observations

approximately once per week. They detected 8 transient sources, four of which have no optical counterparts or quiescent radio emission. They estimate that at MIRANdA sensitivity, approximately 1 transient source per square degree at any given time.

At this stage we can only surmise what MIRANdA will end up detecting, but a regular all-sky survey covering timescales from minutes to months will be a gold mine for radio transient science.

Chapter 9

Other Science

9.1 Exploring the Unknown

Most of the phenomena we observe today, using telescopes to observe across the electromagnetic spectrum, were unknown a few decades ago and were discovered by radio astronomers using increasingly powerful instruments.

In his book "Cosmic Discovery", Harwit (1981) addressed the question of what factors lead to new discoveries in astronomy. He argues that a large fraction of the discoveries have been associated with improved coverage of the electromagnetic spectrum or better resolution in the angle, time, or frequency domain. He also notes that astronomical discovery is often closely linked to innovative new technology introduced into the field.

MIRANdA is the first of a new generation of radio telescopes using innovative phased array feed technology to explore a greatly enlarged survey area parameter space. This wide field of view is essential for many of the science cases presented here, but we can also anticipate discovery of new rare and unexpected phenomena.

The next two sections describe one recent and unexpected discovery and one unusual proposal which would open a new field of particle astrophysics. One explores the highest frequency resolution and the other the highest time resolution.

9.2 OH Megamasers with MIRANdA

9.2.1 Survey

A rich series of transitions in OH, H2O and methanol molecules can be driven into population inversions to generate powerful maser emission (Darling et al. 2003). Especially important for observations out to high redshifts are likely to be the 1665/1667 MHz OH maser lines and 1612/1720 MHz conjugate lines (Darling 2004).

The wide field of view of MIRANdA makes blind surveys for extragalactic OH megamasers a possibility. An appropriate channel width for OH megamaser detection is about 30 kms^{-1}, or 0.17 MHz at z=0. For a 12-hour integration, we expect an rms noise level of 0.4 mJybm^{-1}, or 2 mJy at 5σ significance. One can expect to detect all OH gigamasers ($L_{\mathrm{OH}} > 10^4$) out to z = 1 and all OH megamasers with $L_{\mathrm{OH}} > 10^3$ out to z = 0.5 (834 and 1112 MHz, respectively). $L_{\mathrm{OH}} = 10^3$ $\mathrm{L}_\odot$ roughly represents the median luminosity of known OH megamasers.

Based on the OH megamaser luminosity function, the expected number of OH megamasers detected at $0 < z < 0.5$ per 30 square degree region of the sky is conservatively of order 1.3. One new OH megamaser per MIRANdA field of view would be fantastic in terms of enhancing numbers, pushing to higher redshifts, and studying the merging rate of galaxies (along with associated black hole feeding and merging and extreme bursts of star formation). If the survey were to cover the entire southern sky, we might expect the detection of ∼10000 new OH megamasers (just over 100 are known today).

Including an OH megamaser search in the planned H I search should be possible, it would not cost anything extra in terms of bandwidth or survey design - the OH megamasers would essentially be free additional data products. A survey with 300 MHz of instantaneous bandwidth from 1400 to 1100 MHz would be an ideal OH megamaser survey for this facility, and highly compatible with the H I survey. No other facility will be competitive in identifying new OH megamasers, particularly in a "blind" host-independent manner.

9.2.2 Magnetic Fields

The recent measurement of Zeeman splitting in extra-galactic OH megamasers by Robishaw et al (2007) using Arecibo opens a new and exciting field of research with these objects.

OH megamasers are typically found in ULIRGs so these Zeeman observations provide the first magnetic field estimates in powerful starburst

galaxies at significant redshifts. ARP220 and IIIZw35 were detected with good S/N but required the full sensitivity of Arecibo. Extended MIRANdA has just enough sensitivity to do the Zeeman experiment but will require a few days integration for the strongest OH megamasers.

To interpret the results Robishaw et al (2007) had to use previous VLBI measurements to separate the different components of the velocity profile which correspond to different OH megamaser sites inside the starburst galaxy. The unique advantage of MIRANdA for this research will be the baselines to the east coast which can use VLBI to separate the multiple components in the starburst galaxy. The OH megamaser spots will still be unresolved (Diamond, private communication) and only a single high sensitivity baseline (e.g. MIRANdA to Parkes) is needed to separate the maser spots in the Zeeman measurement while smaller dishes can images the OH megamaser sites.

9.3 Lunar Cherenkov Technique for UHE Particle Astronomy

The origin of the most energetic particles observed in nature, the ultra high energy (UHE) cosmic rays, which have energies extending up to at least 2×10^{20} eV, is currently unknown. Finding the origin of these particles will have important astrophysical implications as they may be accelerated in active galaxies or radio galaxies and could be directly or indirectly responsible for much of the non-thermal emission in these objects. One promising non-acceleration scenario is the generation of UHE particles due to the decay of super-massive dark matter particles which would form cold dark matter halos, with the highest concentration near centres of galaxies. In this scenario we would expect a strong UHE neutrino flux from the Galactic Centre region.

A key to untangling the origin of the UHE cosmic rays will be observations of UHE neutrinos. Despite the fact that for extragalactic UHE cosmic rays almost all spectral information above the GZK cut-off is lost, significant information on the cosmic ray spectrum at the sources is preserved in the spectrum of neutrinos (Protheroe & Clay 2004) and of course the neutrinos are not deflected by magnetic fields and so should point back to where they were produced. The Moon can be used as a large volume neutrino detector, adopting a powerful method first proposed by Dagkesamanskii & Zheleznykh (1989) and first applied by Hankins et al. (1996) using the Parkes radio telescope. The coherent radio Cherenkov emission (Askar'yan

effect) from neutrino-induced electromagnetic cascades in lunar regolith (the ∼10 m deep sandy lunar surface layer) is observed with ground based radio telescopes.

9.3.1 Coherent Radio Cherenkov Emission

Askar'yan (1962) first predicted coherent Cherenkov emission in dielectric media at radio and microwave frequencies. Cherenkov radio pulses are much shorter (sub-nanosecond duration) than any signals normally encountered in radio astronomy, so special signal processing techniques are required.

The spectrum of coherent Cherenkov emission rises approximately linearly with frequency until a peak value is reached, after which de-coherence and/or attenuation in the regolith result in a relatively sharp cut-off at about 5 GHz. Far from the Cherenkov angle, and deeper in the regolith, the peak moves down to about a hundred MHz.

MIRANdA is an array of small dishes which is the optimum way to do this experiment. The dishes are small enough to see all the moon (< 20 m at 1.4 GHz) and the array and site provide essential discrimination against RFI. To gain the advantage of the large number of small dishes, signals have to be combined and analysed with nanosecond timing accuracy. This can be done by using the phased array beam forming hardware. The extremely short Cherenkov pulses suffer dispersion in the ionosphere which must be corrected in real time at the output of the phased array beams to maximise the signal to noise. This will be similar to the pulsar back-end requirements. We need enough phased array beams to cover all the limb of the moon and this will depend on frequency and resolution. For a 5 km array at 1.5 GHz this would already need 250 beams which is impractical. For a reasonable system of say 25 beams we will only be able to use the inner 0.5 km so a high central concentration or an ultra compact configuration is a huge advantage. Note that the compact core with a large fraction of the collecting area is needed to optimise the s/n for the event trigger, but once triggered buffered data from the longer baselines can be used for position determination. Although there has been no explicit discussion of the MIRANdA phased arra y beam forming machinery needed for VLBI, pulsars or neutrino pulses it is interesting to note that it may be possible to reconfigure the FPA beam forming hardware for use as the antenna array beam formers when large fields of view are not required.

9.3.2 Comparison with Other Facilities

In the UHE neutrino energy range applicable to this experiment, $10^{18} - 10^{23}$ eV, the ANITA balloon-borne experiment (Barwick et al. 2006), which observes the Antarctic ice shield looking for coherent radio Cherenkov emission in ice from cascades initiated by UHE neutrinos, has the greatest sensitivity to UHE neutrinos . Because the Antarctic ice shield is at the pole, ANITA is only sensitive to UHE neutrinos from the equatorial plane region from declinations approximately $|\delta| < 15°$. Hence, the lunar Cherenkov technique will play a very important and complementary role in UHE neutrino and cosmic ray astronomy at $|\delta| > 15°$, inaccessible to ANITA. This includes the nearby blazar Mark 421 and nearby FRI radio galaxy Cen A, as well as the Galactic Centre, all likely sources of UHE cosmic rays and neutrinos but not visible to ANITA.

9.3.3 Optimum Frequency Range

The dependence of the peak frequency on shower geometry makes the choice of an optimum observation frequency non-trivial. Higher frequencies have a narrower acceptance angle and this reduces the effective aperture. But lower frequencies have reduced the sensitivity, increasing the particle energy threshold to above 10^{21} eV. Since the flat-spectrum Z-burst models of cosmic-ray production have been already ruled out by the ANITA-lite and FORTE limits, we place greater emphasis on observing below 10^{21} eV and hence the higher frequencies. By observing at higher frequencies the de-dispersion needed to correct for the ionosphere is smaller and easier to correct and the increased sensitivity to shower geometry provides more information on the energy and arrival direction of the primary particle.

There are very strong and complementary arguments in favour of observing at low frequencies (Scholten 2006). This applies especially to cosmic ray primaries for which only radiation far from the Cherenkov angle is likely to escape the regolith (cosmic rays will interact immediately so the bulk of their radiation will be directed into the Moon, while neutrinos can penetrate enough of the limb to produce showers parallel to the surface). The low frequency observations proposed for LOFAR and also possible with the MWA provide complementary information on UHF particles.

9.3.4 Observing time

The effective aperture of the full SKA as a function of neutrino energy is comparable to ANITA and reaches the flux level at which GZK neutrinos must

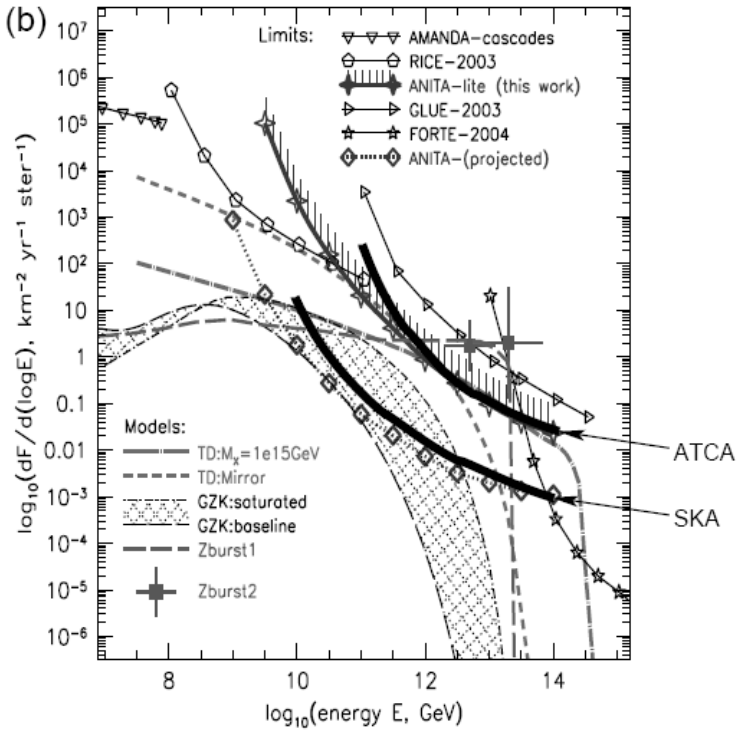

Figure 9.1: Existing limits on diffuse neutrino intensity, and expected sensitivity of ANITA compared to a range of models based on Fig. 3 of Barwick (2006). Our estimated sensitivities for 40 days using ATCA and SKA are overlaid as thick solid lines (C. James et al. in preparation).

be seen (see figure 9.1). Sensitivities have been modelled for MIRANdA, and compared with the published apertures for GLUE and ANITA (James, private communication). The neutrino flux sensitivities for a 40 day exposure with MIRANdA at 10^{12} GeV is 100 times the sensitivity of GLUE or Parkes, 5 times better than ATCA but still 20 times less than the proposed ANITA or SKA sensitivity. LOFAR (or MWA) has no sensitivity at 10^{12} GeV but exceeds the sensitivity of all other experiments at energies greater than 10^{13} GeV.

9.3.5 Summary of Key Observing Specifications

- The pulse-detection equipment will require a non-standard back-end, with very fast special purpose signal processing.
- Full polarisation.
- The largest possible bandwidth.
- 0.8 - 1.7 GHz frequency range is optimum for neutrino energy sensitivity and for neutrino vs. cosmic ray discrimination.
- Extension of the upper frequency to 3 GHz would give more information on particle energy and direction and would become very important when UHE neutrinos are detected.

References

Afonso, J., et al. 2003, ApJ, 597, 269
Amy, S., Large, M., Vaughan, A. 1989, PASA, 8, 172
Appleton, P. N., et al. 2000, ApJS, 154, 147
Armstrong, J., Rickett, B., Spangler, S. 1995, ApJ, 443, 209
Askar'yan, G. A., 1962, Sov.Phys. JETP, 14, 441
Barwick, S. et al, 2006, Phys. Rev. Lett., 96, 171101
Basilakos, S., et al., 2007, astro-ph/0703713
Baugh, C. M. et al. 2004, NewAR, 48, 1239
Baugh, C. M. et al. 2005, MNRAS, 356, 1191
Baugh, C. M. 2006, Rep. Prog. Phys., 69, 3101
Beck, R., et al., 1996, ARA&A, 34, 155
Beck, R. 2001, Space Science Reviews, 99, 243
Beck, R., Gaensler, B. M., 2004, NewAR, 48, 1289
Berger, E. 2006, ApJ, 648, 629
Beswick, R. J., et al. 2006, astro-ph/0612077
Bignall, H. et al., 2006, ApJ, 652, 1050
Bignall, H. et al., 2003, ApJ, 585, 653
Binney J., 2004, MNRAS 347, 421
Blasi, P. et al., 1999, ApJ, 514, L79
Blundell, K.M., Rawlings, S., Willott, C.J., 1999, ApJ, 117, 677
Bond, H. et al., 2002, PASP, 114, 1359
Boughn, S., Crittenden, R., 2004, Nature, 427, 45
Bower, R. G. et al. 2006, MNRAS, 370, 645
Boyle, B. J. et al. 2007, MNRAS, 276, 1182
Braun, R., Thilker, D. A. 2004, A&A, 417, 421
Brentjens, M. A., de Bruyn, A. G. 2005, A&A, 441, 1217
Brisken, W. F., et al. 2002, ApJ, 571, 906
Brown, J. C., Taylor, A. R. 2001, ApJ, 563, L31
Brown, J. C., et al. 2007, ApJ, In Press (astro-ph/0704.0458)
Brüns, C., Kerp, J., Pagels, A. 2001, A&A, 370, L26
Brüns, C. et al., 2000, A&A, 357, 120
Burgasser, A., Putman, M. 2005, ApJ, 626, 486

Butcher, H., Oemler, A. Jnr. 1978, ApJ, 219, 18
Carilli, C. L. et al., 1992, ApJ, 399, L59
Carilli, C., Ivison, R., Frail, D. 2003, ApJ, 590, 192
Carilli, C. et al., 2004, NewAR, 48, 1029
Chamaraux, P., Masnou, J.-L. 2004, MNRAS, 347, 541
Chang, T.-C., Refregier, A., Helfand, D., 2004, ApJ, 617, 794
Clegg, A. W. et al., 1992, ApJ, 386, 143
Cole S., et al. 2000, MNRAS, 319, 168
Condon, J. J., et al. 1998, AJ 115, 1693
Condon, J. J., 1992, ARA&A, 30, 575
Cordes, J. M., Lazio, T. J. W. 2002, astro-ph/0207156
Cordes, J. M., McLaughlin, M. 2003, ApJ, 596, 1142
Dagkesamanskii, R., Zheleznykh, I. 1989, Sov. Phys. JETP, 50, 233
Darling, J., et al. 2003, AJ, 125, 1177
Darling, J., 2004, ApJ, 612, 58
Davé, R., et al., 1999, ApJ 511, 521
Davé, R., Cen R., Ostriker J. P., 2001, ApJ, 552, 473
de Avillez, M., Breitschwerdt, D. 2004, Ap&SS, 292, 207
De Breuck, C., et al. 2006, MNRAS, 366, 58
Deller, A., et al., 2007a, PASP, 119, 318
Deller, A. et al. 2007b, ATel #1037
Dennett-Thorpe, J., de Bruyn, G. 2002, Nature, 415, 57
Dickey, J. M. 1997, ApJ, 488, 258
Dickey, J. M., Crovisier, J., Kazes, I. 1981, A&A, 98, 271
Dove, J. B., Shull, J. M., 1994, ApJ 423, 196
Draine, B. T. 1998, ApJ, 509, L41
Dressler, A. 1984, ARAA, 22, 185
Dulk, G., et al., 1983, ApJ, 273, 249
Dumke, M. et al., 1995, A&A, 302, 691
Elmegreen, B. G. 1991, ApJ, 378, 139
Fender, R. 2004, NewAR, 48, 1399
Ferrière, K. 2005, *The Magnetized Plasma in Galaxy Evolution*, 147
Feulner, G., et al., 2005, ApJ, 633, L9
Fiedler, R., et al. 1987a, ApJSS, 65, 319
Fiedler, R., et al. 1987b, Nature, 326, 675
Fiedler, R., et al. 1994, ApJ, 430, 581
Frick, P. et al., 2001, MNRAS, 325, 649
Gaensler, B. M., Beck, R., Feretti, L. 2004, NewAR, 48, 1003
Gaensler, B. M. et al., 2005, Science, 307, 1610
Gal-Yam, A., et al. 2006, ApJ, 639, 331

Geller, R.M., et al. 2000, ApJ, 539, 73
Goldsmith, P. F., Li, D., Krčo, M. 2007, ApJ, 654, 273
Goldsmith, P. F., Li, D. 2005, ApJ, 622, 938
Gomez, P. L., et al., 2003, ApJ, 584, 210
Gunn, J., Peterson, B., 1965, ApJ, 142, 1633
Gunn, J. E., Gott, J. R. III 1972, ApJ, 176, 1
Han, J. L., Qiao, G. J. 1994, A&A, 288, 759
Han, J. L., et al. 2006, ApJ, 642, 868
Hankins, T., Ekers, R., O'Sullivan, J., 1996, MNRAS, 283 1027
Hansen, B., Lyutikov, M. 2001, MNRAS, 322, 695
Harwit, M., "Cosmic Discovery - The Search, Scope & Heritage of Astronomy", Basic Books, Inc., New York (1981).
Heiles, C., Troland, T. H. 2003, ApJS, 145, 329
Heiles, C., Troland, T. H. 2005, ApJ, 624, 773
Hewish, A., et al. 1968, Nature, 217, 709
Hobbs, G. 2005, PASA, 22, 179
Hopkins, A., et al. 2000, ExA, 10, 419
Horiuchi, S. et al. 2004, ApJ, 616, 110
Hulse, R. A., Taylor, J. H. 1975, ApJ, 195, L51
Hyman, S., et al. 2005, Nature, 434, 50
Irwin, M. J. et al 2007, ApJ, 656, 13
Jackson, C. 2004, NewAR, 48, 1187
Jackson, C. A., Wall, J. V. 1999, MNRAS, 304, 160
Jackson, C. 2005, PASA, 22, 36
Jenet, F. A., et al. 2005, ApJ, 625, L123
Johnston, S., Gray, A. 2006, SKA Memo Series #72
Johnston, S., Romani, R. 2003, ApJ, 590, L95
Johnston, S., et al. 2005, MNRAS, 364, 1397
Juneau, S. et al. 2005, ApJ, 619, L135
Kalberla, P. M. W., Kerp, J. 1998, A&A, 339, 745
Karastergiou, A., Johnston, S. 2006, MNRAS, 365, 353
Katz, C., et al. 2003, PASP, 115, 675
Kedziora-Chudczer, L. 2006, MNRAS, 369, 449
Kedziora-Chudczer, L., et al. 1997, ApJ, 490, L9
Keller, S. C., et al. 2007, astro-ph/0702511
Kenney, J. D. P., van Gorkom, J. H., Vollmer, B. 2004, AJ, 127, 326
Keres, D. et al., 2005, MNRAS, 363, 2
Kilborn, V. A. et al. 2005, MNRAS, 356, 77
Klamer, I. J. et al. 2006, MNRAS, 371, 852
Kolatt, T. 1998, ApJ, 495, 564

Kramer, M. et al. 2004, NewAR, 48, 993.
Kramer, M. et al. 2006, Science, 312, 549
Kronberg, P. P. 1994, Rep. Prog. Phys., 57, 325
Lah, P. et al 2007, MNRAS, 376, 1357
Lazio, T. et al. 2004, NewAR, 48, 985
Lenc, E., Tingay, S. 2006, AJ, 132, 133
Levinson, A., Ofek, E., Waxman, E., Gal-Yam, A. 2002, ApJ, 576, 923
Lewis, I., et al., 2002, MNRAS, 334, 673
Li, D., Goldsmith, P. F. 2003, ApJ, 585, 823
Lockman, F. J. 2002, ApJ, 580, L47
Lovell, J. at al., 2003, AJ 126, 1699
Lovell, J. et al., 2007, ASP Conf Series, astro-ph/0701601
Lyne, A., et al. 1998, MNRAS, 295, 743
Macquart, J.-P., de Bruyn, A.G. 2007, MNRAS, Submitted
Maggiore, M. 2000, Phys. Rep., 331, 283
Manchester, R. N., et al. 2005, AJ, 129, 1993
Manchester, R. N., et al. 2001, MNRAS, 328, 17
Matsumura, N., et al. 2007, AJ, 133, 1441
Mauch, T. et al., 2003, MNRAS, 342, 1117
McClure-Griffiths, N. M., et al. 2005, ApJS, 158, 178
McLaughlin, M. A. et al. 2006, Nature, 439, 817
Merloni, A., Heinz, S., di Matteo, T. 2003, MNRAS, 345, 1057
Mesa, D., et al. 2002, A&A, 396, 463
Meyer, M. et al. 2004, MNRAS, 350, 1195
Meyer, M. et al. 2007, ApJ, 654, 702
Minter, A. H., Spangler, S. R. 1996, ApJ, 458, 194
Moore, B., et al., 1996, Nature, 379, 613
Mulchaey, J. S., Zabludoff, A. I. 1998, ApJ, 496, 73
Norris, R. P., et al. 2006, AJ, 132, 2409
Norris, R.P. et al. 2007, MNRAS, In Press
Omar, A., Dwarakanath, K. S. 2005, JApA, 26, 71
Padovani, P., et al., 2007, astro-ph/0701493
Papovich, C., et al., 2006, ApJ, 640, 92
Peek, J. E. G., et al., 2007, ApJ, 656, 907
Péroux, C., et al., 2003, MNRAS, 346, 1103
Phillips, C.J. et al. 2007, MNRAS, submitted
Phinney, E., Taylor, J. 1979, Nature, 360, 137
Poggianti, B. M., et al., 2006, ApJ, 642, 188
Prochaska, J.X., Herbert-Fort, S., Wolfe, A.M. 2005, ApJ, 635, 123
Protheroe, R. J., Clay, R. W. 2004, PASA, 21, 1

Putman, M. E., et al., 2003, ApJ, 586, 170
Putman, M. E. 2000, PASA, 17, 1
Rao, S. M., Turnshek, D. A., Nestor, D. B. 2006, ApJ, 636, 610
Rao, S. M., Briggs F. 1993, ApJ, 419, 515
Rawlings, S. et al., 2004 NewAR, 48, 1013
Rees, M. J., Ostriker, J. P., 1977, MNRAS 179, 541
Reynolds, R. J. 1985, ApJ, 294, 256
Robishaw, T. et al. 2007, IAU Symposium 242, In Press
Romani, R., Blandford, R. D., Cordes, J. M. 1987, Nature 328, 324
Ruzmaikin, A. A., Sokolov, D. D., Shukurov, A. M., 1988, *Magnetic Fields of Galaxies*
Ryan-Weber, E. V. 2006, MNRAS, 367, 1251
Scholten, O. et al., 2006, Astropart. Phys., 26, 219
Sholomitskii, G.B., Yaskovitch, A.L., 1990, Soviet Astron. Lett, 16, 383
Simpson, C., et al. 2006, MNRAS, 372, 741
Solanes, J. M. et al. 2001, ApJ, 548, 97
Spangler, S., Gwinn, C. 1990, ApJ, 353, 29
Springel, V. et al. 2005, Nature, 435, 629
Springob, C. M., Haynes, M. P., Giovanelli, R. 2005, ApJ, 621, 215
Stairs, I. H., Lyne, A. G., Shemar, S. 2000, Nature, 406, 484
Staveley-Smith, L. 2006, ATNF SKA Memo Series #6
Storrie-Lombardi, L. J., 2000, ApJ 543, 552
Tingay, S. J. et al. 2002, ApJS, 141, 311
Tingay, S. J., Murphy, D. W. 2001, ApJ, 546, 210
Tingay, S. J. et al. 1996, ApJ, 464, 170
Tingay, S. J. et al. 1995, Nature, 374, 141
Totani, T., Panaitescu, A. 2002, ApJ, 576, 120
Treu, T. et al. 2003, ApJ, 591, 53
Tucci, M., et al., 2004, MNRAS, 349, 1267
Tully, B. 1987, ApJ, 321, 280
Tüllmann, R. et al., 2000, A&A, 364, L36
Vranesevic, N., et al. 2004, ApJ, 617, L139
Walker, M. A. 2006, ASP Conf. Series, astro-ph/0610737
Wall, J. V. 1994, Aus. J. Phys., 47, 625
West, J. L., et al., 2007, ApJ, 656, 914
Widrow, L. M. 2002, Rev. Mod. Phys., 74, 775
Windhorst, R. A. 2003, NewAR, 47, 357
Windhorst, R. A., et al. 1999, ASPC, 193, 55
Wolleben, M., et al,. 2006, A&A, 448, 411
Xu, Y. et al., 2006, ApJ, 637, 19

Yun, M. S., Ho, P. T., Lo, K. Y. 1994, Nature, 372, 530
Zheng, X. Z., et al. 2007, astro-ph/0702208
Zwaan, M., et al. 1997, ApJ, 490, 173
Zwaan, M. et al. 2003, AJ, 125, 2842
Zwaan, M. et al. 2005, MNRAS, 359, 30
Zweibel, E. G. & Heiles, C. 1997, Nature, 385, 131